

Copyright

by

Fernando Eguiarte-Solomon 2020

The Dissertation Committee for Fernando Eguiarte-Solomon Certifies
that this is the approved version of the following dissertation:

The Role of Twist1 in UVB-induced Skin Carcinogenesis

Committee:

John DiGiovanni, Supervisor

Karen Vasquez

Stefano Tiziani

Dawit Kidane-Mulat

The Role of Twist1 in UVB-induced Skin Carcinogenesis

by

Fernando Eguiarte-Solomon

Dissertation

Presented to the Faculty of the Graduate School of

The University of Texas at Austin

in Partial Fulfillment

of the Requirements

for the Degree of

Doctor of Philosophy

The University of Texas at Austin

December 2020

Acknowledgements

First and foremost, I would like to thank my advisor Dr John DiGiovanni for all of his support and guidance during the graduate program. He always demanded more of me and challenged me to become a better graduate student, shaping me into a more organized and analytical scientist. Many are the lessons that I treasure and will continue to live by in my professional career ahead.

I thank my dissertation committee members Dr. Karen Vasquez, Dr Stefano Tiziani and Dr. Dawit Kidane for taking the time of their busy schedules to supervise my work and provide invaluable guidance and feedback throughout my presentations.

I would also like to thank the DiGiovanni Lab members past and present for their moral support and help with my experiments. Dr. Lisa Tremmel was a senior graduate student when I first started in the lab who taught me a lot of the skills I have used in my project, from handling and treating the mice to collecting tissues and running efficient Western blots. Dr. Okkyung Rho provided tremendous help throughout my project, particularly with figuring out the mouse models and PCR techniques. Dr. Nicholas Blazanin often offered great insight into theoretical aspects of my projects and helped me develop strong skills for experimental design.

The DiGiovanni lab members have been extremely supportive, especially when my experiments were not working, and make the lab a fun place to work. Thank you: Sabin Kshattray, Carly Wilder, Steve Carbajal, Achinto Saha, Zhao Chen, Songyeon Ahn, Megha Thakur and Eleanor Shaul, I will greatly miss all of you.

Lastly, I would like to thank my partner, parents, family and friends. Without your support and encouragement over the last years I would not be where I am today.

The Role of Twist1 in UVB-induced Skin Carcinogenesis

Fernando Eguiarte-Solomon Ph.D.

The University of Texas at Austin, 2020

Supervisor: John DiGiovanni

The transcription factor Twist1 has been reported to be essential for the formation and invasiveness of chemically induced tumors in mouse skin. However, the impact of keratinocyte specific Twist1 deletion on carcinogenesis caused by UVB radiation has not been clarified.

In the current studies, we demonstrate that deletion of Twist1 in skin keratinocytes *in vivo* (using K5-Cre x Twist1^{flox/flox} mice; Twist1 KO mice) significantly suppressed UVB-induced skin carcinogenesis. Twist1 KO led to reduced UVB-induced epidermal hyperproliferation. Proliferation analysis by Ki67 immunofluorescence staining as well as BrdU incorporation showed a significant decrease in Twist1 KO epidermis. In addition, Twist1 was also found to control the differentiation of keratinocytes in the bulge region and in the interfollicular epidermis, suggesting that exit from cell cycle in Twist1 KO keratinocytes is linked to induction of differentiation. Deletion of Twist1 *in vivo* and in culture showed significant induction of early and late differentiation markers including TG1, K1, OVOL1, Loricrin and Filaggrin. In contrast, overexpression of Twist1 in cultured keratinocytes suppressed expression of calcium-induced differentiation markers. Additionally, deletion of Twist1 in epidermal and bulge region

keratinocytes led to depletion of several hair follicle stem/progenitor markers, including CD34, Lrig1, Lgr5 and Lgr6. These findings further support the hypothesis that Twist1 may have direct role in regulating proliferation, differentiation and self-renewal processes in the epidermis.

We also discovered that the natural compound, Harmine, leads to degradation of Twist1 in keratinocytes and inhibits UVB-induced epidermal proliferation while stimulating keratinocyte differentiation similar to Twist1 KO. Collectively, the current data demonstrate an important role for Twist1 in UVB skin carcinogenesis and the potential for this transcription factor as a target for skin cancer prevention.

Table of Contents

LIST OF FIGURES	X
LIST OF TABLES	XII
CHAPTER 1. BACKGROUND.....	1
1.1. <i>Biology of the skin</i>	1
1.1.1 Architecture of skin layers and cell types	1
1.1.2 Hair follicle and bulge region	2
1.1.3 Differentiation and proliferation programming	3
1.2. <i>Skin cancer</i>	6
1.2.1. Non-Melanoma Skin Cancers	6
1.2.2. UV radiation.....	7
1.2.3. Other risk factors for SCC	7
1.2.4. Animal models to study SCC.....	8
1.3. <i>Transcription factor Twist1</i>	10
1.3.1 Oncogenic functions and target pathways	10
1.3.2 Pharmacological inhibitors of Twist1	13
1.3.2.1 Harmine.....	13
1.3.2.2 Emodin	13
1.3.2.3 SKP2 inhibitors	14
1.3.2.4 Atalantlaflavone	14
1.4. <i>Overall Goals and Objectives</i>	15

CHAPTER 2. METHODS.....	16
2.1 <i>Transgenic Animals & Study Protocols</i>	16
2.1.1 In vitro Knockout of Twist1 with AdeCre	16
2.1.1.1 Cell cycle	16
2.1.1.2 Apoptosis	17
2.1.2 K5.Twist1 KO mice.....	17
2.1.2.1 K5 Twist1 KO in vivo studies	17
2.1.2.2 Short-term UV radiation protocol.....	19
2.1.2.3 Long-term UVB carcinogenesis protocol	19
2.1.2.1 Pharmacological inhibition using Harmine	23
2.1.3 <i>Inducible K5.rTA.Twist1 overexpressing model</i>	23
2.1.3.1 Calcium-induced differentiation studies	23
2.1.4 <i>K15.Twist1 KO model</i>	25
2.1.4.1 Treatment for K15.Twist 1 KO.....	25
2.1.4.2 Keratinocyte Stem Cell Isolation and Staining.....	25
2.1.4.3 Colony Formation Efficiency Assay.....	26
2.2 <i>Western Blot Analyses</i>	26
2.3 <i>RT-qPCR Analyses</i>	27
2.4 <i>Histological and Immunohistochemical Analyses</i>	27
2.5 <i>Flow cytometry Analyses</i>	28
2.6 <i>Statistical analyses</i>	28

CHAPTER 3. DELETION OF TWIST1 IN KERATINOCYTES INDUCES DIFFERENTIATION	29
3.1 INTRODUCTION	29
3.2 RESULTS	31
3.3 DISCUSSION	42
CHAPTER 4. DELETION OF TWIST1 INCREASES APOPTOSIS AND REDUCES UVB- INDUCED PROLIFERATION AND TUMORIGENESIS	46
4.1 INTRODUCTION	46
4.2 RESULTS	49
4.3 DISCUSSION	65
CHAPTER 5. PHARMACOLOGICAL INHIBITOR OF TWIST1, HARMINE, INDUCES KERATINOCYTE DIFFERENTIATION AND INHIBITS UVB-INDUCED EPIDERMAL PROLIFERATION	68
5.1 INTRODUCTION	68
5.2 RESULTS	69
5.3 DISCUSSION	82
CHAPTER 6. CONCLUSIONS AND FUTURE DIRECTIONS.....	85
6.1 CONCLUSIONS	85
6.2 FUTURE DIRECTIONS	91
REFERENCES	95

List of Figures

FIGURE 1.1 THE EPIDERMAL DIFFERENTIATION PROCESS (SANDILANDS <i>ET AL</i> 2019)	4
FIGURE 1.2 THE MARKERS IN THE HAIR FOLLICLE AND BULGE REGION (JAKS <i>ET AL</i> 2010).....	5
FIGURE 1.3 UV RADIATION CAUSES NON MELANOMA SKIN CANCERS (COELHO <i>ET AL</i> 2016)	9
FIGURE 1.4 MULTIPLE FUNCTIONS OF TWIST1 IN CANCER. (ZHAO <i>ET AL</i> 2017)	12
FIGURE 2.1 IN VITRO KO OF TWIST1 USING ADECRE FOR CELL CYCLE AND APOPTOSIS ANALYSIS	18
FIGURE 2.2 SHORT-TERM UVB CARCINOGENESIS EXPERIMENT USING K5.TWIST1 KO MICE	18
FIGURE 2.3 LONG-TERM UVB CARCINOGENESIS PROTOCOL USING K5.TWIST1 KO MICE.....	20
FIGURE 2.4 HARMINE TREATMENT STUDIES USING WILD-TYPE PRIMARY KERATINOCYTES	24
FIGURE 2.5 CALCIUM-INDUCED DIFFERENTIATION USING K5.RTA.TWIST1 PRIMARY KERATINOCYTES	24
FIGURE 3.1 TWIST1 KO IS CONFIRMED IN SKIN SECTIONS AND IN RNA FROM EPIDERMAL SCRAPINGS.....	32
FIGURE 3.2 TWIST1 DELETION LEADS TO DECREASED EMT DOWNSTREAM EFFECTORS AND INCREASED KERATINOCYTE DIFFERENTIATION MARKERS AND PROLIFERATION INHIBITORS	33
FIGURE 3.3 TWIST1 DELETION LEADS TO INCREASED DIFFERENTIATION MARKERS IN SKIN SECTIONS	34
FIGURE 3.4 TWIST1 OVEREXPRESSION REVERSES EFFECTS OF CALCIUM-INDUCED DIFFERENTIATION	36
FIGURE 3.5 TWIST1 KO IN BASAL KERATINOCYTES ALTERS EXPRESSION OF STEM/PROGENITOR CELL MARKERS IN VIVO	38
FIGURE 3.6 TWIST1 KO IN K15 POSITIVE BULGE REGION KERATINOCYTES ALTERS EXPRESSION OF STEM/PROGENITOR CELL MARKERS IN VIVO	39
FIGURE 3.7 DELETION OF TWIST1 IN KSC RESULTS IN DECREASED STEM MARKERS.....	40
FIGURE 3.8 DELETION OF TWIST1 IN KSC RESULTS IN IMPAIRED CLONOGENICITY	41
FIGURE 4.1 TWIST1 DELETION LEADS TO REDUCED KERATINOCYTE SURVIVAL FOLLOWING UVB EXPOSURE.	52
FIGURE 4.2 IN VITRO TWIST1 DELETION LEADS TO ALTERATIONS IN CELL CYCLE.	53
FIGURE 4.3 TWIST1 DELETION IN PRIMARY KERATINOCYTES LEADS TO ALTERED LEVELS OF APOPTOTIC AND CELL CYCLE REGULATORS.....	54
FIGURE 4.4 TWIST1 DELETION IN KERATINOCYTES IN VIVO LEADS TO ALTERED LEVELS OF CELL CYCLE REGULATORY PROTEINS FOLLOWING UVB EXPOSURE.....	56
FIGURE 4.5 TWIST1 DELETION DECREASES UVB-INDUCED EPIDERMAL THICKNESS, BRDU INCORPORATION AND KI67 STAINING	57
FIGURE 4.6 TWIST1 KO INCREASES CARCINOMA-FREE SURVIVAL AND INHIBITS UVB-INDUCED SCC DEVELOPMENT	61
FIGURE 4.7 IMMUNOSTAINING OF SCC MARKERS CONFIRMING TUMOR CLASSIFICATIONS OBTAINED FROM UVB CARCINOGENESIS PROTOCOL.	62

FIGURE 4.8 REPRESENTATIVE SCC TUMORS FROM BOTH TWIST1 WT AND KO GROUPS SHOWED HIGH LEVELS OF TWIST1.....	63
FIGURE 4.9 TWIST1 KO YIELDS NO SIGNIFICANT DIFFERENCE IN UVB-INDUCED SARCOMAS.....	64
FIGURE 5.1 TREATMENT WITH HARMINE AND CALCIUM IN VITRO AFFECTS KERATINOCYTE MORPHOLOGY INDUCING DIFFERENTIATION.....	70
FIGURE 5.2 HARMINE TREATMENT OF CULTURED KERATINOCYTES MIMICS CALCIUM-INDUCED DIFFERENTIATION.....	71
FIGURE 5.3 BMI1 INHIBITION REPLICATES P-16 AND E-CADHERIN INCREASES OF HARMINE BUT NOT OVOL1 INDUCTION.	73
FIGURE 5.4 OVOL1 INHIBITION REDUCES HARMINE-INDUCED DIFFERENTIATION.	74
FIGURE 5.5 TWIST1 DELETION IMPACTS WNT PATHWAY VIA PKC-MEDIATED DEGRADATION OF B-CATENIN.	76
FIGURE 5.6 PKC INHIBITION RESULTS IN REDUCED HARMINE-INDUCED OVOL1 AND P-STAT3.	77
FIGURE 5.7 HARMINE TREATMENT OF IN VIVO INDUCES DIFFERENTIATION MARKERS AND OVOL1.....	79
FIGURE 5.8 HARMINE TREATMENT IN VIVO INHIBITS UVB-INDUCED ACTIVATION OF CELL CYCLE MARKERS.....	80
FIGURE 5.9 HARMINE TREATMENT IN VIVO INHIBITS UVB-INDUCED INCREASES IN EPIDERMAL THICKNESS AND BRDU INCORPORATION.	81
FIGURE 6.1 WORKING MODEL FOR THE EFFECTS OF TWIST1 DELETION ON DOWNSTREAM PATHWAYS CONTROLLING PROLIFERATION, DIFFERENTIATION, STEMNESS AND EMT IN KERATINOCYTES.....	90

List of Tables

TABLE 1. UV-CARCINOGENESIS TWIST1 WT GROUPS (FE.UVTUM.WT).....	21
TABLE 2. UV-CARCINOGENESIS TWIST1 KO GROUPS (FE.UVTUM.KO).....	22
TABLE 3. TUMOR ONSET AND MULTIPLICITY FOR TWIST1 WT AND TWIST1 KO COHORTS IN UVB CARCINOGENESIS PROTOCOL	59

CHAPTER 1. Background

1.1. Biology of the skin

1.1.1 Architecture of skin layers and cell types

As the external barrier of mammalian organisms, the skin is the largest organ of the body. It represents the first line of defense against pathogens and environmental stimuli. The skin contributes to the regulation of body temperature and hydration, amongst other protective functions, organized in two main layers: the dermis and the epidermis [1].

The dermis is the mesenchymal component of the skin that provides strength and elasticity due to the presence of collagen and elastin fibers in the papillary and reticular layers [2].

The epidermis is a stratified squamous epithelium that is constituted of several cell layers (Fig 1.1). Resting on the basement membrane that separates it from the dermis is the basal layer, consisting of proliferating cells called keratinocytes. The basal layer gives rise to three differentiated cell layers: the spinous layer, granular layer and the stratum corneum [1]. Keratinocytes line these layers and confer the epidermis with durability and cohesion that together serve as a renewable barrier. Other important cell types conferring the epidermis with an array of vital functions are: melanocytes (to protect against ultraviolet radiation), Langerhans cells (for immune response), and Merkle cells (to allow sensorial impulses) [2, 3].

1.1.2 Hair follicle and bulge region

In addition to the transiently amplifying cells whose descendants are organized spatially and temporally to form the supra basal layer, the epidermal basal layer maintains reservoirs of multipotent keratinocyte stem cells (KSC) [4]. These serve to replenish all the different compartments in the hair shaft so that follicles can periodically undergo cycles of growth (anagen), destruction (catagen), and rest (telogen) [5]. The hair follicle consists of an outer root sheath at the surface of the basal epidermal layer and extends into the deep dermis. There are three important segments of hair follicles: the infundibulum, the isthmus, and the lower follicle/inferior segment, which includes the bulb (Fig 1.2). The hair bulb is made from proliferating matrix cells that terminally differentiate to generate the different cell types of the follicle. The hair follicles also host the sweat glands, which associate to an extensive vascular supply into the dermis where with the help of adipose tissue allow for proper thermoregulation [2, 3]. The dermal component of the hair follicle is the dermal papilla, which consists of specialized mesenchymal cells surrounded by the hair matrix cells [2, 3].

The bulge region is part of the outer root sheath and is where epidermal KSC reside. The self-renewal capability of the KSC located in the bulge region of the hair follicle is essential for the development of oncogenic lineages that can result in different types of epidermal malignancies [6, 7]. Thus, KSC are recognized as target cells for the initiation of non-melanoma skin cancers [8, 9].

1.1.3 Differentiation and proliferation programming

Epidermal homeostasis is maintained through a balance between proliferation and differentiation of keratinocytes residing throughout the hair follicle (HF) and in the supra-basal cell layers of the inter follicular epidermis (IFE) [10, 11]. Within mammalian epidermis there are two well characterized terminal differentiation pathways, the endpoints of which are the cells of the hair shaft and the outermost cornified layers of IFE [12, 13]. As seen in Figure 1.1, the main markers of the early differentiation process that occurs in the epidermal spinous layer above the basal layer are: Keratin 10 (K10), Keratin 1 (K1), and Transglutaminase (TG1) [10, 14]. Those that are characteristic of terminal differentiation in the granular and cornified layers are: Loricrin [15], Involucrin [16], and Filaggrin [17]. It is also widely recognized that extracellular calcium (Ca^{2+}) concentrations induce terminal differentiation [18], which represents a well-established model for induction of differentiation in cultured keratinocytes.

Given the nature of the differentiation programming, cells that are located in the upper layers of the epidermis are not actively proliferating and therefore are not capable of accumulating genetic mutations required for tumorigenesis [19]. Consequently, poorly differentiated states are considered a hallmark in most cancers [20] and, for over a decade, evidence of successful drug-induced differentiation therapies (i.e retinoic acid) have been proposed to induce terminal maturation and loss of self-renewal in stem-like tumor cells in gliomas, leukemias, and pancreatic cancers and other cancers [21, 22].

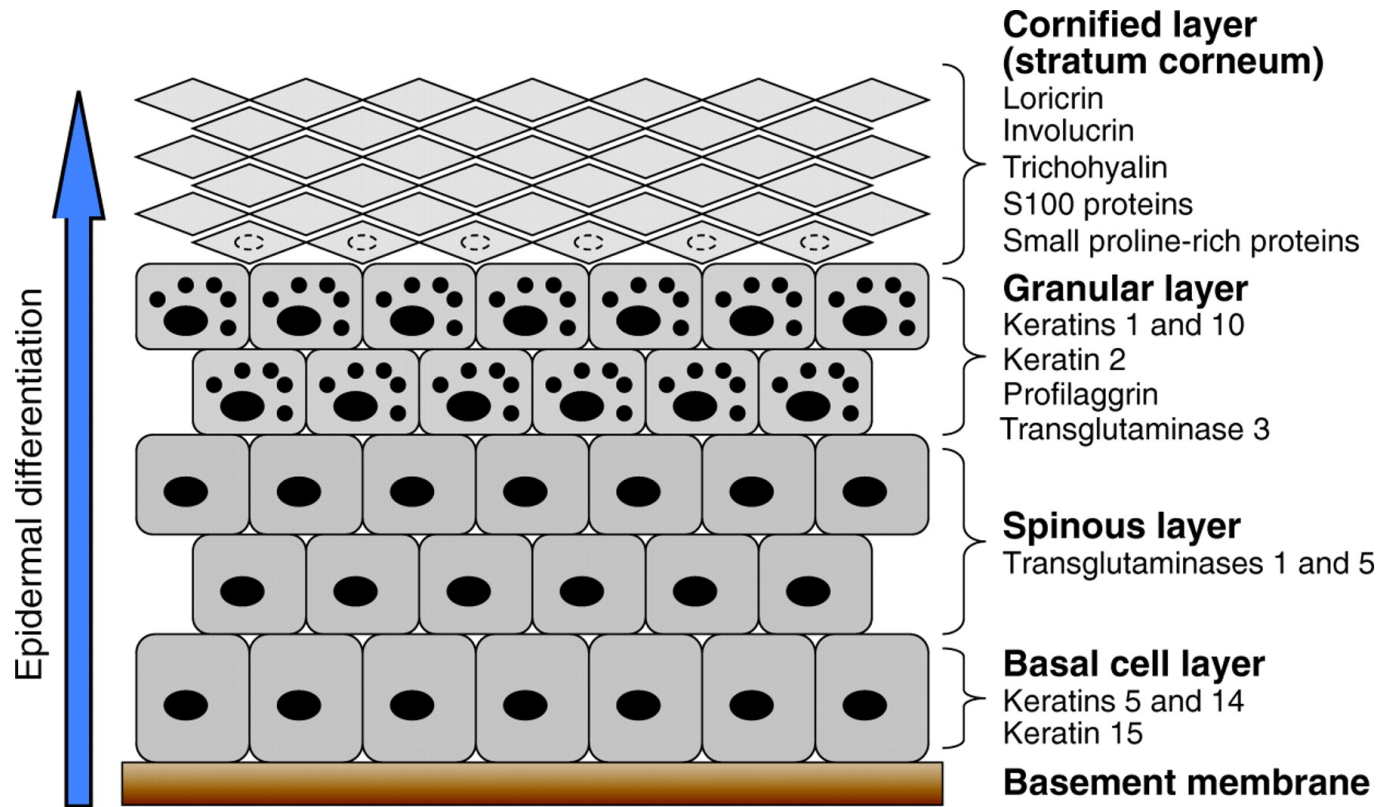


Figure 1.1 The Epidermal Differentiation Process (Sandilands *et al* 2019)

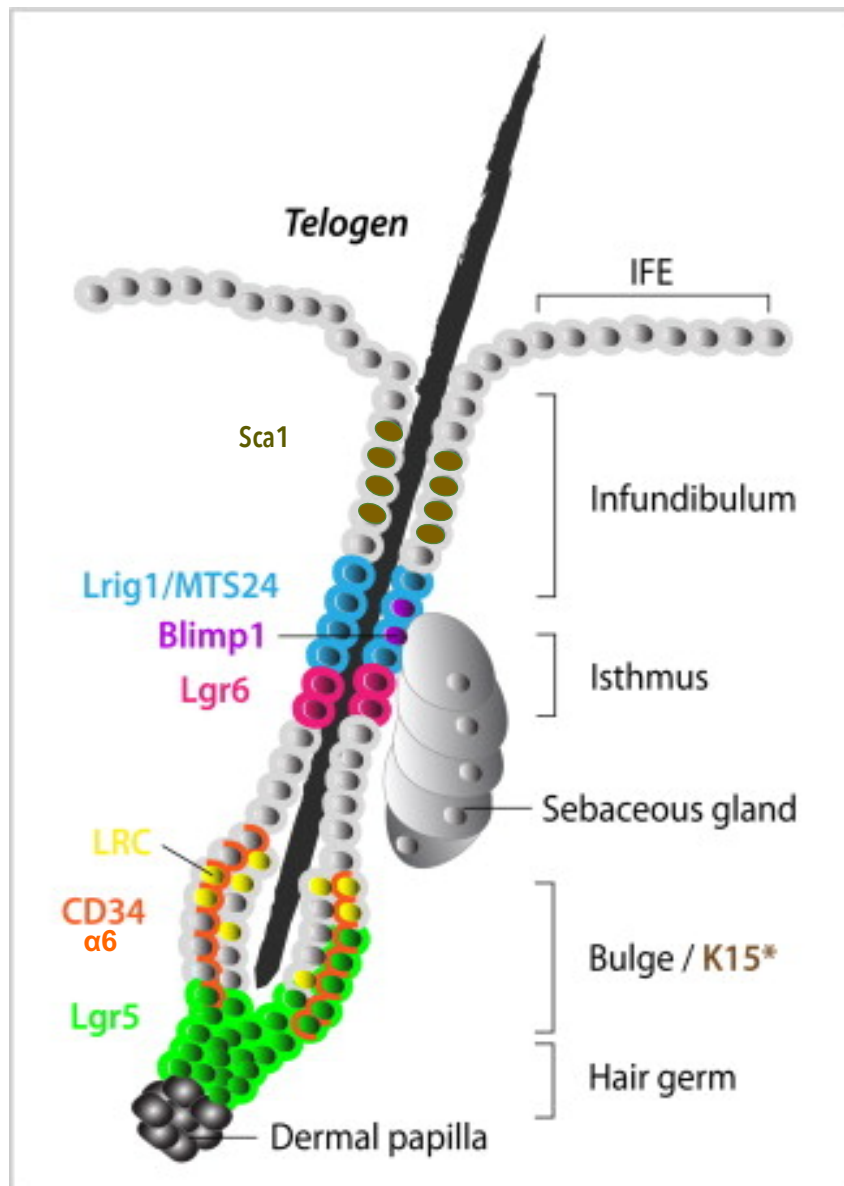


Figure 1.2 The markers in the Hair Follicle and Bulge Region (Jaks *et al* 2010)

1.2. Skin cancer

1.2.1. Non-Melanoma Skin Cancers

Non-melanoma skin cancers (NMSC) are the most diagnosed type of cancer worldwide [23]. NMSC are divided into two subtypes, squamous and basal cell carcinomas (SCC, BCC), depending on the cell type they originate from in the epidermis and the degree of dermal invasion they sustain. BCC and SCC together have one of the highest rising incidences in the United States with over 5 million diagnoses every year [24].

BCC arise from epidermal basal cells and are the least aggressive of the two despite of the capability of local invasion, tissue destruction, and recurrence [25]. BCC usually present as an enlarging, nonhealing lesion that may bleed. BCC vary in color and shape and can be described as flesh-colored round growth, pearl-like bump, or just pink patches of skin [26, 27].

SCC are the second most frequent type of NMSC, with over 250,000 new cases per year in the US [24]. SCC usually present as red firm bumps, scaly patches, recurrent sores [28]. They usually have favorable prognosis, although 4% of patients develop metastases and about 1.5% ultimately die [25]. SCC have been seen to progress from a precursor lesion called Actinic Keratoses (AK) to SCC in situ, then invasive SCC, and finally metastatic SCC [29]. Most patients develop multiple AK which results in a risk of developing invasive SCC ranging between 0.15 to 80% [30]. Additionally, males have a higher predisposition over females for the development of AK and SCC [31, 32].

1.2.2. UV radiation

Ultraviolet (UV) radiation plays the most important role in NMSC pathogenesis as the main risk factor for both subtypes (Fig 1.3). UVB is the major carcinogen that damages DNA most in the epidermis and continuously affects functions in keratinocytes resulting in their uncontrolled proliferation [33, 34]. Freckles, age spots, patches of discolored skin, and deep wrinkles are caused by UV radiation and make patients more susceptible to development of both NMSC, which implies that age itself is a major risk factor for these diseases. The median age recorded for NMSC diagnoses is at 67 years of age although it is not exclusive to the elderly demographic [23-25]. According to a few studies, history of sunburns in childhood tend to be associated with SCC development in adulthood [35].

1.2.3. Other risk factors for SCC

As stated above, BCC develops primarily on sun-exposed skin, mostly head and neck, and is rarely found on palmoplantar surfaces [24]. Gender has also been documented as a risk factor for BCC, appearing more commonly (2 : 1) in males [26]. Other individual risk factors for BCC include immunosuppression, arsenic poisoning, Fitzpatrick skin types I and II, and genetic diseases like the Gorlin–Goltz syndrome [26]. Similar risk factors have been reported for progression of AK into SCC, including family history of skin cancer, aging, fair complexion, chronic skin ulcers, burn scars, and exposure to chemical carcinogens [24, 28].

1.2.4. Animal models to study SCC

The DMBA/TPA chemical carcinogenesis model has been the benchmark methodology to study NMSC for decades. Many studies have also modeled the appearance of these cancers with transgenic and knockout mice, as reviewed by Huang *et al* in 2014 [36]. However, given the well-known etiology for NMSC, UV induced carcinogenesis studies are more physiologically relevant to study the underlying mechanisms of skin carcinogenesis leading to SCC. Our group uses acute and long-term UV radiation protocols, described further in Chapter 2, that facilitate the study of new strategies to prevent and treat NMSC. Figure 1.3 provides a conceptual framework for our current knowledge of skin carcinogenesis produced by exposure to solar UV (a combination of UVA and UVB at an approximate ratio of 20:1) [34, 37, 38].

The use of these mouse models of skin carcinogenesis has provided us with invaluable insight into the role of STAT3 in regulating the initiation and promotion of papillomas and cutaneous SCC. STAT3 was found to play an important role in skin carcinogenesis through its ability to regulate multiple keratinocyte growth properties, especially proliferation and differentiation [39-41]. During the course of studies in our laboratory, Twist1 was discovered to be a transcriptional target of STAT3 in keratinocytes [42, 43] confirming studies published from other laboratories using other cells and tissues [44-48]. It was therefore hypothesized that Twist1 might mediate some of the effects of STAT3 during skin carcinogenesis.

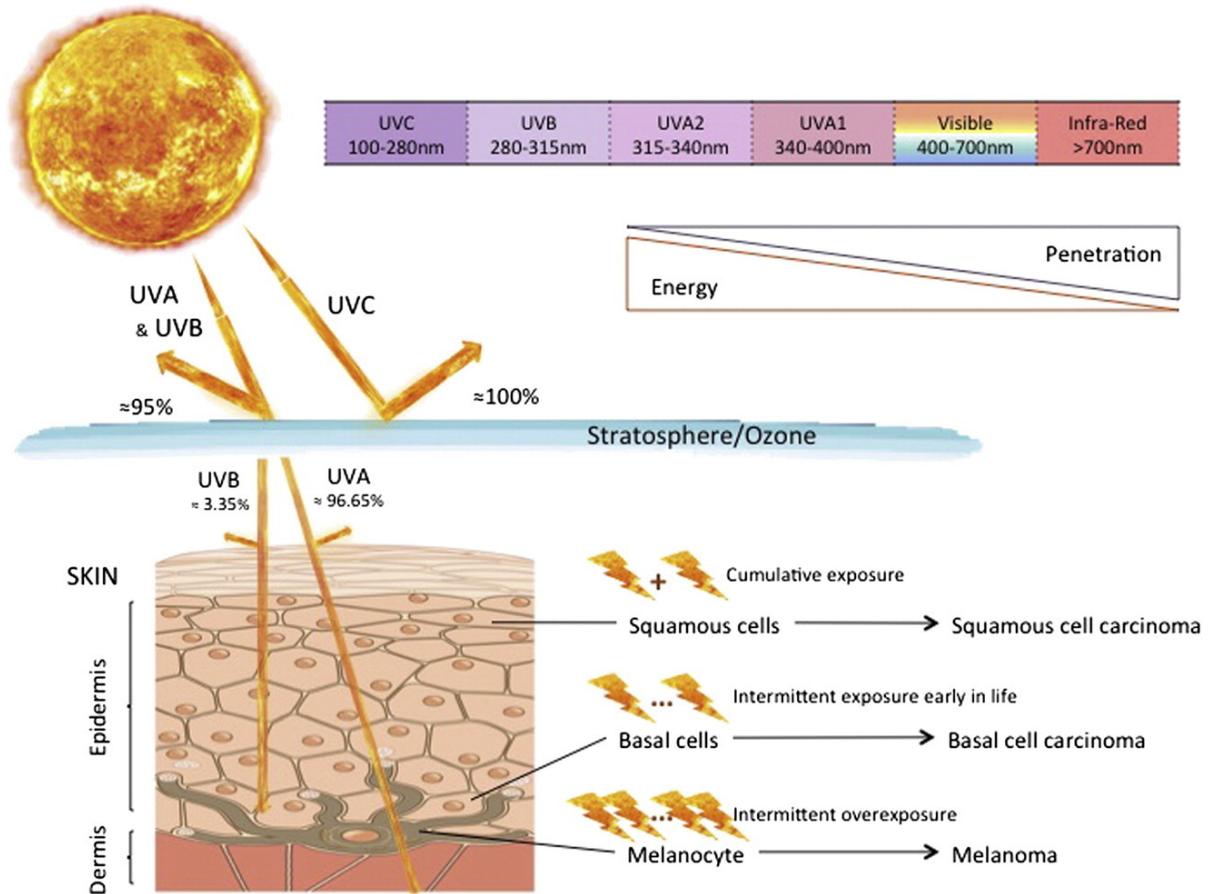


Figure 1.3 UV Radiation causes Non Melanoma Skin Cancers (Coelho *et al* 2016)

1.3. Transcription factor Twist1

The transcription factor Twist1 belongs to the basic helix-loop-helix family and was identified in *Drosophila* as a regulator of development and differentiation in embryos. The name derived from the “twisted” shape of internal organs in embryos with mutated Twist1. Accordingly, mutations in the Twist1 human gene cause craniosynostosis and hypertelorism, which are characteristics of the Saethre-Chotzen syndrome [49]. In humans, Twist is known to be expressed in two sequentially similar isoforms: Twist1 and Twist2 [50, 51]. The dimerization of the HLH domains of Twist1 is an essential for the interaction with E-box sequences (CANNTG), commonly found in promoter and enhancer regions of a large variety of regulatory genes [52]. Transcriptional functions of Twist1 differ depending on either homodimer or heterodimer associations and adjacent nucleotide variability flanking the E-boxes [53, 54]. Twist1 binds to E-box sequences to activate transcription of multiple signaling pathways involved in tumor progression, most commonly associated with pathways regulating the epithelial-mesenchymal transition (EMT) [55]. Studies have shown that Twist1 activation can result from environmental stimuli such as cytokines, hormones, and γ -irradiation, and, when stimulated, Twist1 regulates vital cellular activities such as evasion of apoptosis, cell migration, and invasion [51].

1.3.1 Oncogenic functions and target pathways

Twist1 is overexpressed in many cancers and is a positive regulator of proliferative and metastatic signaling (Fig 1.4) [56-58]. The aggressiveness imprinted in cancers by Twist1 makes this a marker and indicator for poor prognosis and disease recurrence [59]. However, only

limited data is available on the role of Twist1 in NMSC, and only a few papers have reported that Twist1 is upregulated in human cutaneous squamous cell carcinomas (cSCCs) [60, 61]. In more recent years, Twist1 has been reported to be involved in other oncogenic pathways regulating not only the invasiveness of tumors but also pathways contributing to tumor initiation (Fig 1.4) [62]. Evidence indicates that Twist1 plays an essential role in tumor initiation by evading p53-induced cell senescence and apoptosis [63]. Investigations into the regulation of Twist1 expression have revealed that STAT3 and NF- κ B are positive transcriptional regulators of Twist1 [64-66]. Activation of STAT3 via signaling through the EGFR leads to increased expression of Twist1 [64, 65, 67]. It has also been proposed that cytokine (e.g. TNF- α) mediated activation of NF- κ B activates Twist1, which in turn subsequently leads to the repression of NF- κ B transactivation [68-70]. As reported in several studies, Twist1 promotes EMT via regulation of proteins such as E-cadherin/ N-cadherin [71-73], MMP-1 [74] and Bmi1 [75]. In fact, there are reports of a connection between EMT and cancer stemness mediated by Twist1 and Bmi-1, interdependently [76]. Twist1 also promotes stemness properties independent of EMT as shown by the regulation of CD24 expression in a breast cancer study with Twist1 overexpression [77].

In summary, Twist1 can induce EMT when overexpressed but will stably inhibit stemness upon deactivation, implying a mutually exclusive system between these two pathways mediated by Twist1 [78]. Correspondingly, Beck *et al* showed that low levels of Twist1 are insufficient to induce EMT but can regulate tumor-associated proliferation and tumor stemness independently of p53 [56]. Furthermore, by deleting Twist1 in pre-existing skin tumors, they confirmed its essential role for tumor maintenance and propagation in K14.CreER x Twist1^{flox/flox} NOD/SCID/Il2Rg null mice [56].

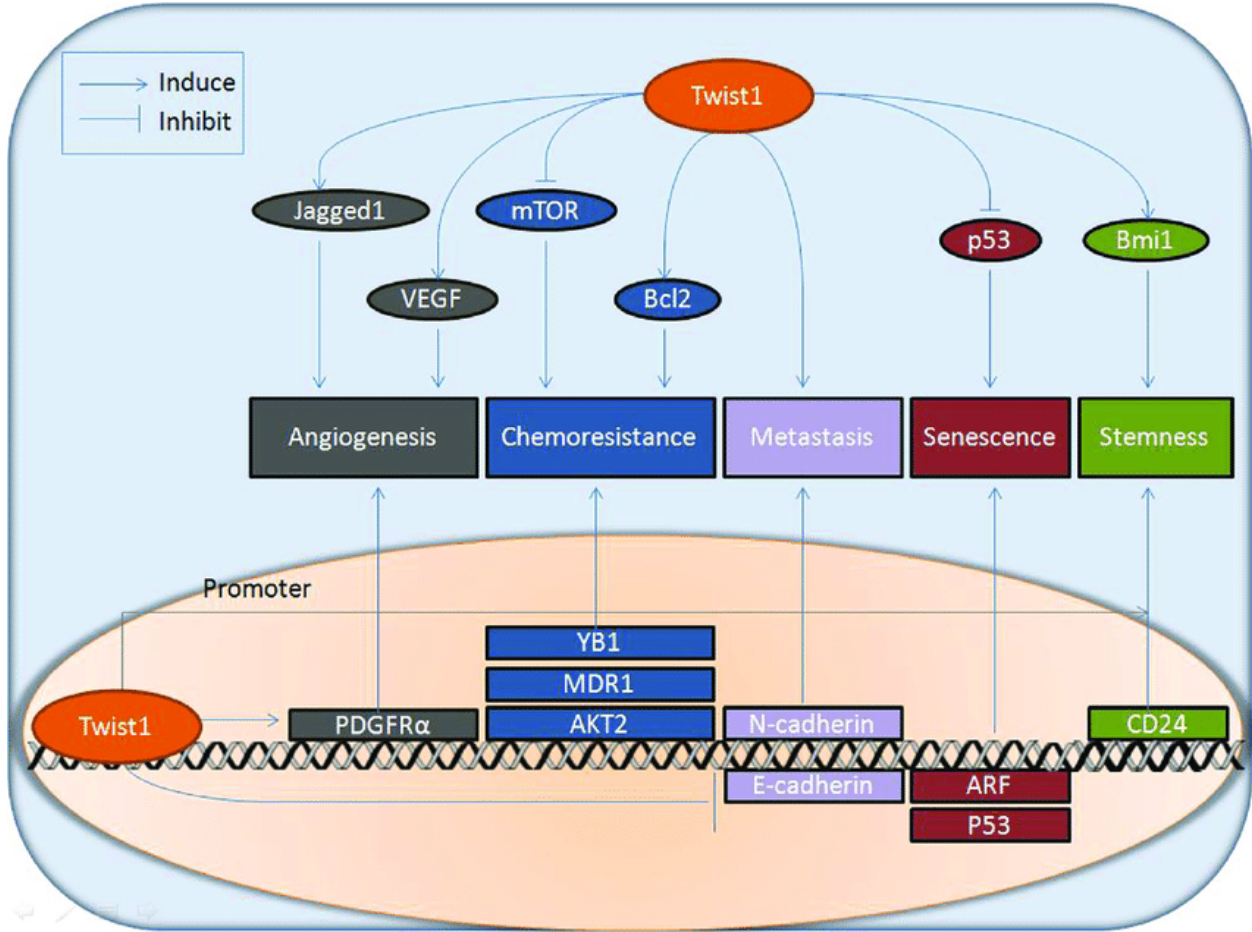


Figure 1.4 Multiple functions of Twist1 in cancer. (Zhao *et al* 2017)

1.3.2 Pharmacological inhibitors of Twist1

1.3.2.1 Harmine

Harmine is an alkaloid present in many medicinal plants used in traditional remedies and was named when first isolated from seeds of the *Peganum harmala* plant [79, 80]. Harmine has been shown to inhibit different cancers by impacting proliferation and invasion mechanisms [81]. It specifically inhibits the cell cycle G0/G1 phase by impairing activity of cyclin-dependent kinases [82]. Yochum *et al* in 2017 identified Harmine as a cytotoxic agent in several lung cancer models. The mechanism described upon treatments with Harmine involved the degradation of Twist1 protein as well as its dimerization, which is critical for its downstream functions [83]. Based on this information, we used Harmine on primary keratinocytes and *in vivo* as a control for the effects of Twist1 inhibition, and a proof of principle that it can be used to prevent progression of NMSC. This data will be presented in Chapter 5.

1.3.2.2 Emodin

Emodin is a chemical compound isolated from the root of *Rheum palmatum*, most commonly known as rhubarb, and is widely used as a laxative in traditional Chinese medicine. This anthraquinone is reported to possess anti-bacterial, anti-inflammatory and immunosuppressive effects [84]. Recent studies have described its anti-proliferative and pro-apoptotic effects in leukemia, ovarian, lung, and head and neck cancers [85]. Way *et al* [86] showed that Emodin significantly inhibits Twist1-induced cell invasion by dysregulating β -

catenin and Akt pathways. Emodin treatments led to inhibition Twist1 expression and EMT seen in downregulated vimentin mRNA and protein levels and upregulated E-cadherin expression [86]. In summary, they demonstrated that Twist1 inhibition is key for emodin-mediated reduction of pathways related to tumor initiation and invasion.

1.3.2.3 SKP2 inhibitors

The S-phase kinase associated protein-2 (Skp2) is a substrate recognition protein of the E3 ligase complex that regulates protein substrates through ubiquitination. Skp2 is believed to promote tumorigenesis through mechanisms involving many oncogenic substrates [87]. Ruan *et al* showed that when Skp2 interacts with Twist1, it prevents proteasomal degradation by promoting the non-degradative ubiquitination of Twist1 instead, thus stabilizing Twist1 protein expression [88]. They tested a library of potential inhibitors and found that the protein expression of Twist and its ubiquitination promoted by Skp2 were impaired by compound SKP2C25. In conclusion, the inhibition of the stabilization of Twist1 regulated by Skp2 restricted cancer stem cell traits and tumor progression in their adenocarcinoma mouse prostate model.

1.3.2.4 Atalanttraflavone

Atalanttraflavone (AFL) is a natural product isolated from leaves of the *Atalantia monophylla* plant and tested for antioxidant activity and acetylcholine esterase inhibition important in Alzheimer's disease [89]. Yuan *et al* recently described the tumor suppressive function for AFL in a NSCLC model via a mechanism of increasing Twist1 degradation [90].

AFL promoted ubiquitin mediated proteasomal degradation of Twist1 while Twist1 overexpression partially reversed the effect of AFL. The consequences of a Twist1 inhibition on EMT deregulation and apoptotic rescue seem to inhibit metastatic characteristics of cancer cells and imply that AFL can be used to reversed cisplatin resistance in some NSCLC cell lines.

1.4. Overall Goals and Objectives

The overall goal of the current project was to determine the role of Twist1 in UV induced skin carcinogenesis, especially early in the carcinogenic process. In addition, we sought to determine if Twist1 could be a potential target for prevention of cSCC. Novel mouse models (i.e., K5.Cre x Twist1^{flox/flox} mice, K5.rTA x tetotwist1 mice and K15.CrePR1 x Twist1^{flox/flox} mice) were used to not only determine the role of Twist1 in UV induced skin carcinogenesis but to further understand the mechanism(s) involved within. The current results demonstrate that Twist1 is required for skin carcinogenesis by UVB showing that Twist1 directly regulates keratinocyte differentiation. These data help to further explain the evidence of reduction in tumor response seen in Twist1 KO groups using the DMBA-TPA model [91] as well as in immunodeficient mice [56]. Furthermore, the current data pave the way for future studies targeting Twist1 for prevention of NMSC.

CHAPTER 2. Methods

2.1 Transgenic Animals & Study Protocols

2.1.1 In vitro Knockout of Twist1 with AdeCre

Primary epidermal keratinocytes were obtained from Twist1^{lox/lox} and wild-type mice as previously described [16]. At 80% confluence, the cells were infected for 5 hours with a CMV adenovirus expressing GFP-tagged nuclear permeable Cre recombinase (AdeCre). After 24 hours of replacing the adenoviral treatment with EMEM2, the keratinocytes were exposed to 25mJ/cm² of UVB or sham radiation for control dishes in 1 mL of PBS (Fig 2.1).

2.1.1.1 Cell cycle

These adult primary keratinocytes (Fig 2.1) were also harvested for Cell Cycle analysis via Propidium Iodide staining. An approximate of 5×10^5 cells was suspended in 1mL of PBS and added with 70% ethanol for fixation using the drop titration method with constant vortexing. Cells were incubated overnight at -20°C and then resuspended in 1mL of PBS-Propidium Iodide (1%). After a 30min incubation with this intercalating agent at room temperature, cells were aspirated into a FACS-Aria flow cytometer to quantify DNA content and classify cells into four different cell cycle phase populations: SubG1, G1, S, G2/M.

2.1.1.2 Apoptosis

Treated primary keratinocytes (Fig 2.1) were also harvested for Apoptosis analysis via Annexin V/7AAD staining following the Guava protocol. An approximate of 5×10^5 cells was suspended in 0.1mL of PBS and added with 5uL of Annexin V solution. After a 30min incubation at room temperature with this intercalating agent, cells were aspirated into a Guava flow cytometer and Annexin V staining was quantified to identify apoptotic population using 7AAD as a viability indicator to characterize the necrotic and late apoptotic populations.

2.1.2 K5.Twist1 KO mice.

K5.Cre^{+/-} x Twist1^{flox/flox} mice were generated in our animal facility at the Dell Pediatric Research Institute to obtain a keratinocyte specific genetic deletion of Twist1. The original Twist1^{flox/flox} mice were backcrossed from a C57B6 genetic background onto a FVBN background over 10 generations prior to crossing with the K5.Cre mice (Fig 2.2).

2.1.2.1 K5 Twist1 KO *in vivo* studies

Cohorts of 6 mice were used for *in vivo* UVB experiments and divided into two treatment groups: Twist1 KO mice [K5.Cre^{+/-} x Twist1^{flox/flox}] and control mice [K5.Cre^{+/-} x Twist1^{wt/wt}] at 7-8 weeks of age. The dorsal skin of each mouse was shaved 48 hours before processing the skin for analyses. (Fig 2.2)

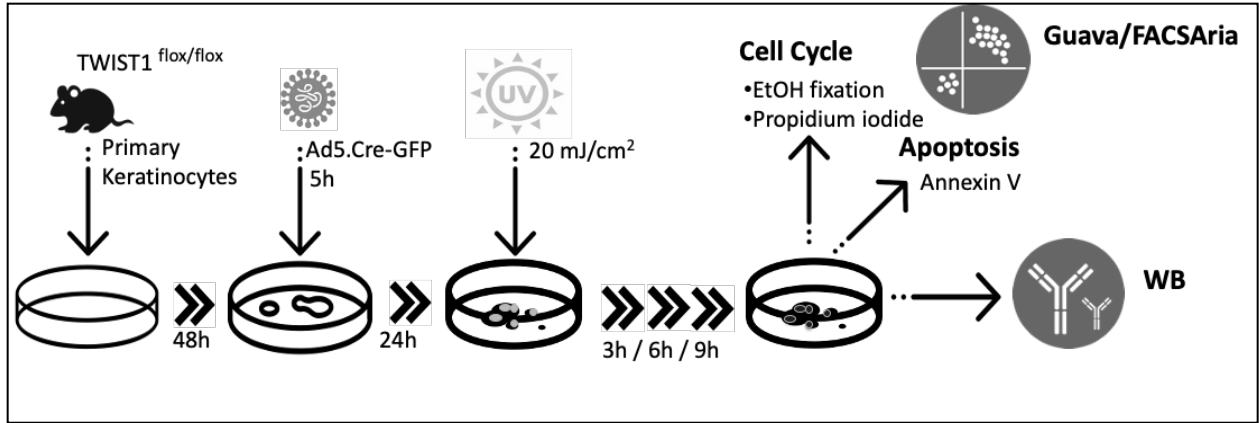


Figure 2.1 In vitro KO of Twist1 using AdeCRE for Cell Cycle and Apoptosis Analysis

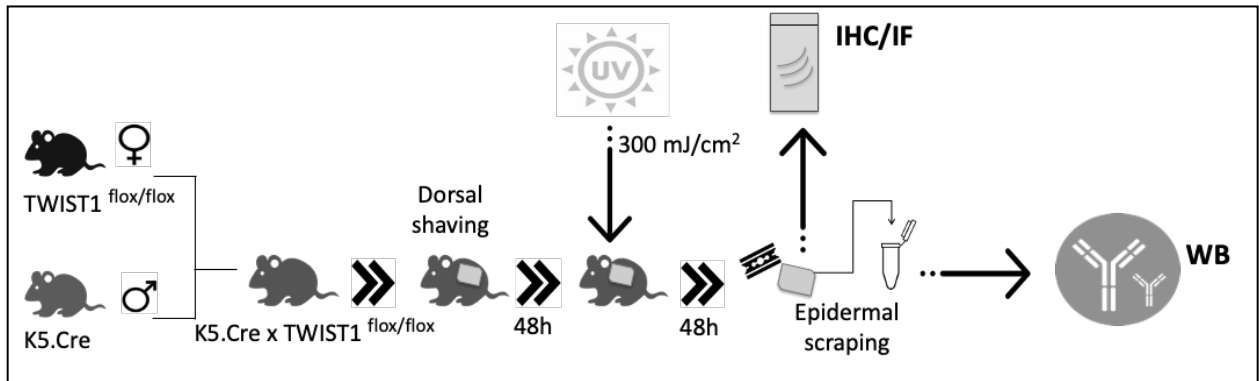


Figure 2.2 Short-term UVB carcinogenesis experiment using K5.Twist1 KO mice

2.1.2.2 Short-term UV radiation protocol

To evaluate the effects of the keratinocyte specific deletion of Twist1 on UVB radiation, mice from the two groups Twist1 WT (K5.Cre × Twist1^{wt/wt}) and Twist1 KO (K5.Cre × Twist1^{flox/flox}) were subjected to single treatment with UVB radiation in doses ranging in from 120-300mJ/cm². These studies were done in a custom-made UV chamber using an ILT140 Portable Radiometer/Photometer detector (International Light Technologies, Peabody, MA). Untreated mice were submitted to “sham” radiation and were subjected to the same handling procedures as the UVB-treated specimens but without the radiation treatment itself (Fig 2.2).

2.1.2.3 Long-term UVB carcinogenesis protocol

To evaluate the consequences of a deletion of Twist1 on UVB-induced carcinogenesis, different cohorts of mice in two groups: 26 control Twist1 WT (K5.Cre × Twist1^{wt/wt}) (Table 1) and 14 Twist1 KO (K5.Cre × Twist1^{flox/flox}) mice (Table 2) were subjected to treatments with UVB radiation 3 times a week (MWF) for 52 weeks. In order to avoid negative effects of erythema and to reduce ear papilloma formation, we used an incrementally graded UV protocol previously verified by our laboratory. All mice were exposed to 220mJ/cm² of UVB 3 times per week for weeks 1–6, 260mJ/cm² of UVB for weeks 7–8, 300mJ/cm² of UVB for weeks 9–10, 360mJ/cm² of UVB for weeks 11–12, 405mJ/cm² of UVB for weeks 13–14, and 450mJ/cm² of UVB for weeks 15–30 and 480mJ/cm² through the rest of the protocol to week 52. Mice were monitored for tumor formation weekly to establish tumor incidence and multiplicity. Skin tumors that developed on dorsal skin were counted following the first tumor appearance to establish tumor onset. At the termination of the experiment, mice were sacrificed and tumors were collected for histopathologic evaluation and for Western blot analysis.

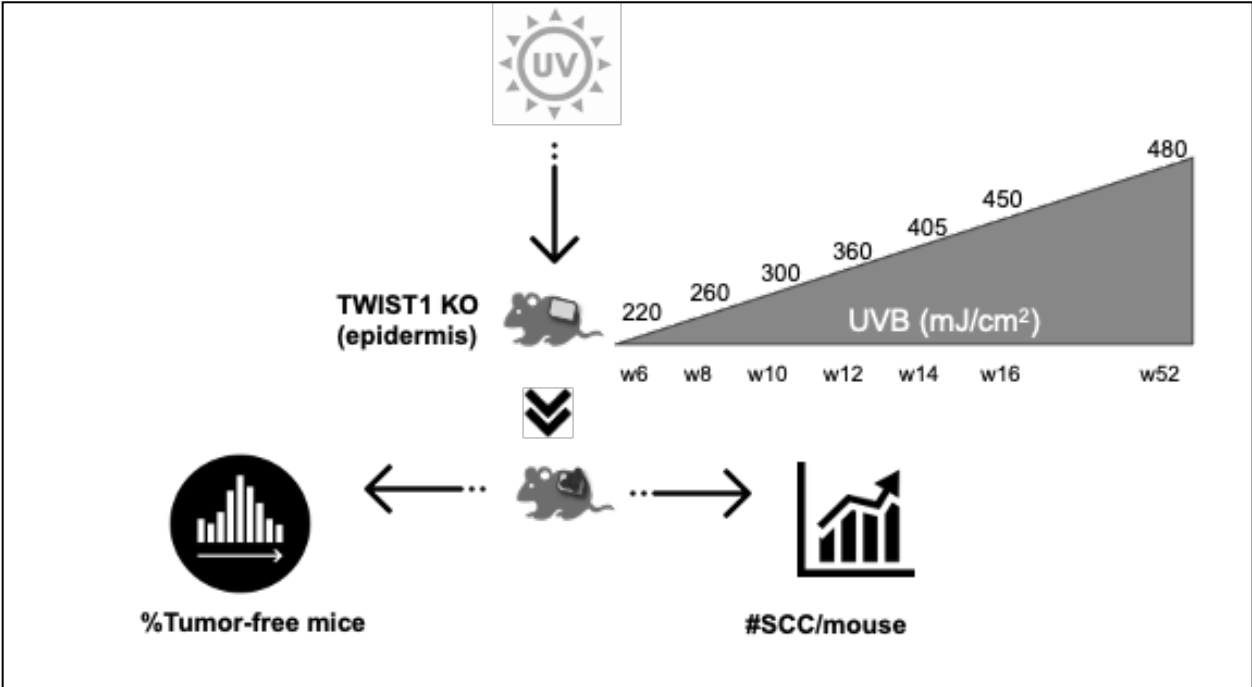


Figure 2.3 Long-term UVB carcinogenesis protocol using K5.Twist1 KO mice

Table 1. UV-Carcinogenesis Twist1 WT Groups (FE.UVTUM.WT)

Exp	#	JD.920	DOB	Age(w)	CRE	TWIST	Gender	Tx start
302	87	12	10/6/18	7.3	-	Flox	F	11/26/18
302	93	13	10/6/18	7.3	-	Flox	F	11/26/18
302	90	5	10/6/18	7.3	-	Flox	M	11/26/18
303	97	4	10/25/18	6.6	-	Flox	M	12/10/18
303	98	17	10/25/18	6.6	-	Flox	M	12/10/18
303	102	14bis	10/25/18	6.6	-	Flox	F	12/10/18
303	103	16bis	10/25/18	6.6	-	Flox	F	12/10/18
303	30	14	10/21/18	7.1	+	WT	M	12/10/18
303	31	19	10/21/18	7.1	+	WT	M	12/10/18
303	32	3	10/21/18	7.1	+	WT	M	12/10/18
303	33	18	10/21/18	7.1	+	WT	M	12/10/18
303	34	15	10/21/18	7.1	+	WT	F	12/10/18
303	35	2	10/21/18	7.1	+	WT	F	12/10/18
304	37	22	11/20/18	8.0	+	WT	M	1/15/19
304	40	21	11/20/18	8.1	+	WT	F	1/16/19
304	41	20	11/20/18	8.3	+	WT	F	1/17/19
305	53	26	2/27/19	7.7	+	WT	M	4/22/19
305	54	27	2/27/19	7.7	+	WT	M	4/22/19
305	55	28	2/27/19	7.7	+	WT	M	4/22/19
305	60	23	2/27/19	7.7	+	WT	M	4/22/19
305	61	24	2/27/19	7.7	+	WT	M	4/22/19
305	65	29	2/27/19	7.7	+	WT	F	4/22/19
305	62	30	2/27/19	7.7	+	WT	F	4/22/19
305	68	31	2/27/19	7.7	+	WT	F	4/22/19
305	70	25	2/27/19	7.7	+	WT	F	4/22/19
305	71	32	2/27/19	7.7	+	WT	F	4/22/19

Table 2. UV-Carcinogenesis Twist1 KO Groups (FE.UVTUM.KO)

Experiment	#	JD.920	DOB	Age(w)	CRE	TWIST	Gender	Tx start
302	80	1	10/6/18	7.3	+	Flox	M	11/26/18
302	82	6	10/6/18	7.3	+	Flox	M	11/26/18
302	83	8	10/6/18	7.3	+	Flox	F	11/26/18
302	86	7	10/6/18	7.3	+	Flox	F	11/26/18
302	88	11	10/6/18	7.3	+	Flox	F	11/26/18
302	91	9	10/6/18	7.3	+	Flox	M	11/26/18
303	94	10	10/15/18	8.0	+	Flox	M	12/10/18
303	96	-	10/15/18	8.0	+	Flox	M	12/10/18
303	99	16	10/21/18	7.1	+	Flox	F	12/10/18
303	100	15bis	10/21/18	7.1	+	Flox	F	12/10/18
304	105	-	11/20/18	8.9	+	Flox	F	1/21/19
304	106	-	11/20/18	8.9	+	Flox	F	1/21/19
304	107	-	11/20/18	8.9	+	Flox	M	1/21/19
304	108	-	11/20/18	8.9	+	Flox	M	1/21/19

2.1.2.1 Pharmacological inhibition using Harmine

Primary epidermal keratinocytes from adult Twist1 KO mice [K5.Cre^{+/-} x Twist1^{fllox/fllox}] and control mice [K5.Cre^{+/-} x Twist1^{wt/wt}] were obtained as previously described [6]. Keratinocytes were plated under standard conditions in EMEM2 media and were treated with Harmine (5 μ M) for 18 hours to inhibit Twist1 expression and functions. A different set of primary keratinocytes was simultaneously treated with Ca²⁺ (1.4mM) as a differentiation control. Protein was collected for Western blot analysis described below (Fig 2.4).

2.1.3 *Inducible K5.rTA.Twist1 overexpressing model*

K5.rTA mice were obtained from Dr. Adam Glick's Lab and then crossed with tetoTwist1 mice in our animal facility at the Dell Pediatric Research Institute to obtain a Doxycycline-inducible overexpression model of Twist1.

2.1.3.1 Calcium-induced differentiation studies

Primary epidermal keratinocytes were obtained from Single transgenic (ST) or Double transgenic (DT) K5.rTA x tetoTwist1 newborn mice. After plating and incubating for 48 hours, the primary keratinocytes were treated with Doxycycline (1 μ g/mL) for 24 hours to induce Twist1 expression in the DT culture and generate the Twist1 overexpression group (OE). Twist1 OE and Twist1 WT primary keratinocytes were cultured with Ca²⁺-added EMEM2 (1.4mM) for an additional 24 hours and RNA and protein were collected for RT-qPCR and Western blotting analyses (Fig 2.5).

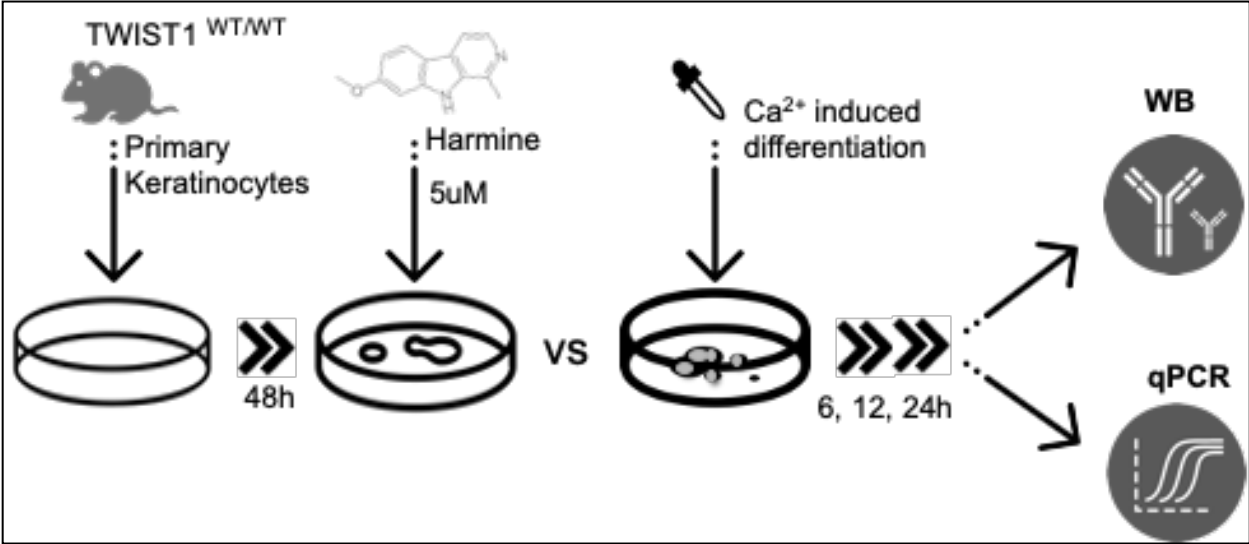


Figure 2.4 Harmine treatment studies using wild-type Primary keratinocytes

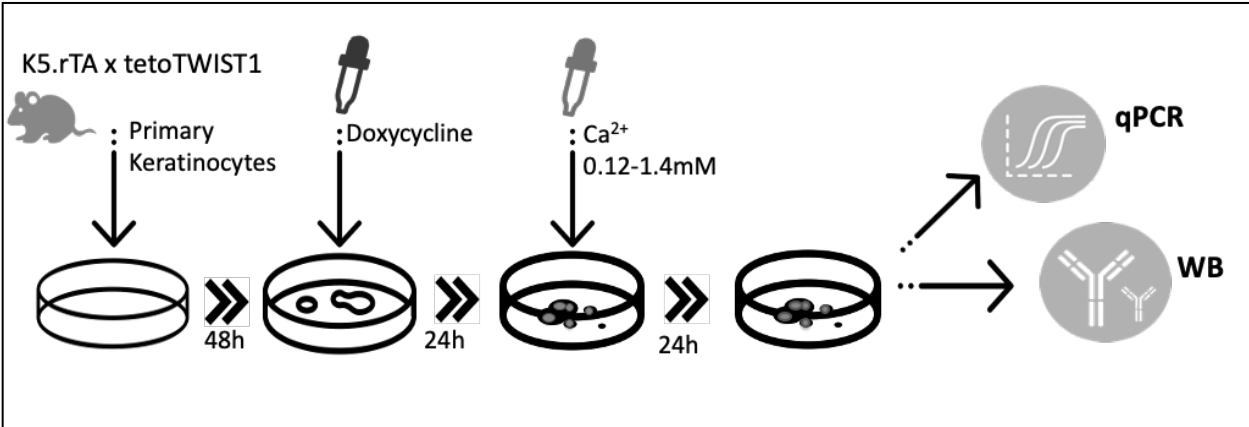


Figure 2.5 Calcium-induced differentiation using K5.rTA.Twist1 Primary keratinocytes

2.1.4 K15.Twist1 KO model

K15.CrePR1 x Twist1^{flox/flox} mice were generated in our animal facility at the Dell Pediatric Research Institute to obtain deletion of Twist1 in the K15 positive bulge region of the hair follicle.

2.1.4.1 Treatment for K15.Twist 1 KO

Groups of at 7 weeks old mice (n = 6) were treated topically with 2mg of RU486 or acetone for 5 consecutive days and comprising two groups: K15.Twist1 KO [K15.CrePR1 x Twist1^{flox/flox}] mice and K15.Twist1 WT [K15.CrePR1 x Twist1^{wt/wt}] mice. The dorsal skin of each mouse was shaved 48 hours before processing the skin for analyses.

2.1.4.2 Keratinocyte Stem Cell Isolation and Staining

Mouse dorsal skin was harvested from K15.Twist1 KO and K15.Twist1 WT mice by established protocols [22]. Fat underlying the subcutis was removed by scraping and the skins were incubated in dispase (5mg/ml) overnight at 48°C. Epidermis was scraped and discarded, and the dermis was incubated in 1% collagenase for 2 hours at 37°C. The resulting solution was first centrifuged at 300G and subsequently at 52G for 5 min at 48°C. The resulting pellet was resuspended in 0.25% Trypsin-EDTA and incubated at 37°C for 12 min. The solution was homogenized by pipetting multiple times and strained through 70mm and 40mm filters. Viability of KSC was analyzed using trypan blue exclusion and KSC counted using hemocytometer. RNA was extracted from the KSC for RT-qPCR analyses. KSC were also labeled with Lgr5-APC

(Miltenyi130111390). Cell sorting and isolation were performed on a BD LSR Fortessa flow cytometer equipped with the BD FACS Diva 6.0 software (BD Biosciences).

2.1.4.3 Colony Formation Efficiency Assay

KSC were also plated to assess the number cells with high growth potential through counts of holoclones (closely packed clones made up of at least 5 cells) and mero/paraclones (loosely packed clones of at least 5–8 cells). Approximately 5×10^5 KSC were plated onto a feeder layer of mitomycin C treated NIH3T3 cells and cultured for 4 weeks in DMEM 10% FBS under standard incubation conditions.

2.2 Western Blot Analyses

Protein lysates were obtained from the primary keratinocytes and from the scrapings of dorsal skins of the Twist1 KO and control wild-type mice as previously described [18-20]. Protein quantification was performed through the Lowry protein assay following a standard protocol from the manufacturer (DC BioRad) and normalized to 35-50 μ g of protein per well. Results were quantified with densitometry analysis using ImageStudioLite and normalized with β -actin and Vinculin loading controls. The following antibodies were used for Western Blotting: Twist1 (Acris AM10230PU-N), Bmi1 (CST 5856), Slug (CST 9598), Zeb1 (CST 3396), Vimentin (CST 5741), E-cadherin (CST3195), p21 (SC 6246), p53 (SC 98), cdk4 (SC 56277), cdk2 (CST 2546), p-cdk1(CST 9114), cyclin D1 (CST 2922), cyclin B1 (SC 245), E2F1 (SC251), TG1 (SC166467), OVOL1 (ProteinTech140821), Loricrin (Covance 145PAF62), Filaggrin (GTX 37695), K1 (Covance PRB160), K10 (Covance PRB159), p27 (BD610242), p16

(SC1661), p63 (Millipore4135), Sox-2 (Millipore4343), c-myb (Sigma SAB4501936), HDAC (CST 2062), Id2 (CST3431), OVOL2 (ThermoFisher PA541619), pMDM2 (CST 3521), cleaved PARP(CST9468), Bcl-2(SC 7382), Bcl-XL (SC1041), cleaved caspase 7 (CST9491), sestrin-2 (SC 393195), β -actin (BioLegend 643807) and Vinculin (CST139015).

2.3 RT-qPCR Analyses

Epidermal or primary keratinocyte RNA samples were isolated using TRIzol reagent (Invitrogen, Carlsbad, CA) according to the manufacturer's protocol. cDNA was then prepared using the High Capacity cDNA Reverse Transcription Kits (Applied Biosystems, Grand Island, NY) according to the manufacturer's protocol. For qRT-PCR analysis, 2 μ L of cDNA was mixed with 5 μ L of 2X iTaq universal SYBR green supermix (Bio-Rad, Hercules, CA), 1 μ L of 10 μ M forward primers, 1 μ L of 10 μ M reverse primers and 1 μ L of RNase-free water for a total volume of 10 μ L. qRT-PCR reactions were performed and analyzed on a Viia 7 (Applied Biosystems, Carlsbad, CA) using the comparative CT method and normalized to housekeeping gene 18S.

2.4 Histological and Immunohistochemical Analyses

The mice in the *in vivo* studies were injected with BrdU (100 μ g/g body weight) 30 minutes prior to sacrifice. A portion of the dorsal skin was excised and processed for H&E and BrdU staining to determine epidermal thickness and Labeling Index (LI) as previously described [21]. Other skin sections were kept for immunofluorescence staining of Ki67 (CST 9129),

OVOL1 (ProteinTech14082-1), Loricrin (Covance 145PAF62), Filaggrin (GTX 37695), Lgr5 (Bioss 1117R), Lgr6 (SC99123), and CD34 (Abcam 8158).

2.5 Flow cytometry Analyses

At 12, 24 and 48 hours post UVB exposure the primary keratinocytes from the *in vitro* Knockout of Twist1 with AdeCre model were harvested and stained for Annexin V and Propidium Iodide in triplicates for apoptosis and cell cycle analyses respectively in the Guava system. For the K15.Twist1 KO experiments, KSC were isolated and stained as described above. Cell sorting and isolation were performed on a BD LSR Fortessa flow cytometer equipped with the BD FACS Diva 6.0 software (BD Biosciences).

2.6 Statistical analyses

For the proliferation analyses counting histological positive staining, we compared triplicate means \pm SEM from control Twist1 WT vs. Twist1 KO groups using the Mann Whitney U test. This test was also used for the comparisons of cumulative counts of SCC and Sarcomas in the UVB carcinogenesis experiments. For the comparisons in the Kaplan-Meier survival curves we used the Mantel-Cox Chi square test. For the RT-qPCR analyses we used one-way ANOVA/Tukey's test. For flow cytometry histogram analyses we used using Welch's corrected unpaired t-test. Significance in all cases was set at * $p < 0.05$, ** $p < 0.005$, *** $p < 0.0005$, **** $p < 0.0001$.

CHAPTER 3. Deletion of Twist1 in Keratinocytes Induces Differentiation

3.1 INTRODUCTION

Epidermal homeostasis is maintained through a balance between proliferation and differentiation of keratinocytes in the hair follicle (HF) and in the supra basal layer of the interfollicular epidermis (IFE) [10]. The keratinocytes from the basal layer transiently migrate upward and become senescent as they repress proliferation regulators and induce expression of differentiation-associated proteins. These proteins have a structural function in the stratification of the supra basal layers of the epidermis [2]. As shown in Figure 1.1 in Chapter 1, the early differentiation markers Transglutaminases 1 and 3 and Keratins 1 and 10 dominate the spinous layer while, in the granular layer, terminal differentiation proteins Loricrin and Filaggrin aggregate keratin filaments and support the cornified layer [2, 14]. The epidermal basal layer is constantly replenished from multipotent keratinocyte stem cells (KSC) that reside in the HF bulge region and are also found at the base of epidermal proliferative units in the IFE [4].

In previous work from our laboratory, STAT3 was found to play an important role in skin carcinogenesis through its ability to regulate multiple keratinocyte growth properties, especially proliferation and differentiation [39-41]. In particular, STAT3 was found to play an important role in survival of bulge-region KSC during tumor initiation and also to control proliferation of initiated keratinocytes during tumor promotion [43, 92]. In additional studies, elevated STAT3 activity (using constitutively active form STAT3C) in basal keratinocytes *in vivo* led to depletion of hair follicle KSC along with a concomitant increase of stem/progenitor cells above the bulge

region [93, 94]. These latter studies indicated that STAT3 plays an important role in keratinocyte stem/progenitor cell homeostasis. Finally, targeting STAT3 in keratinocytes using STA-21 was found to induce differentiation markers *in vitro* [95].

During the course of studies in our laboratory, Twist1 was discovered to be a transcriptional target of STAT3 in keratinocytes [42, 43] confirming studies published from other laboratories using other cells and tissues [44-48]. Twist1 is a transcription factor that binds to E-BOX sequences to activate transcription of multiple signaling pathways involved in epithelial-mesenchymal transition (EMT) and tumor progression in multiple cancers [55]. Twist1 is overexpressed in many cancers including invasive squamous cell carcinomas (SCC) [56], and is a positive regulator of proliferative and metastatic signaling [56-58]. In more recent years, Twist1 has been reported to be involved in other oncogenic pathways regulating not only the invasiveness of tumors but also pathways contributing to earlier stages of tumorigenesis [62]. We recently reported that deleting Twist1 in basal keratinocytes of mouse epidermis resulted in arrested cell cycle progression (in response to TPA treatment) and inhibition of tumor formation in two-stage skin carcinogenesis experiments. Deletion of Twist1 in basal keratinocytes also led to reductions in the number of label-retaining cells and CD34⁺/a6 integrin⁺ cells in the bulge region [96]. More recent studies have shown that Twist1 plays an important role in maintaining stemness in a number of different tissue specific stem cell compartments [77, 78, 97-102].

In the work presented here, we have further examined the role of Twist1 in keratinocyte proliferation, differentiation and HF stem/progenitor cell behavior in mouse skin. Deletion of Twist1 in basal keratinocytes *in vivo* led to upregulation of epidermal differentiation markers

including TG1, K1, OVOL1, Loricrin and Filaggrin. In contrast, overexpression of Twist1 in cultured keratinocytes suppressed expression of calcium-induced differentiation markers. Deletion of Twist1 *in vivo* and in culture resulted in upregulation of cell cycle inhibitors indicating an arrested keratinocyte proliferation. Finally, deletion of Twist1 in epidermal and bulge region keratinocytes led to depletion of several hair follicle stem/progenitor markers, including CD34, Lrig1, Lgr5 and Lgr6. The current findings support the hypothesis that Twist1 is an important transcription factor in regulating the balance between proliferation and differentiation in keratinocytes and for maintaining HF stem/progenitor cell populations.

3.2 RESULTS

Twist1 deletion leads to decreased EMT downstream effectors and increased keratinocyte differentiation markers and proliferation inhibitors

Deletion of Twist1 in basal keratinocytes was achieved by crossing K5.Cre with Twist1^{fllox/fllox} mice (K5.Cre x Twist1^{fllox/fllox} mice) as previously described [96]. Deletion of Twist1 in epidermis was first established by RT-qPCR (Figure 3.1A) indicating a significant 55% reduction in mRNA level. The Twist1 KO was confirmed by IHC staining shown in Figure 3.1B, where Twist1 nuclear staining was reduced in the epidermal basal layer of K5.Cre x Twist1^{fllox/fllox} mice. As shown in Figure 3.2A-B, the achieved Twist1 KO (with 55-74% reductions in Western Blots) led to decreases in EMT downstream effectors including Bmi1, Slug, Zeb1, and Vimentin

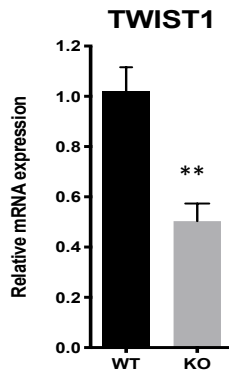
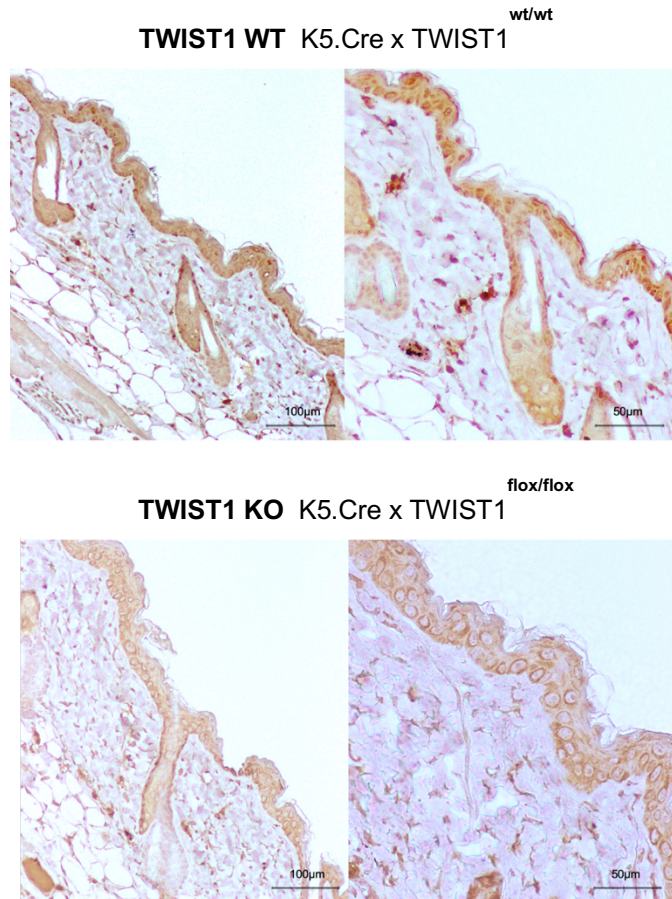
A**B**

Figure 3.1 Twist1 KO is confirmed in skin sections and in RNA from epidermal scrapings.

A. Quantification for RT-qPCR analysis of Twist1 mRNA from epidermal scrapings from both [K5-Cre^{+/-} x Twist1^{wt/wt}] and [K5-Cre x Twist1^{flox/flox}] mice. Values were calculated using Δ CCT method, normalized to the housekeeping gene GAPDH and quantified using mean \pm SEM from triplicates. Statistical analysis performed using Mann Whitney's Test **p>0.005. B. Skin sections from [K5-Cre^{+/-} x Twist1^{wt/wt}] and [K5-Cre^{+/-} x Twist1^{flox/flox}] mice stained for Twist1 immunohistochemical assessment showing decreased nuclear staining in the keratinocytes of the basal layer.

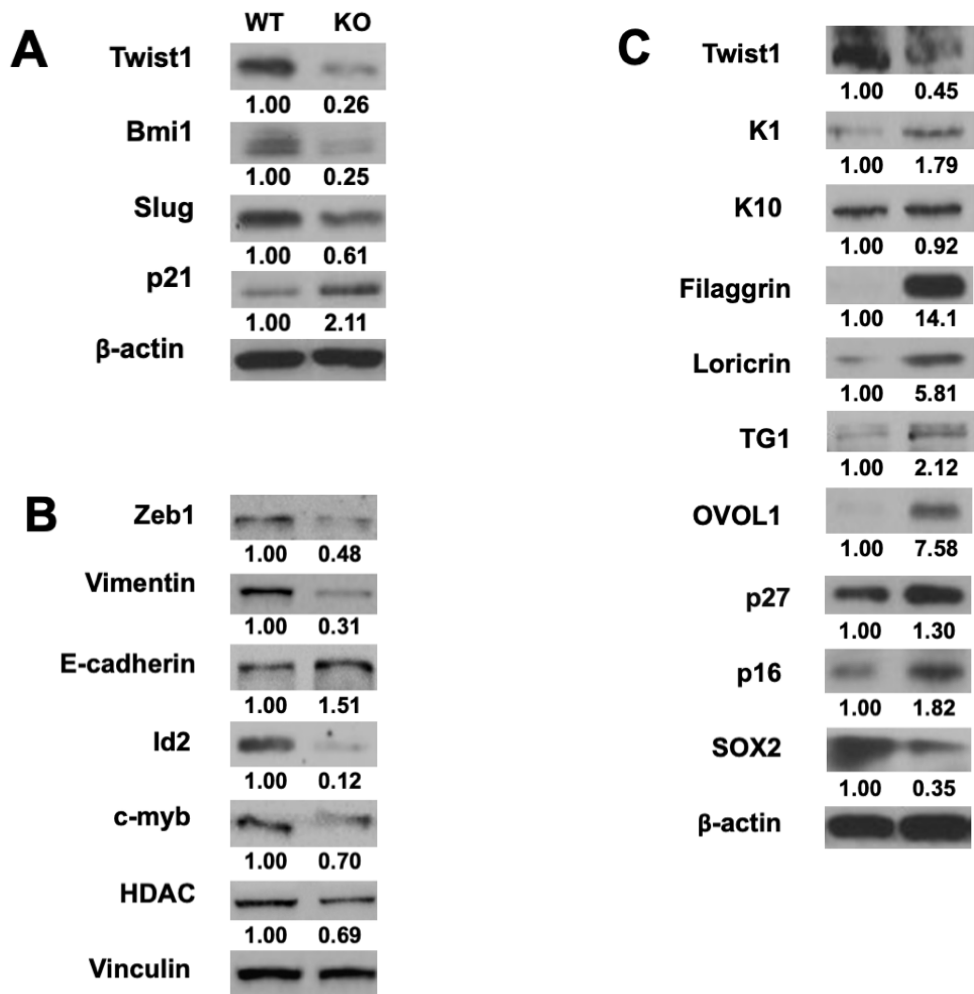


Figure 3.2 Twist1 deletion leads to decreased EMT downstream effectors and increased keratinocyte differentiation markers and proliferation inhibitors

Western blotting analysis of epidermal scrapings from K5-Cre^{+/-} x Twist1^{wt/wt} and K5-Cre^{+/-} x Twist1^{flox/flox} mice confirming A-B) decreases in Twist1 and altered downstream EMT targets and C) increases in proliferation inhibitors and differentiation markers. All values were normalized to respective β -Actin, Vinculin or GAPDH loading controls but a representative loading control for all samples originating from the same experiment was selected for display.

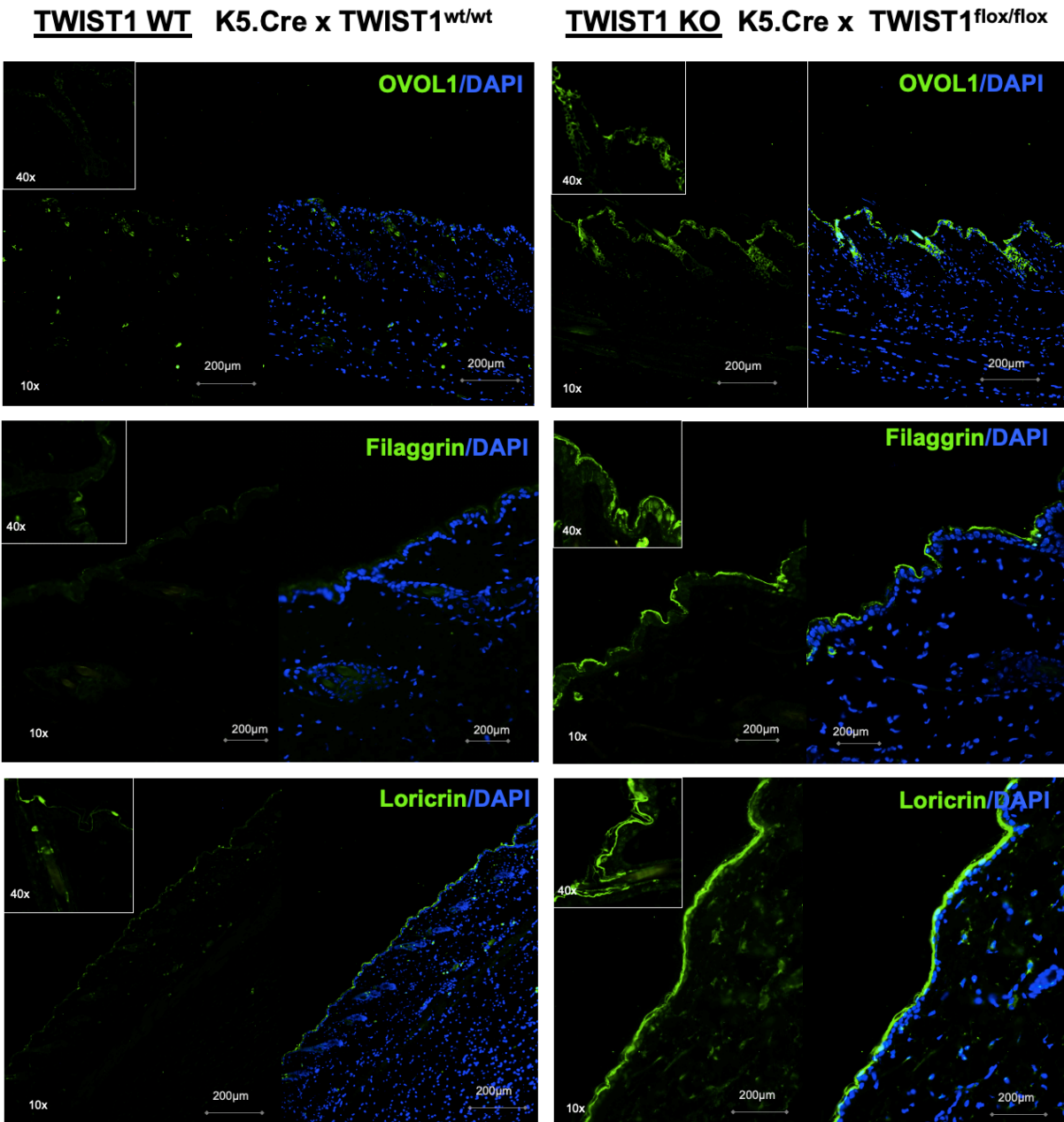


Figure 3.3 Twist1 deletion leads to increased differentiation markers in skin sections

Immunofluorescence staining of dorsal skin sections of both groups identifying differentiation markers (OVOL1, Filaggrin, and Loricrin) in the interfollicular epidermis (IFE).

along with increased levels of E-cadherin (0.25, 0.61, 0.48, 0.31, and 1.51 fold respectively) when compared to Twist1 WT epidermal lysates. Other transcription associated proteins that appeared inhibited were c-myc (30%), HDAC (31%), Id2 (88%), and SOX2 (65%). Additionally, increases in levels of proliferation inhibitors p16, p21 and p27, confirmed previous observations of arrested cell cycle. In Figure 3.2C, we present the findings in increased levels of differentiation related proteins in Twist1 KO epidermis. In this regard, deletion of Twist1 in basal keratinocytes led to increased protein levels of early differentiation markers including a 1.79 fold increase in Keratin 1 (K1) and a 2.12 fold in Transglutaminase-1 (TG1) with a robust increase in the late differentiation indicators Filaggrin (14.1 fold) and Loricrin (5.86 fold). Notably, the protein levels of OVOL1, a transcriptional regulator of Loricrin and Filaggrin [103] and potentiator of differentiation [104], were significantly higher (7.58 fold) in epidermis of Twist1 deficient mice compared to wild-type controls. The increases in OVOL1, Filaggrin, and Loricrin were further confirmed in skin sections by immunofluorescence (Figure 3.3).

TWIST1 overexpression led to inhibition of calcium-induced differentiation

In order to corroborate the induction of differentiation seen in the Twist1 deficient epidermis, we performed *in vitro* calcium-induced differentiation experiments using a DOX-inducible K5.rTA x tetO.Twist1 overexpression model. Compared to primary keratinocytes with normal Twist1 expression, the tetO.Twist1 keratinocytes failed to respond to an induction of terminal differentiation in culture conditions with high calcium concentrations (1.4mM) shown

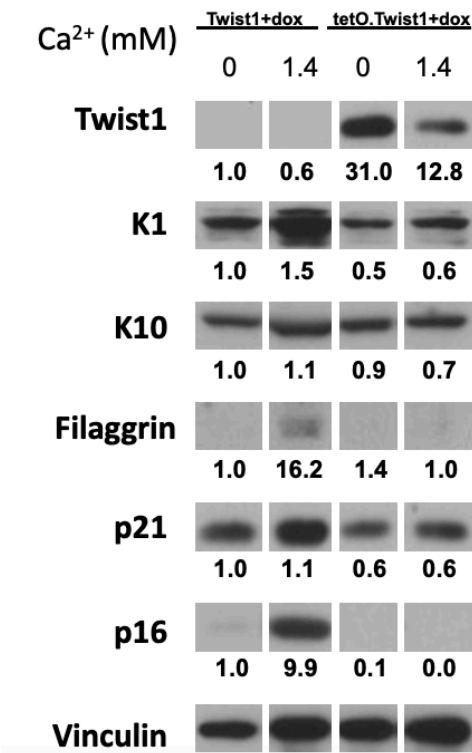
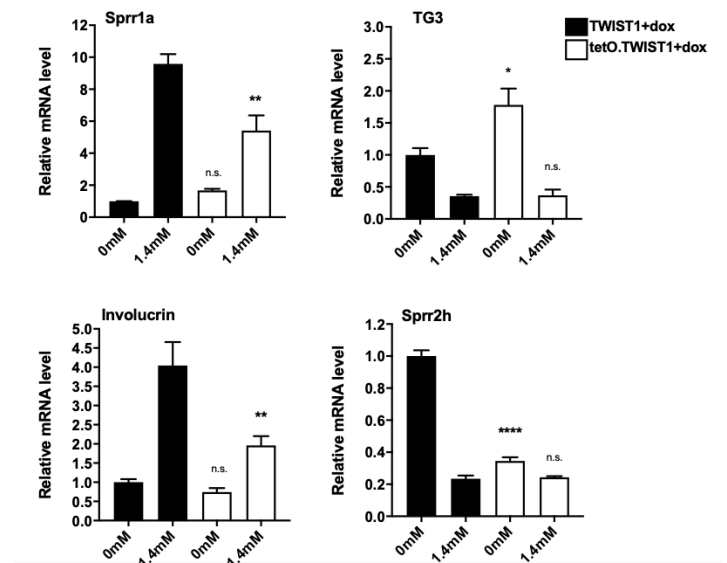
A**B**

Figure 3.4 Twist1 overexpression reverses effects of calcium-induced differentiation

A. Western blot analysis of differentiation markers using protein lysates from primary keratinocytes isolated from single transgenic [K5rTA] or double transgenic [K5rTA x tetO.Twist1] mice. Cells were treated with Doxycycline (1 μ g/mL) and Ca²⁺ (1.4mM) for 24 hours as indicated. Values were normalized to loading control Vinculin. B. mRNA levels of differentiation markers from primary keratinocytes treated as in A and assessed by RT-qPCR analysis. Values were calculated using Δ CCT method, normalized to the 18S and represent mean \pm SEM from triplicates. Statistical analysis performed using One-way ANOVA/Tukey's test *p<0.05.

by the comparably smaller increases in protein levels of K1 (1.5 vs 0.5 fold), K10 (1.1 vs 0.7 fold), Filaggrin (16.2 vs 1.0 fold) (Fig 3.4A). In Figure 3.4B, the mRNA levels of differentiation targets like Involucrin and Sprr1a were significantly decreased in the Twist1 overexpressing keratinocytes (One-way ANOVA/Tukey's test $**p < 0.005$). Interestingly, where the calcium treatment did not show significant differences, the Twist1 overexpression by itself did, as shown by the basal increments in Transglutaminase-3 (TG3) and reduction of Sprr2h (Fig 3.4B). Complementarily, the calcium-induced increase in protein levels of p21 and p16 did not occur as robustly in the Twist1 overexpressing keratinocytes as it did in the Twist1 wild-type keratinocytes (1.0 vs 0.6 and 9.9 vs 0.0, respectively) (Fig3.4A).

Keratinocyte and bulge region specific Twist1 deletion led to depletion of several HF stem/progenitor markers

Further analyses of skin sections from the keratinocyte specific Twist1 KO [K5.Cre^{-/-} x Twist1^{flox/flox}] mice showed decreased immunofluorescence staining for stem/progenitor markers in HF including CD34, Lgr5, and Lgr6 (Fig3.5). With the goal of mapping the fate of the Twist1 deficient KSC, we used K15.CrePR1^{+/-} x Twist1^{flox/flox} mice and control littermates. Dorsal skins were isolated from mice following 5-day treatment with 2mg RU486 and subjected to immunofluorescence staining analyses. As shown in Figure 3.6, Twist1 deletion induced after 5 days of RU486 topical treatment directly affected the stem-like characteristics of the K15(+) KSC niche. Specifically, the same markers from Figure 3.5 appeared decreased or displaced upward from in skin sections from bulge region specific inducible K15 Twist1 KO mice.

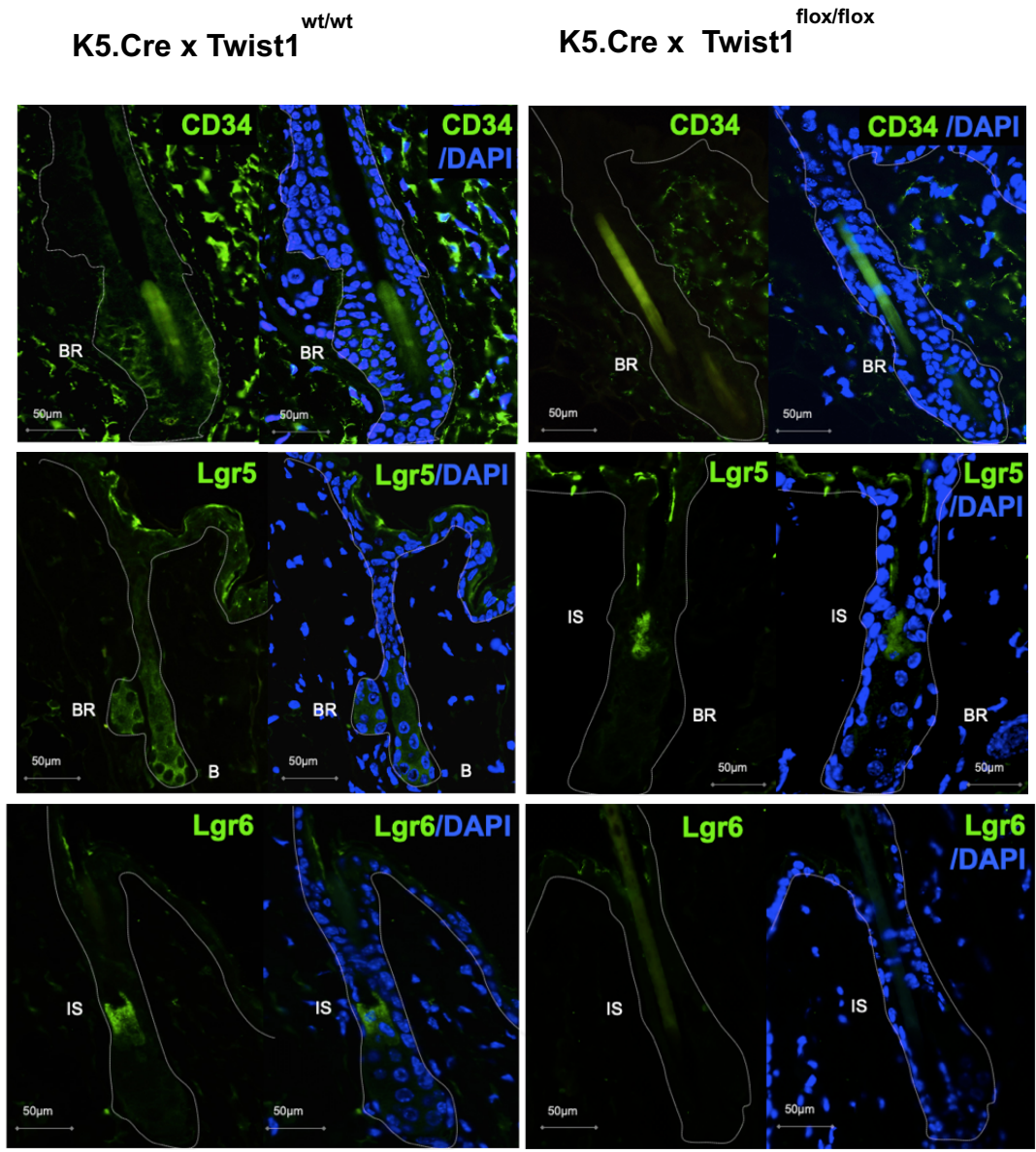


Figure 3.5 Twist1 KO in basal keratinocytes alters expression of stem/progenitor cell markers in vivo

Immunofluorescence staining of dorsal skin sections from K5-Cre x Twist1^{wt/wt} and K5-Cre x Twist1^{flox/flox} mice for CD34, Lgr5 and Lgr6 in hair follicles.

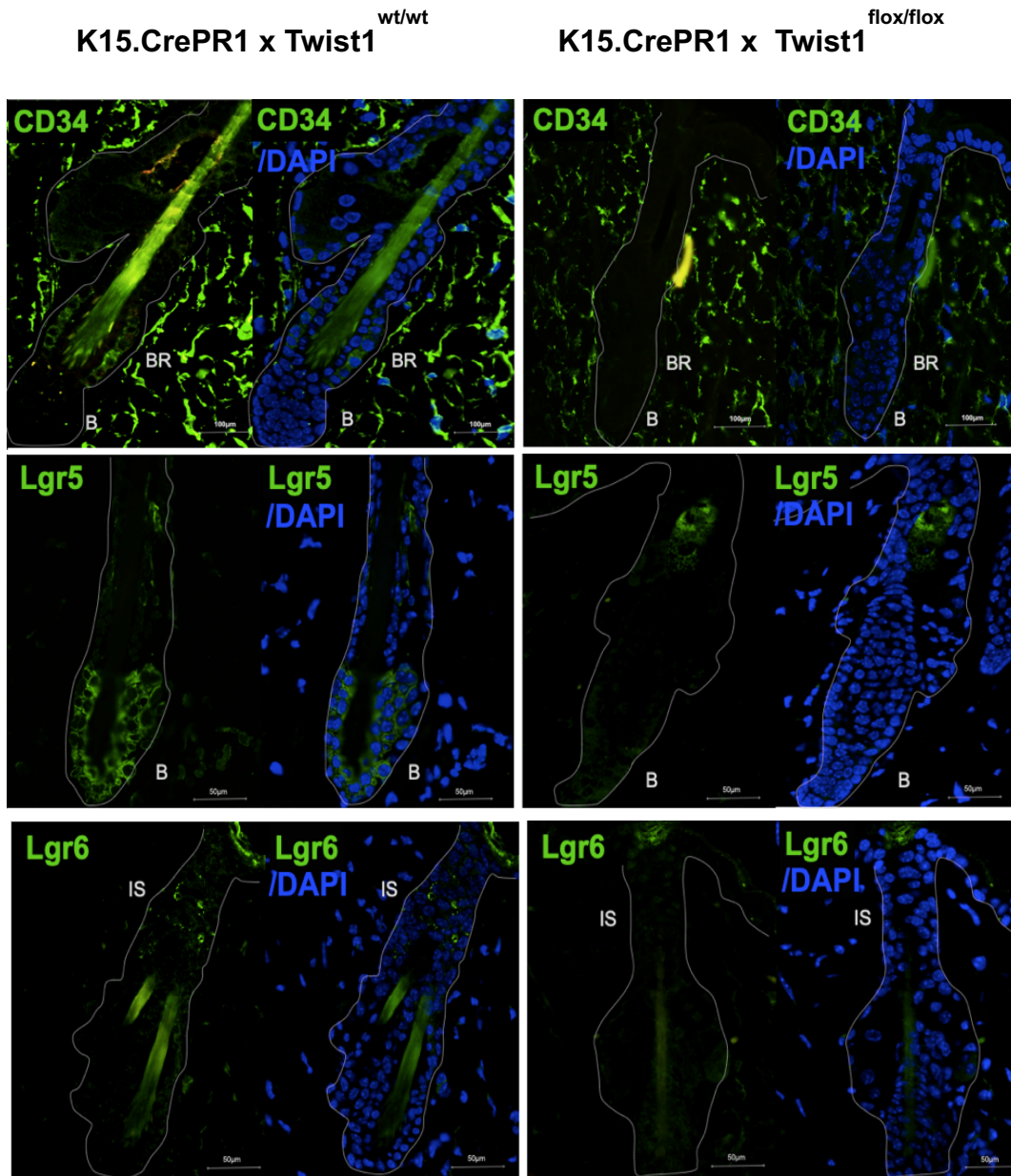


Figure 3.6 *Twist1* KO in *K15* positive bulge region keratinocytes alters expression of stem/progenitor cell markers *in vivo*.

Skin sections from *K15.CrePR1 x Twist1^{wt/wt}* and *K15.CrePR1 x Twist1^{flox/flox}* mice treated with RU486 showing staining for CD34, Lgr5 and Lgr6 in hair follicles. Bulge Region (BR) and Bulb (B).

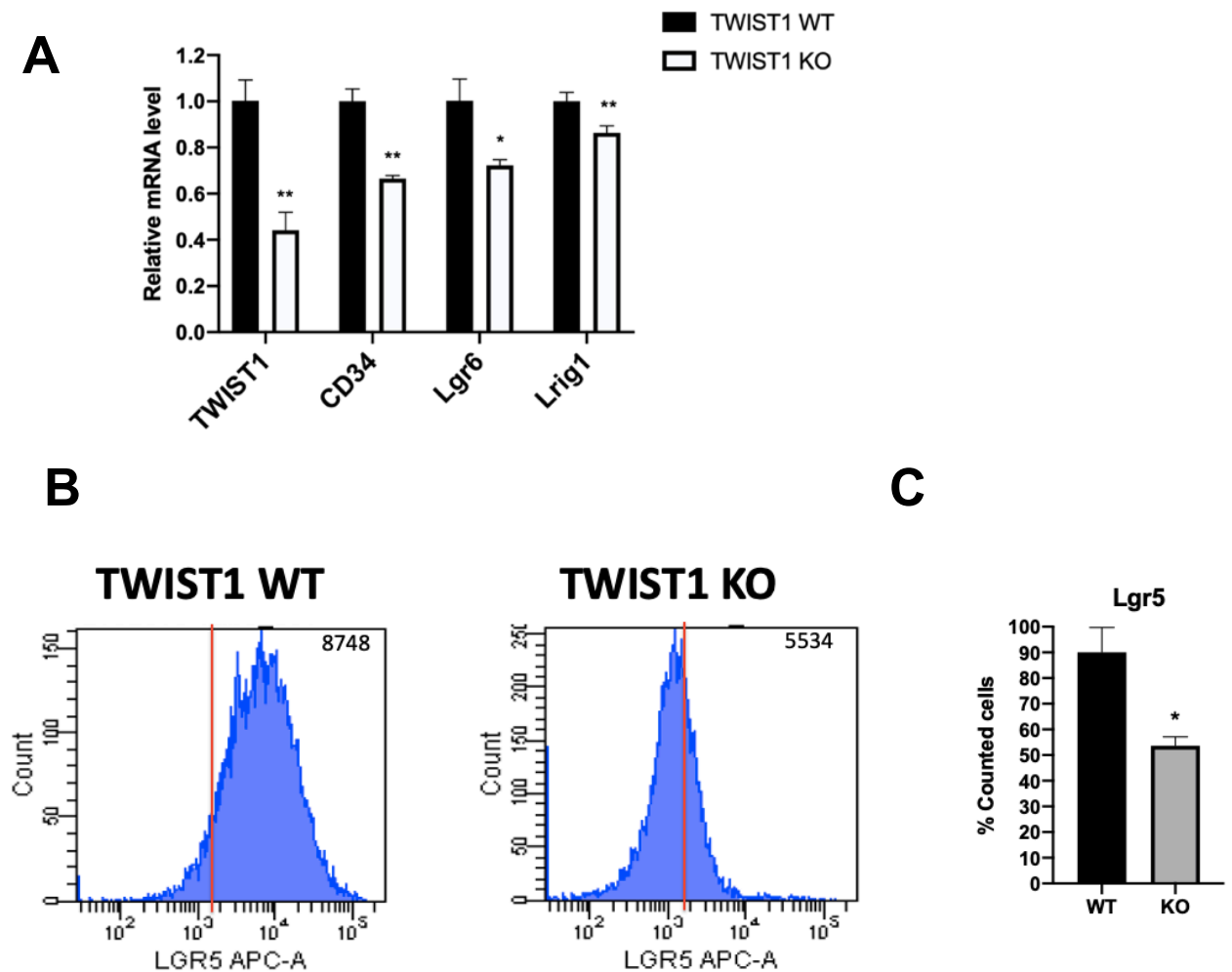
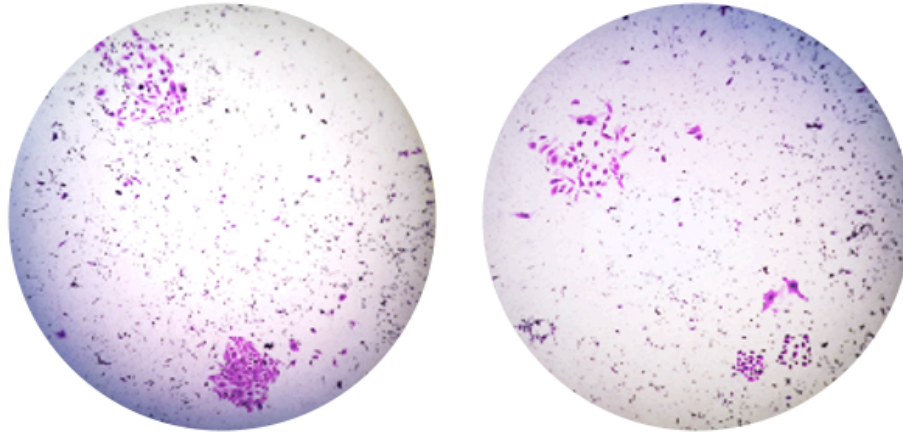


Figure 3.7 Deletion of Twist1 in KSC results in decreased stem markers.

A. mRNA from KSC from [K15.CrePR1 x *Twist1*^{wt/wt}] and [K15.CrePR1 x *Twist1*^{fllox/fllox}] mice was isolated for RT-qPCR analysis. Values were calculated using Δ CCT method, normalized to the housekeeping gene 18S and quantified using mean \pm SEM from triplicates. Statistical analysis performed using Welch's t-test * $p < 0.05$, ** $p > 0.005$. B. KSC were analyzed through a Fortessa flow cytometer for Lgr5-APC. C. Histograms of positive counts in 10,000 events were quantified using mean \pm SEM from triplicates. Statistical analysis performed using Welch's corrected unpaired t-test * $p < 0.05$.

TWIST1 WT



TWIST1 KO

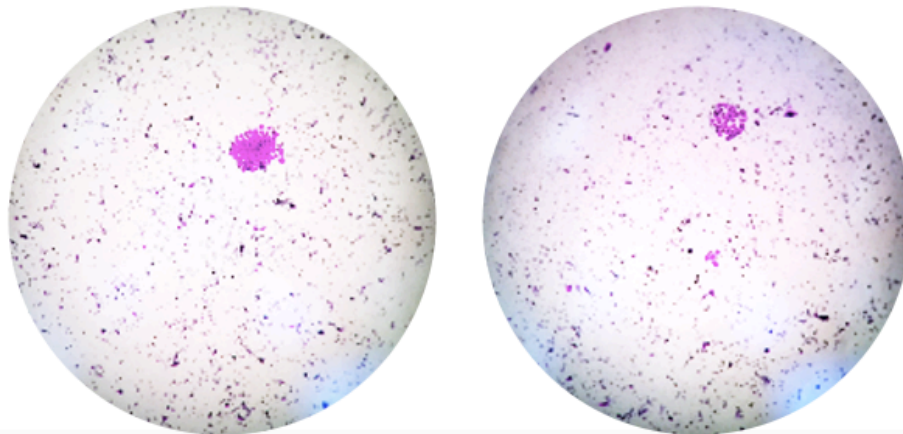


Figure 3.8 Deletion of Twist1 in KSC results in impaired clonogenicity

Isolated KSC from K15.CrePR1 x Twist1^{wt/wt} and K15.CrePR1 x Twist1^{flox/flox} mice treated with RU486 were plated on a feeder layer of 2.5×10^6 3T3 cells under standard incubation conditions for 3 weeks. The K15.Twist1KO KSC formed less paraclones that were also densely packed compared to WT.

Deletion of Twist1 in KSC results in inhibition of colony formation efficiency and decreased stem markers

The isolation of primary KSC allowed the characterization of these migration effects by quantifying mRNA levels and via single cell staining of stemness markers using flow cytometry. As shown in Figure 3.7A. RT-qPCR analysis performed with RNA extracted from isolated KSC corroborated the decrease in Lgr6 levels as well as levels of Lrig1 and CD34 in the K15.Twist1 KO mice. The flow cytometry analysis in Figure 3.7B showed that the KSC with Twist1 deletion showed a robust reduction in the Lgr5-positive population by half (16 %to 7.5 %) according to the FACS analysis and quantification (Figure 3.7C). Moreover, when plating the KSC on a feeder layer of 3T3 cells as described in published protocols [94, 105, 106], we found that the Twist1 KO specific for this K15 positive niche, resulted in reduced clonogenicity as shown by the decreased density of free forming holoclones in Figure 3.8.

3.3 DISCUSSION

Twist1 KO in epidermis resulted in induction of late differentiation markers, particularly Loricrin and Filaggrin (Fig 3.2 and 3.3), which was rescued in our inducible Twist1 overexpression model (Fig3.4). Of particular interest to us were the observed increases in OVOL1 expression in epidermal samples and skin sections of Twist1 KO mice (Fig 3.2 and 3.3). OVOL1 is a transcription factor that is known to regulate keratinocyte differentiation and stemness [103, 104, 107]. In this regard, OVOL1 has been identified as an inducer of terminal

differentiation and negative regulator of the progenitor cell state in the interfollicular epidermis and in the hair follicle [103, 104]. The migration of keratinocytes to the suprabasal layers in the terminal differentiation program can be traced by compartment specific markers K1 and K10 (early stage) and Loricrin and Filaggrin (latest stage) [14]. As a potentiator of terminal differentiation, OVOL1 is known to directly activate transcription of Loricrin and Filaggrin [108-110]. The growth inhibitory functions of OVOL1 have been associated with its negative regulation of c-Myc and Id2 [108]. Id2 is considered a dominant-negative antagonist of basic helix-loop-helix transcription factors and is a direct transcriptional target of c-Myc [111]. Moreover, OVOL1 binding motifs are found in regulatory regions of Zeb1, Vimentin and Snai2 genes, making OVOL1 also an inhibitor of key EMT pathway proteins [112-114]. Accordingly, knockdown of OVOL1/OVOL2 in an SCC model showed increased mRNA and protein levels of Zeb1 [115].

As seen in our results, Twist1 KO also resulted in downregulation of c-myb1 and HDAC (Fig 3.2B), which are both needed in the competitive OVOL1 self-repression mechanism reported previously [116]. This represents an interesting potential mechanism that compels future examination by which Twist1 may regulate OVOL1 expression. Supporting this hypothesis is the fact that other groups have reported a regulatory link between Twist1 and c-myb. Kulkeaw *et al* published CHIP analysis results suggesting that Twist1 directly regulates transcription of c-myb [117]. Microarray analysis and RT-qPCR further showed downregulated expression of c-myb transcripts in Twist1 knockout cells, likely due to an E-box located at transcriptional start site of c-myb which is the knowingly bound by Twist1 [117]. The lack of activation of the c-myb promoter in Twist1 deficient epidermis results in decreases of c-myb protein that would

otherwise compete with OVOL1 on the binding of its own promoter to repress it. Thus, OVOL1 potentially goes unrepressed and accumulated in the basal layer activating differentiation markers. Future experiments testing the association of c-myb and HDAC to the OVOL1 promoter in Twist1 deficient models will help resolve this line of inquiry.

Additionally, OVOL1 may also play a role in the effects seen in stem/progenitor behavioral changes induced by Twist1 deficiency. It has been reported that OVOL2 overexpression reduces epidermal stem/progenitor cell population as shown by reduced K15-positive cells in both epidermis and HF bulge and decreased stem-like markers like p63 [114]. In Figures 3.5 and 3.6, we have confirmed that skin sections from both K5 and K15 conditional Twist1 KO mice showed decreased immunofluorescence staining of stem/progenitor markers CD34, Lgr5 and Lgr6. Accordingly, we found significantly decreased basal protein expression of stem marker Sox2 in Twist1 KO epidermis (Fig 3.2C).

As stated above, when assessing Twist1 deficiency in bulge region KSC (using K15.Twist1 KO mice) we found decreases in Lgr6 and Lgr5 immunofluorescence staining, which were further confirmed with a significant reduction in the Lgr5+ KSC population consistent with our previous findings in basal keratinocytes. The mRNA analysis also corroborated the decrease in Lgr6, Lrig1 and CD34 expression in the Twist1 deficient KSC. Correspondingly, Twist1 deletion in KSC inhibited colony formation efficiency which demonstrates that Twist1 has a direct role in maintaining homeostatic self-renewal in the HF. Overall, the findings of these studies demonstrate that Twist1 is an important regulator of the stem/progenitor niche by controlling the differentiation fate of KSC in the bulge region and in the interfollicular epidermis.

The results suggest that Twist1 deletion may reduce the size of the target population for UVB skin carcinogenesis by driving KSC to a more differentiated state. Future studies with Twist1 KO mice exposure to UVB will be needed to confirm that Twist1 regulates proliferation of these KSC during UVB skin carcinogenesis.

CHAPTER 4. Deletion of Twist1 Increases Apoptosis and Reduces UVB-induced Proliferation and Tumorigenesis

4.1 INTRODUCTION

Nonmelanoma skin cancer (NMSC) is the most common cancer [118, 119] and can be divided into two subtypes, squamous and basal cell carcinomas (SCC, BCC), depending on the cell type they originate from in the skin and the degree of dermal invasion. SCC and BCC together have one of the highest rising incidences in the United States with over 5 million diagnoses every year [23]. Although BCC is more common, SCC metastases account for up to 20% of all deaths from skin cancer [120]. Solar ultraviolet radiation (hereafter referred to as UV) is the major risk factor for the development of both BCC and SCC. UVA (320-400 nm) and UVB (280-320nm) both function as initiators and promoters in carcinogenesis and possess immunosuppressive activity [reviewed in 121]. Continuous UVB exposure to epidermal keratinocytes results in deregulation of protein expression and activation of proliferative and survival signaling pathways that contribute to the initiation of tumorigenesis and ultimately skin tumor development [33, 122]. In fact, both UVB and UVA damage DNA in the keratinocytes leading to mutations in hallmark tumor suppressor p53 [123]. Multiple researches in the field have determined that childhood exposure and/or intense intermittent UV exposure are major risk factors for BCC whereas chronic cumulative UV exposure is associated with the development of SCC [124]. Given the prevalence, as well as the social and economic burden of this disease, there remains a pressing need for the development of novel prevention and treatment strategies for NMSC [118, 125-127].

Actinic keratoses (AK) or solar keratoses are premalignant skin lesions with the potential to develop into cutaneous SCC (cSCC). Although these lesions can be found anywhere on the body, they are typically located on sun-exposed areas such as the face, neck, and extremities. In AK, activation or upregulation of Ras, Fyn/Src and Bcl2 coupled with p53 mutations have been identified [30, 128]. These changes coupled with suppression of the cutaneous immune response through inhibiting the ability of Langerhans cells to present antigen to helper TH1 lymphocytes result in the development of AKs. It is important to effectively treat AK given their potential to develop into SCC [30]. In this regard, in a study of 169 people, 65% of SCCs occurred from AK [129]. This was further confirmed by Hurwitz *et al* who found 444 of 459 (97%) subjects had contiguous AK near the site of their SCC [130]. Given the prevalence of AK and the subsequent high risk of malignant conversion of these lesions to SCCs, development of novel strategies to treat these premalignant lesions and prevent their progression could have a significant benefit. The currently approved treatments for AK include, cryosurgery and other surgical methods, topical treatment with 5-fluorouracil, diclofenac sodium, imiquimod or ingenol mebutate as well as photodynamic therapy [30, 131]. The current topical agents used to treat AK have significant negative features, including irritation, decreased quality of life, and limited efficacy.

In recent years, Twist1 has been reported to be involved in other oncogenic pathways regulating not only the EMT-supported invasiveness of tumors but also pathways contributing to earlier stages of tumorigenesis [62]. Several groups have also suggested that Twist1 may also have a role in proliferation of cancer cells [132, 133]. Additional publications suggest that Twist1 expression may signal for evasion of apoptosis, highlighting the importance of future studies probing the mechanisms with which Twist1 regulates cell proliferation [134].

In previous results, deletion of Twist1 in skin led to arrested cell cycle progression by the stabilization of p53 in response to TPA treatment, which in turn stimulated apoptosis and prevented growth of chemically-induced tumors [96]. Other groups also corroborated that Twist1 is an inhibitor of apoptosis in other tissues, proposing different mechanisms to explain its role in activation of oncogenic proliferation [134, 135]. Beck *et al* confirmed that Twist1 prevents apoptosis by promoting Mdm2-mediated p53 degradation and showed that deletion of p53 in Twist1-deficient cells rescued the apoptosis but not the proliferation phenotype, concluding that Twist1 promotes tumor cell proliferation independently of p53 [56]. Based on our preliminary and published data, as well as data from other laboratories, we hypothesized that Twist1 deletion will significantly inhibit UV-induced skin carcinogenesis and that overexpression of Twist1 will enhance UV-induced skin carcinogenesis. The effects of Twist1 on skin carcinogenesis may involve effects on proliferation and differentiation of target cells early during the carcinogenic process as well as effects during progression of SCC via stimulation of EMT.

The evidence presented in Chapter 2 demonstrates that Twist1 controls the differentiation of keratinocytes in the bulge region and in the IFE. However, the impact that the Twist1 deletion specifically in keratinocytes has on UVB-induced skin carcinogenesis, has not yet been clarified. In the work presented here, we have examined the role of Twist1 in UVB induced keratinocyte apoptosis and proliferation. Twist1 deletion led to reduced hyperproliferation induced by UVB *in vivo*. Moreover, our *in vitro* studies corroborated an arrest in cell cycle paired with a sensitization to UVB-induced apoptosis caused by Twist1 deficiency.

Furthermore, the development of UVB-induced SCC was significantly reduced in Twist1 KO mice compared to the wild-type controls. These results demonstrate that Twist1 regulates both proliferation and apoptosis in the overall tumorigenic response to UVB exposure.

4.2 RESULTS

Twist1 deletion leads to reduced keratinocyte survival following UVB exposure

As shown in Figure 4.1, deletion of Twist1 led to increased sensitivity to UVB induced apoptosis. For these experiments, primary keratinocytes with Twist1 deletion were exposed to UVB and then collected at 24 hours. The primary keratinocytes were obtained from Twist1^{fl^{ox}/fl^{ox}} mice and then treated with CMV AdeCre Recombinase (5MOI) for 5 hours. After 24 hours of having confirmed successful infection efficiency with GFP (data not shown), the cells were exposed to UVB radiation (20-25mJ/cm²). The cells were harvested 12 hours after and then subjected to flow cytometry analysis of Annexin V staining. As shown by the increases in keratinocytes in the lower right quadrant of the Figure 4.1, the Twist1 deletion sensitized the cells to UVB-induced apoptosis. Panel B of Figure 4.1 shows the quantitation of Annexin V staining that confirms the apoptotic increase in Twist1 KO conditions after single UVB treatment. The increase in Annexin V staining in the Twist1 deficient keratinocytes was highly significant (p=0.004). The observation of an increase apoptotic population data is consistent with the results in the cell cycle analysis using Propidium Iodide described below that also showed an increased sub-G1 phase following UVB exposure in the Twist1 deficient keratinocytes (Fig4.2).

In vitro Twist1 deletion leads to alterations in cell cycle

The Propidium Iodide staining for cell cycle was performed by following manufacturer's protocols. The Twist1 deficient keratinocytes were generated in the same manner as described above (using AdeCre on Twist1^{flox/flox} primary keratinocytes). Once analyzed in the FACS-Aria flow cytometer, DNA content was quantified to allow identification of four different cell cycle phase populations: subG1, G1, S, G2/M. As seen in Figure 4.2, the Twist1 deficiency *in vitro* alone resulted in significantly increased subG1, increased G1 and decreased G2/M phases compared to the keratinocytes treated with an empty viral vector (i.e. Twist1 WT) . After a single UVB exposure of 25mJ/cm², the Twist1 KO cells showed sensitization to UVB-induced cell death as seen in the increased subG1 population. Moreover, the Twist1 KO cells showed a significant indication of arrested UVB-induced mitosis as seen by the decreases in both G1 and G2/M populations.

Twist1 deletion in primary keratinocytes leads to altered levels of apoptotic regulators

Protein lysates were obtained from the primary keratinocytes with Twist1 deletion referred to above for Western Blot analyses of cell survival and apoptosis related proteins. The primary keratinocytes were treated with 20mJ/cm² of UVB and harvested at 3, 6 and 9 hours. As shown in Figure 4.3, the adenoviral treatment of Cre recombinase on the primary keratinocytes from Twist1^{flox/flox} mice resulted in successful reduction of Twist1 yielding almost undetectable protein levels. Likewise, the levels of the downstream targets Slug and Snail were also fully depleted. When comparing to the UVB-treated wild-type control, the primary keratinocytes with

Twist1 KO showed robust increases in protein levels of apoptotic markers including cleaved PARP (2.2 vs 5.4 fold), active caspase 7 (0.7 vs 84 fold) and sestrin-2 (7.3 vs 15 fold) after a single UVB treatment. These changes were particularly evident at the later time point (9 hours) following UVB irradiation. In addition, altered levels of Bcl-XL and Bcl-2 were recorded and understood as further indication of altered apoptosis (Fig 4.3).

Twist1 deletion leads to alterations in protein levels of cell cycle regulators

As seen in Chapter 3, the deletion of Twist1 *in vivo* in skin keratinocytes led to increased basal protein levels of cell cycle inhibitors p21 (2.79 fold), p27 (1.37 fold) and p16 (1.98 fold). Our Twist1 KO *in vitro* system showed that levels of p21 were also elevated in the Twist1 KO keratinocytes without UVB exposure. When comparing to the Twist1 WT group (Ad5-empty) at the 9 hours time point, the Twist1 KO in primary keratinocytes led to upregulation of UVB-induced levels of p21 (1.4 vs 5.1 fold). Interestingly, this *in vitro* system also corroborated the *in vivo* reduction in Cyclin B1 and p-cdk1 without UVB (Fig 4.3). Lastly, an early decrease in pMDM2 (2 fold at 3 hours) complemented the concomitant increase of p53 levels (1.6 vs 6.3 fold).

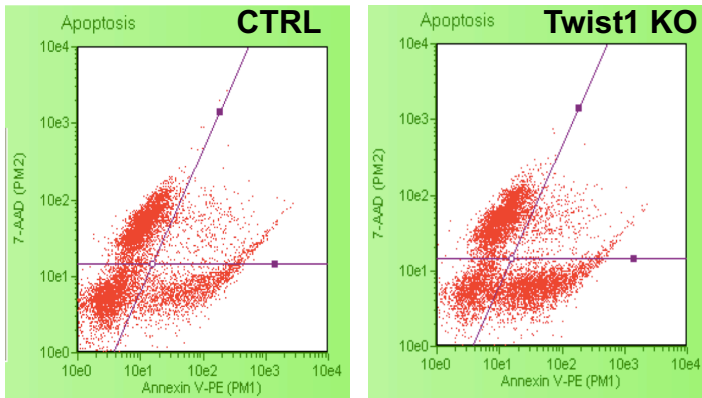
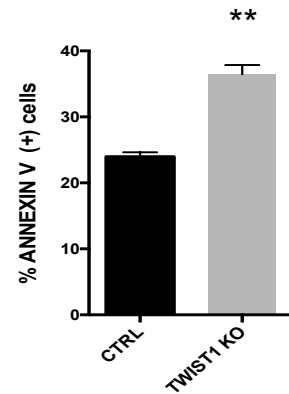
A**B**

Figure 4.1 Twist1 deletion leads to reduced keratinocyte survival following UVB exposure.

A. Dot plot for Annexin V v.s 7-AAD staining from Guava Nexin flow cytometry. Lower right quadrant indicates increased population of Annexin V positive TWIST1 KO primary keratinocytes undergoing apoptosis. B. Quantification of plots using Mann Whitney U test (mean \pm SEM n=4 **p=0.029)

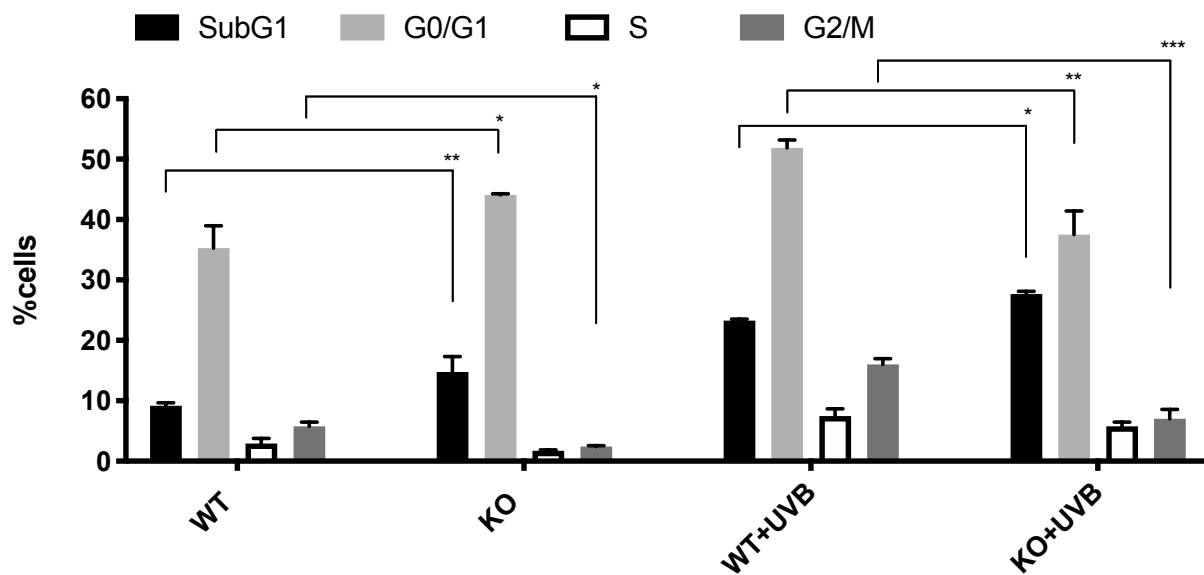


Figure 4.2 In vitro Twist1 deletion leads to alterations in cell cycle.

Quantification of SubG1, G1, S and G2/M phase populations from cell cycle analysis histograms using mean \pm SEM. from histograms for cell cycle analysis from FACS Aria flow cytometer. Each group result is representative of 3 replicates. Statistical analyses performed included One-way ordinary ANOVA and Tukey's comparison test of the KO groups vs the WT groups with or without UVB * $p < 0.05$, ** $p < 0.005$, *** $p < 0.0005$.

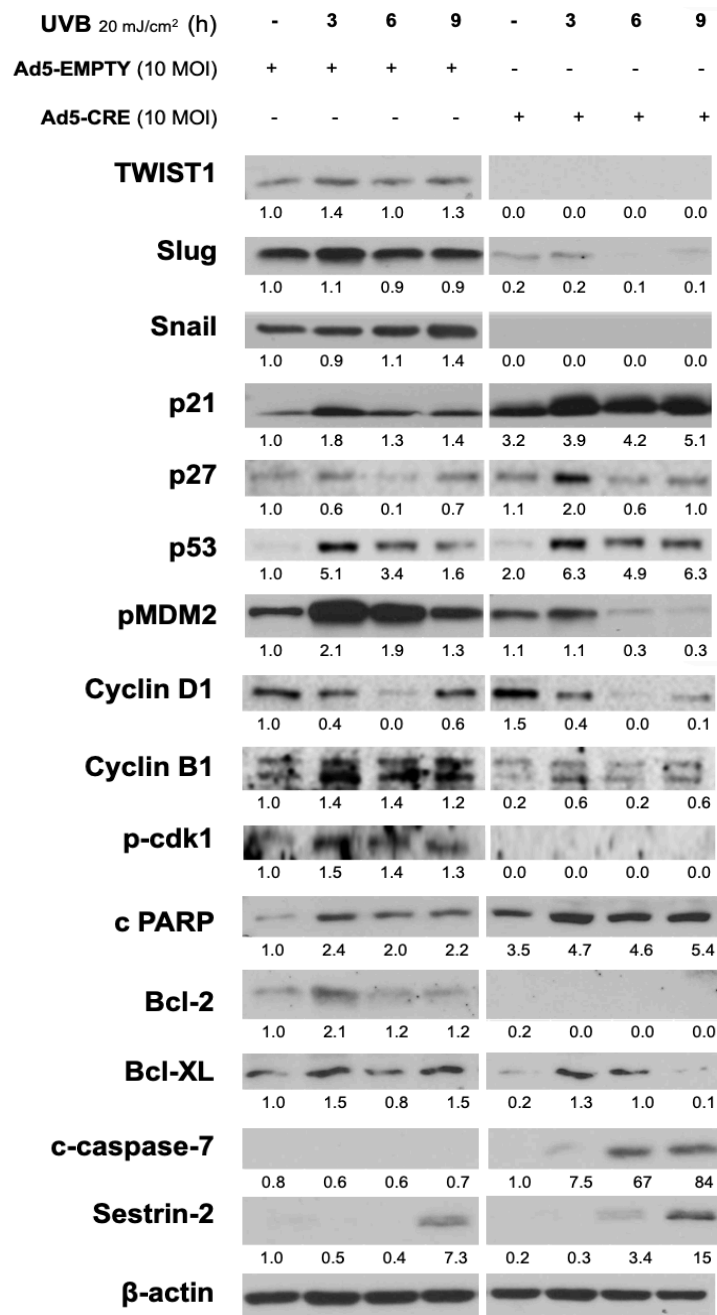


Figure 4.3 Twist1 deletion in primary keratinocytes leads to altered levels of apoptotic and cell cycle regulators.

Western Blot for in vitro treatment of 20mJ/cm² of UVB at 3, 6 and 9 hours on Ad5-Cre or Ad5-Empty treated primary keratinocytes from TWIST1flox/flox mice (10MOI). Densitometric quantification for protein targets using values normalized to β-actin.

Twist1 deletion in keratinocytes in vivo leads to altered levels of cell cycle regulatory proteins following UVB exposure

In the Western Blot analysis shown in Figure 4.4, we show changes in cell cycle regulators at 48 and 72 hours after 300mJ/cm² of UVB. The untreated control showed a 50% decrease in Twist1 protein levels along with significant increases in protein levels of p53 (2.3 fold) and p21 (5.4 fold). Importantly, levels of p-cdk1 (0.3 fold) and E2F1 (0.4 fold) were reduced after Twist1 deficiency without UVB exposure. At the 48 hours time point after UVB, the Twist1 KO epidermis showed dramatically increased levels of p21 (10.7 fold) together with reductions in cyclins D1 (0.7 fold), B1 (0.7 fold), cdk4 (0.3 fold), p-cdk1 (0.2 fold), and E2F1 (0.3 fold). After 72 hours of UVB radiation, increases in p53 were higher than the wild-type control (6.5 fold) while levels of cyclin B1 and p-cdk1 were almost fully depleted in the Twist1 deficient epidermis.

Twist1 deletion decreases keratinocyte hyperproliferation in vivo after acute UVB treatment

For these experiments, K5.Twist1 WT and KO mice were exposed to 300mJ/cm² of UVB and dorsal skin sections were harvested at 48 hours after UVB. Skin sections were processed for IF and IHC as previously described [40, 92]. As shown in Figure 4.5, deletion of Twist1 in epidermal keratinocytes of K5.Cre x Twist1^{lox/lox} mice led to a significant inhibition of epidermal proliferation at 48 h after exposure to UVB. The keratinocyte specific deletion of Twist1 in the K5.Twist1 KO mice led to inhibition of UVB-induced increases in epidermal thickness as well as epidermal hyperproliferation compared to wild-type mice. In this regard, proliferation analysis by both Ki67 immunofluorescence staining as well as BrdU incorporation and staining showed a

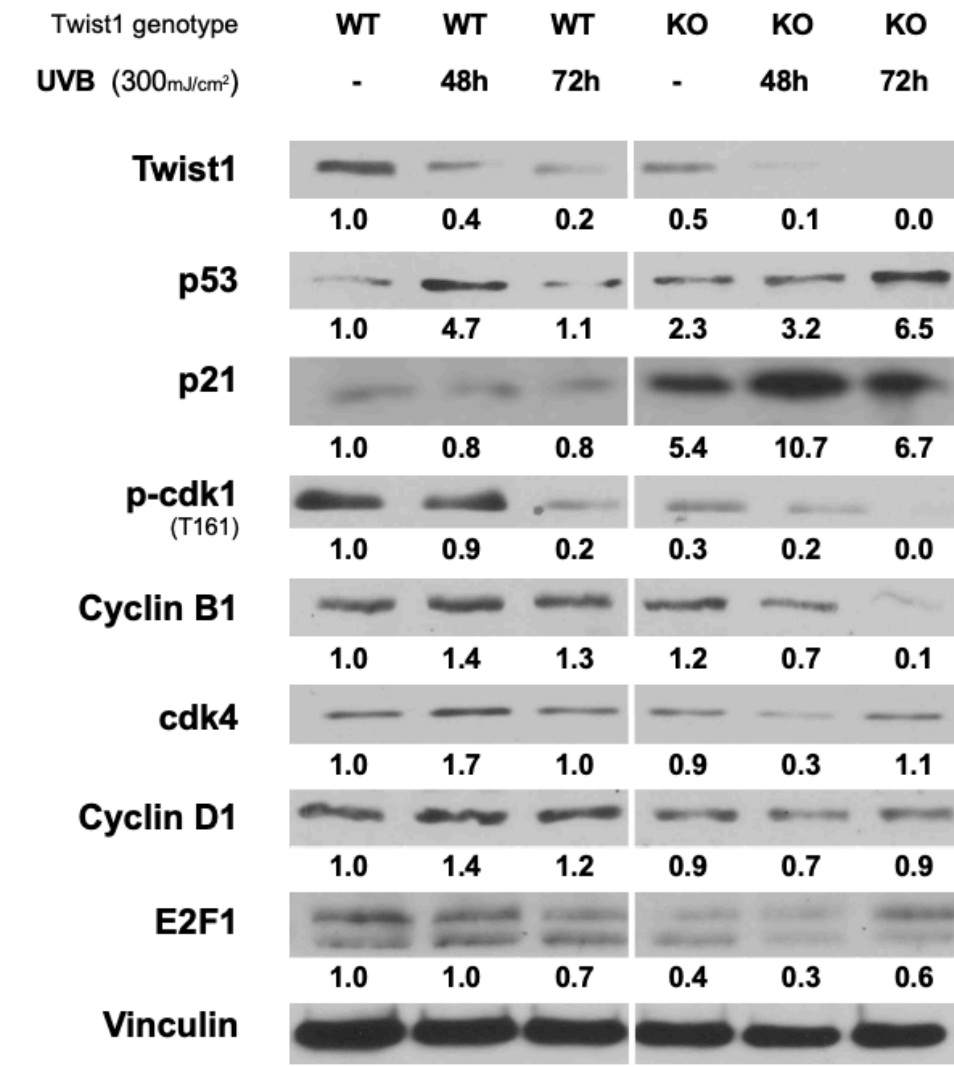


Figure 4.4 Twist1 deletion in keratinocytes in vivo leads to altered levels of cell cycle regulatory proteins following UVB exposure.

Western blotting analysis of proliferation regulators using protein lysates obtained from epidermal scrapings from both [K5-Cre^{+/-} x Twist1^{wt/wt}] and [K5-Cre x Twist1^{flox/flox}] mice treated with 300mJ/cm² of UVB and harvested at 48 and 72 hours. Values were normalized to loading control Vinculin.

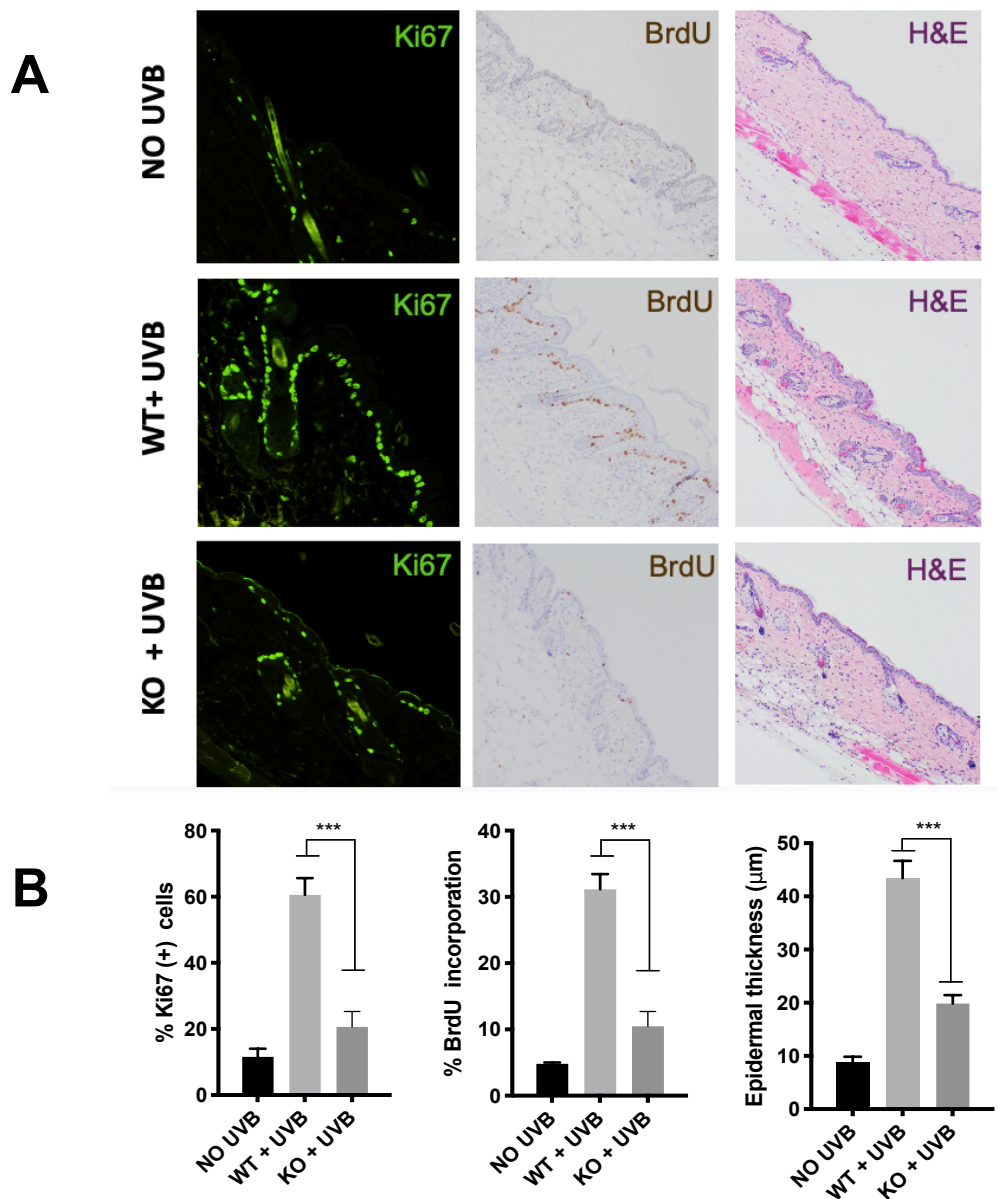


Figure 4.5 Twist1 deletion decreases UVB-induced epidermal thickness, BrdU incorporation and Ki67 staining.

A. IF staining of Ki67, IHC staining of BrdU and H&E staining of dorsal skin sections from Control and K5.Cre x Twist1^{flox/flox} mice treated with 300mJ/cm² of UVB and harvested at 48 hours. B. Quantification of positive staining in 500 cells per section presented as means \pm SEM of 4 sections per treatment group. Quantification of epidermal thickness (mean \pm SEM) of triplicate measurements for 6 H&E stained sections per group. * $p < 0.05$, *** $p < 0.0005$, Mann Whitney U tests.

significant decrease in Twist1 KO epidermis compared to wild-type epidermis (Fig 4.5). Quantitation of epidermal thickness and both Ki67 and BrdU stained cells (i.e., Labeling Index or LI) is shown in Figures 4.5B. All reductions in epidermal thickness and LI were statistically significant.

Twist1 deletion in basal keratinocytes inhibited UVB skin carcinogenesis

After following our previously published UVB protocol [136], we found a significant delay in the onset of squamous cell carcinomas (SCC) in the Twist1 KO cohort as well as significant decreases in tumor incidence and multiplicity when compared to Twist1 WT mice. In Table 3 and Figure 4.6A, the Twist1 KO mice showed significant increased SCC-free survival (Mantel-Cox Test $p < 0.0001$, Chi Square=26.98) presenting the first SCC at week 44. The tumor at week 33 in this group was confirmed as a sarcoma based on the negative staining of K1, K5, and p63 and positive Vimentin staining characteristically found distributed throughout the epithelial portion of the tumors (Fig4.7A). There were no significant differences in incidence, multiplicity and onset of sarcomas when comparing both groups (Fig4.7B). In Table 4 and Figure 4.6B, the cumulative count of SCC/mouse was also significantly reduced in the Twist1 KO mice (2.96 vs 1.07, Mann-Whitney U test $p < 0.001$). The Twist1 KO group presented delayed onset of SCC (44 weeks) compared to the Twist1 KO group (27 weeks) (Table 3). These tumors showed high protein levels of Twist1 (Fig4.8) equally in both groups and were confirmed as cutaneous SCC based on positive immunofluorescence staining for K1, K5, p63 and low staining for Vimentin (Fig4.7B) in tumor sections.

Table 3. Tumor onset for Twist1 WT and Twist1 KO cohorts in UVB carcinogenesis protocol

TWIST1 WT	ONSET FIRST TUMOR (week)	TWIST1 KO	ONSET FIRST TUMOR (week)
MOUSE #		MOUSE #	
87	48	80	33***
93	41	82	50
90	46	83	49
97	40	86	45
98	41	88	48
102	40	91	46***
103	46	94	45***
30	46	96	NO
31	37	99	49
32	30	100	44
33	37***	105	NO
34	40	106	NO
35	27	107	NO
37	39	108	NO
40	41		
41	38		
53	31		
54	29		
55	35		
60	29		
61	35		
65	41		
62	39		
68	40		
70	35		
71	49		

*** Tumors classified as Sarcomas based on staining of Figure 4.7B

Table 4. Tumor multiplicity for Twist1 WT and Twist1 KO cohorts in UVB carcinogenesis protocol

TWIST1 WT		Multiplicity		TWIST1 KO		Multiplicity	
WEEK	#ofTUM	SUM	SUM/n	WEEK	#ofTUM	SUM	SUM/n
26	0	0	0.00	26	0	0	0.00
27	1	1	0.04	27	0	0	0.00
28	0	1	0.04	28	0	0	0.00
29	2	3	0.12	29	0	0	0.00
30	1	4	0.15	30	0	0	0.00
31	1	5	0.19	31	0	0	0.00
32	0	5	0.19	32	0	0	0.00
33	0	5	0.19	33	0	0	0.00
34	3	8	0.31	34	0	0	0.00
35	5	13	0.50	35	0	0	0.00
36	1	14	0.54	36	0	0	0.00
37	5	19	0.73	37	0	0	0.00
38	3	22	0.85	38	0	0	0.00
39	4	26	1.00	39	0	0	0.00
40	7	33	1.27	40	0	0	0.00
41	7	40	1.54	41	0	0	0.00
42	2	42	1.62	42	0	0	0.00
43	2	44	1.69	43	0	0	0.00
44	3	47	1.81	44	1	1	0.07
45	4	51	1.96	45	2	3	0.21
46	5	56	2.15	46	0	3	0.21
47	7	63	2.42	47	1	4	0.29
48	3	66	2.54	48	1	5	0.36
49	5	71	2.73	49	3	8	0.57
50	3	74	2.85	50	1	9	0.64
51	3	77	2.96	51	6	15	1.07
52	0	77	2.96	52	0	15	1.07

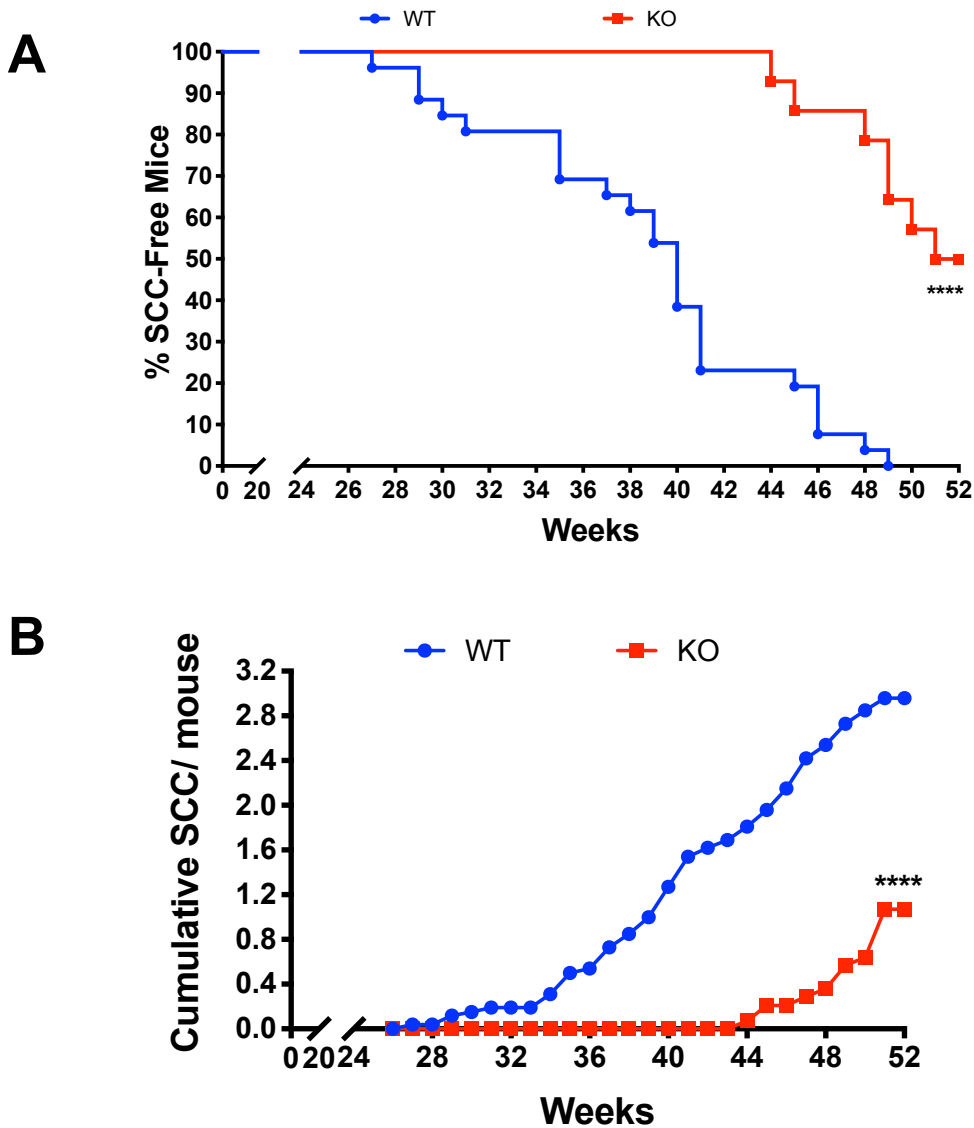


Figure 4.6 Twist1 KO increases carcinoma-free survival and inhibits UVB-induced SCC development.

A. Carcinoma-free survival Kaplan-Meier curve [WT (n=26) vs KO (n=14)] after 3x/week incremental UVB treatments [250-480mJ/cm²] for 52 weeks. Statistical analysis performed using Mantel-Cox Test, Chi square= 26.98, ****p<0.0001. B. Cumulative SCC incidence curve. Statistical analysis performed using Mann Whitney's Test ****p<0.0001

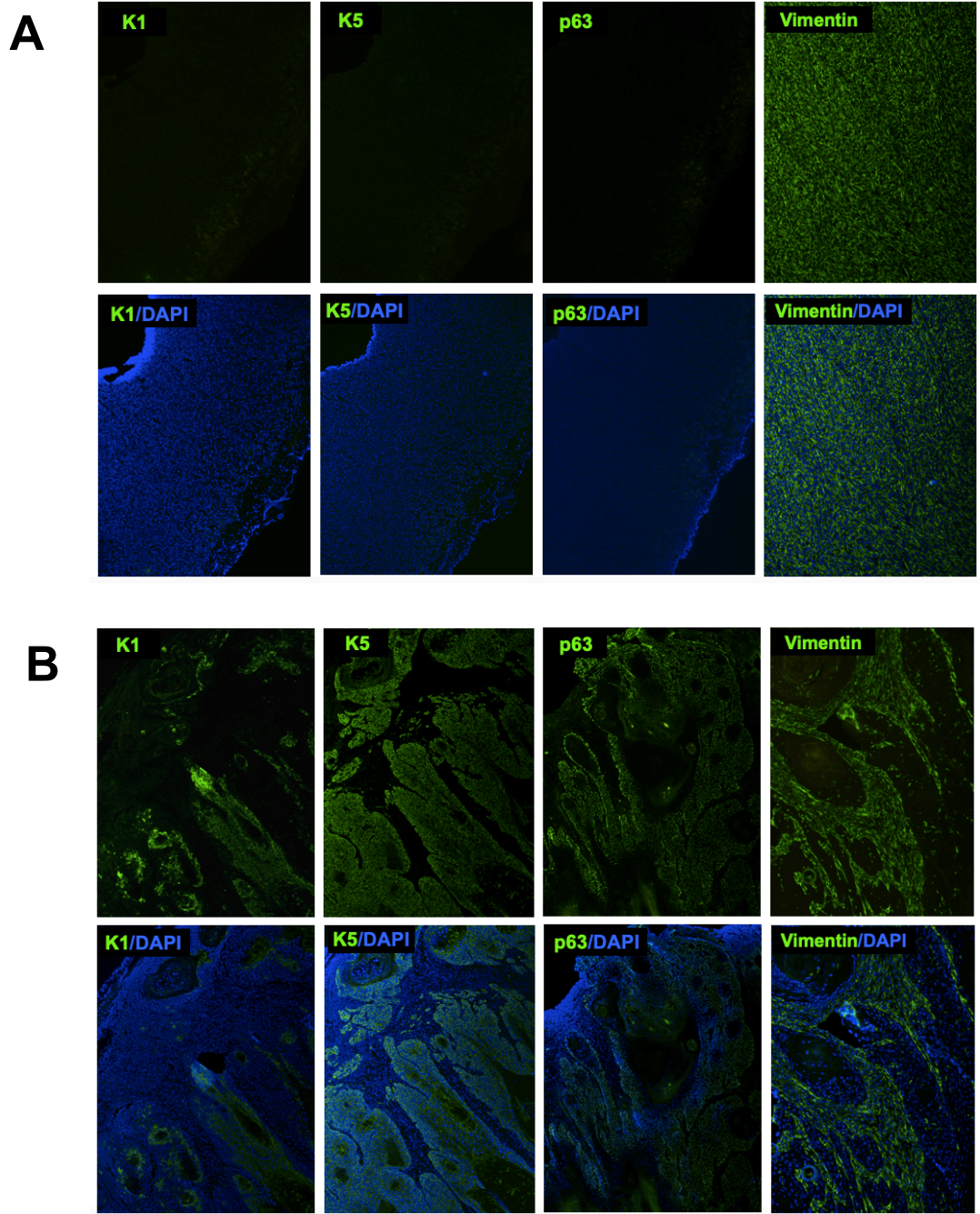


Figure 4.7 Immunostaining of SCC markers confirming tumor classifications obtained from UVB carcinogenesis protocol.

Immunostaining of SCC markers K1, K5 and p63 and of sarcoma-associated marker Vimentin in tumors pre-classified as A. Sarcoma or B. SCC based on H&E keratin pearl development (not shown).

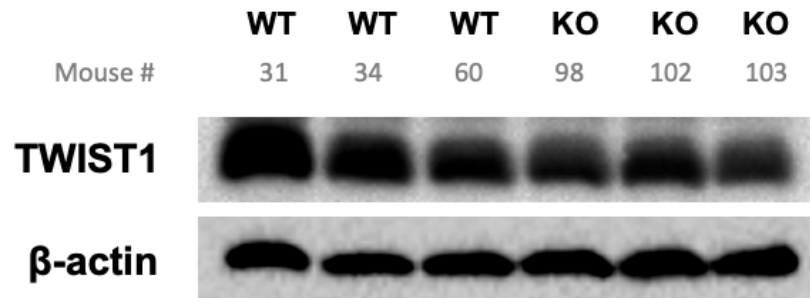


Figure 4.8 Representative SCC tumors from both Twist1 WT and KO groups showed high levels of Twist1.

Western Blot analysis using lysates from UVB-induced SCC showing staining for Twist1 and normalized to β -actin loading control.

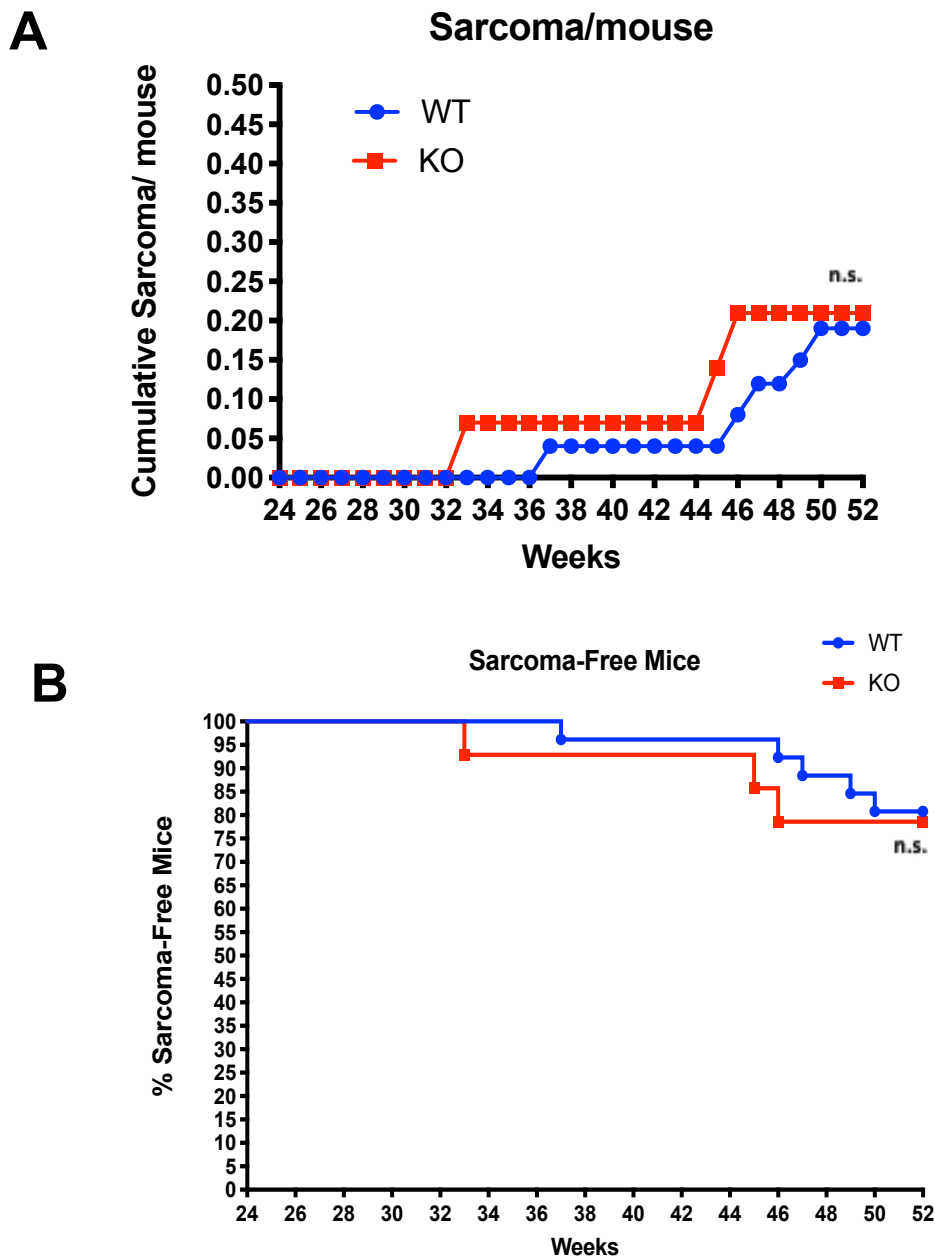


Figure 4.9 Twist1 KO yields no significant difference in UVB-induced sarcomas.

Cumulative Fibrosarcoma incidence [WT (n=26) vs KO (n=14)] after 3 weekly incremental UVB treatments [250-480mJ/cm²] for 52 weeks. Statistical analysis performed using Mann Whitney's Test ****p<0.0001. C) Sarcoma-free survival Kaplan-Meier curve. Statistical analysis performed using Mantel-Cox Test ****p<0.0001.

4.3 DISCUSSION

An oncogenic role for Twist1 in epithelial cancers has been uncovered, in addition to the known functions of Twist1 during EMT and cancer progression. Our published results and other supporting reports have helped in identifying Twist1 as a novel regulator of cell cycle progression and proliferation of epidermal keratinocytes during tumor promotion via direct transcriptional and post-translational regulation of key cell cycle genes [96]. Previously, we showed that constitutive expression of an active form of STAT3 in keratinocytes (i.e., BK5. STAT3C mice) resulted in increased Twist1 expression in both mouse epidermis and mouse skin tumors [42, 94]. Tsai *et al* [137] reported that overexpression of Twist1 in skin keratinocytes accelerated SCC formation and tumor cell metastasis during two-stage skin carcinogenesis using the DMBA-TPA protocol. Moreover, these experiments demonstrate that Twist1 is required for *de novo* development of skin tumors.

We utilized K5.Cre x Twist1^{fllox/fllox} mice and K5.rTA x tetO.Twist1 mice to further evaluate the overall role of Twist1 in UV-induced skin carcinogenesis. In the current study, we found that Twist1 impacts both the proliferation and survival of keratinocytes following exposure to UVB. In particular, the deletion of Twist1 in basal keratinocytes led to significantly reduced epidermal proliferation following exposure to UVB. Both in Twist1 deficient keratinocytes in culture and mouse epidermis *in vivo*, there was evidence for decreased keratinocyte survival. This was demonstrated by the increases of the Annexin V positive apoptotic population in the primary keratinocytes (Fig4.1). The reduced levels of anti-apoptotic proteins (e.g. sestrin-2, Bcl-2, Bcl-XL) along with the arrested sub-G1 phase cells seen by Propidium Iodide staining, also confirmed an increased sensitization to UVB-induced apoptosis (Fig 4.2 and 4.3). Overall, these

findings demonstrate that Twist1 is an important regulator of cell survival pathways following exposure to UVB.

A reduction in epidermal proliferation implies that Twist1 regulates the proliferation of keratinocytes since the deletion of Twist1 occurs in basal keratinocytes (where K5 is expressed) that possess proliferative capacity. Twist1 deletion decreased keratinocyte hyperproliferation *in vivo* after acute UVB exposure as seen by the reduction of epidermal thickness, the inhibition of BrdU incorporation and decreased staining of the proliferation marker Ki67. These data indicate that Twist1 deletion inhibits UVB-induced epidermal proliferation similar to that observed following topical application of TPA and suggests that targeting Twist1 could inhibit development of UVB-induced cSCC. Together with the changes in expression of cell cycle proteins (especially cyclin B1 and p-cdk1 after acute UVB irradiation in Figure 4.4) these results are all indicators of decreased UVB-induced epidermal hyperproliferation in Twist1 KO keratinocytes.

In our previous published studies [96] we provided evidence that Twist1 binds to and transcriptionally regulates both cyclin D1 and cyclin E genes and possibly other cell cycle genes. As shown in Figure 4.4, Twist1 deficient epidermis showed increased induction of p21 and p53 compared to its wild-type counterparts after 72h of UVB exposure. The increased levels of p21 likely resulted in the observed inhibited E2F1 expression, which would prevent continuation of the G1 phase of the cell cycle [138-140]. However, we observed more robust effects on the G2 phase shown by decreased Cyclin B1 and p-cdk1 in the UVB-exposed Twist1 KO epidermis. Charrier-Savournin *et al* have concluded that p21 can also contribute to the establishment of a

G2 arrest by maintaining the inactive state of mitotic cyclin–cdk complexes. In their DNA damage model, p21^{-/-} fibroblasts showed degradation of mitotic cyclin B1 and cdk1 and interfered with their nuclear recruitment compared to wild-type controls. Thus, the current data are consistent with their observations and complement our findings establishing a role for Twist1 in UVB-induced epidermal proliferation. This supports our confirmed hypothesis that the Twist1 deficiency significantly increases tumor-free survival in UVB carcinogenesis (Fig4.6A) and reduces cumulative counts of SCC (Fig4.6B).

In closing, we have provided evidence for the first time for an important role of Twist1 in regulating early responses to UVB exposure in skin keratinocytes, the target cells for formation of SCC. The decreased formation of SCC in the Twist1 KO cohort of the UVB skin carcinogenesis experiments, demonstrate a critical role for Twist1 as a novel target for prevention of NMSC.

CHAPTER 5. Pharmacological inhibitor of Twist1, Harmine, induces keratinocyte differentiation and inhibits UVB-induced epidermal proliferation

5.1 INTRODUCTION

In Chapter 3, we described how that transcription factor Twist1 regulates proliferation in epidermis by inhibiting keratinocyte differentiation and maintaining stem/progenitor functions. Additionally, the deletion of Twist1 *in vivo* and in culture showed significant induction of early and late differentiation markers, which was rescued in an inducible Twist1 overexpression model. Moreover, deletion of Twist1 inhibited stem markers and clonogenicity in keratinocyte stem cells (KSC), which demonstrates that Twist1 plays a direct role in regulating proliferative and self-renewal processes in the epidermis.

Harmine, a harmala alkaloid found in numerous plants [79, 80], has been shown to inhibit different cancers by impacting mechanisms of cell proliferation and invasion [83, 141]. In traditional medicine of Mediterranean cultures, the seeds of *P. harmala* are used to treat skin and subcutaneous tumors [142]. In addition, Harmine has been shown to have anti-tumor activity in both transgenic and patient-derived xenograft mouse models of *KRAS*-mutant NSCLC [141]. Recently, Harmine has been reported as a first in class Twist1 inhibitor [83]. Mechanistic examination indicated that Harmine targeted the Twist1 pathway through elevated degradation of Twist1 protein [83]. Atalantiaflavone, a flavonoid from the leaves of *Atalantia Monophylla* also decreased the stability of Twist1 via elevated ubiquitin mediated proteasomal degradation in a dose-dependent manner, leading to inhibition NSCLC progression [90].

In the work presented here, we demonstrate that treating keratinocytes with Harmine led to Twist1 degradation and increases in K1, K10 and TG1, mimicking the differentiation-inducing effects of high calcium concentrations [13, 14, 18]. Additionally, we have found that topical application of Harmine induces increased expression of keratinocyte differentiation markers similar to that seen in Twist1 KO mice and that Harmine significantly inhibits UVB-induced epidermal proliferation. These additional data suggest that Harmine and possibly other natural compounds that target Twist1 degradation may effectively inhibit UV-induced skin carcinogenesis.

5.2 RESULTS

Harmine treatment of cultured keratinocytes induces expression of differentiation markers

To gain additional insight into the role of Twist1 in keratinocyte differentiation, we treated primary keratinocytes with Harmine. As noted in the Introduction, Harmine is a harmala alkaloid found in a number of different plants [80] and has been identified as a first in class Twist1 inhibitor that works by facilitating the degradation of Twist1 [83]. Primary keratinocytes were treated with Harmine (5 μ M) for 18 hours to inhibit Twist1 protein levels and functions. The effects of Harmine were compared with calcium-switch and with primary keratinocytes from Twist1 KO mice. The main morphological changes seen in the keratinocytes after Harmine and calcium (1.4mM) treatments were similar and included increased cell elongation and increased cell detachment, consistent with induction of differentiation (Fig 5.1). As shown in Figure 5.2, the protein levels of Twist1 were decreased by 50% after treatment with Harmine and 60% after

Harmine (5uM)	-	+	-
Ca²⁺ (1.4mM)	-	-	+

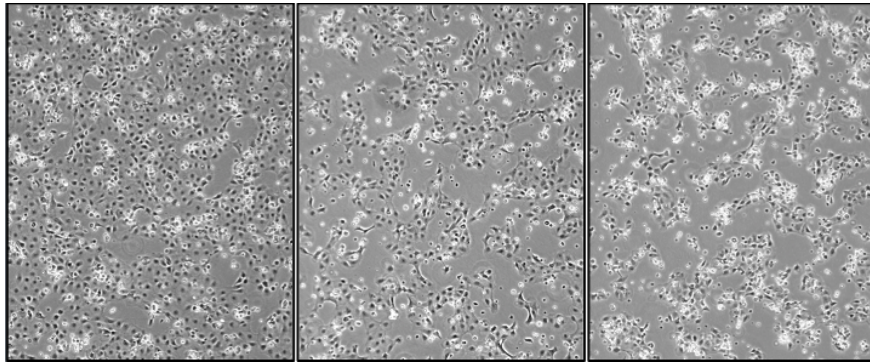


Figure 5.1 Treatment with Harmine and calcium in vitro affects keratinocyte morphology inducing differentiation.

Morphologic characterization of adult primary keratinocytes from control mice [K5.Cre^{-/-} x TWIST1^{WT/WT}] treated for 18 hours with Harmine (5uM) alone or with Ca²⁺ (1.4mM) alone.

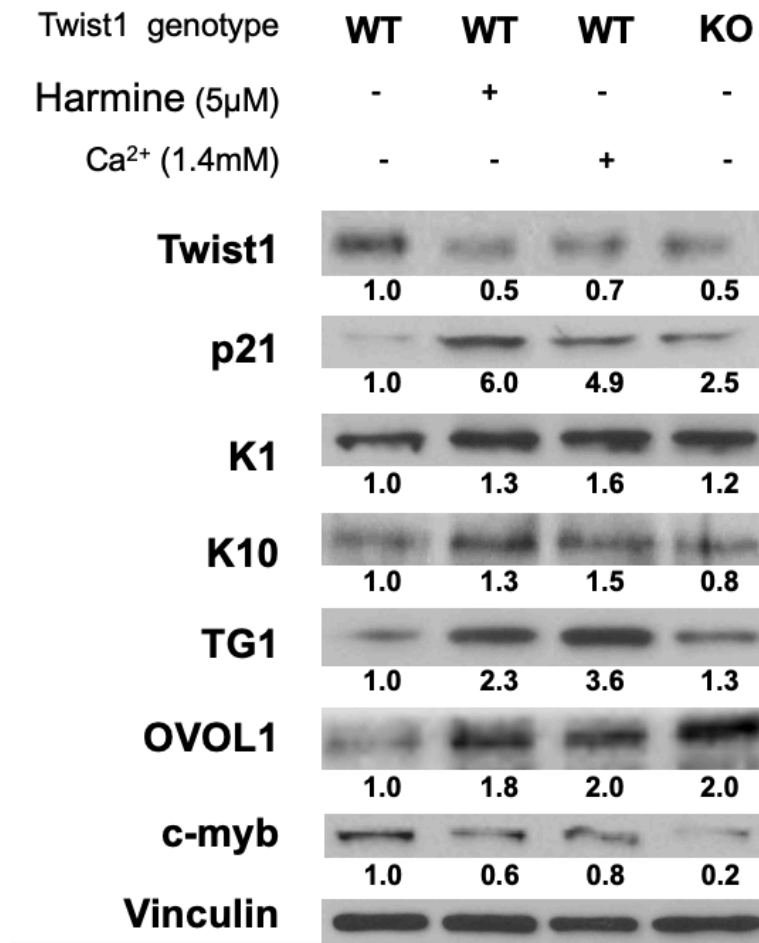


Figure 5.2 Harmine treatment of cultured keratinocytes mimics calcium-induced differentiation.

Western blot analysis of differentiation markers in primary keratinocytes from FVB/N mice after an 18 hour treatment with Harmine (5 μ M) alone or with Ca²⁺ (1.4mM) alone compared to protein samples from Twist1 KO [K5.Cre^{+/-} x Twist1^{flox/flox}] keratinocytes. Values were normalized to the Vinculin loading control.

calcium-switch. The Harmine treated keratinocytes and those treated only with high calcium showed similar increases in protein levels of p21 (7.7 and 5.0- fold, respectively), TG1 (2.3 and 2.8-fold, respectively) and K1 (1.9 and 1.8- fold, respectively). Furthermore, primary keratinocytes from Twist1 KO mice exhibited increased levels p21 (3-fold), TG1 (1.3-fold) and K1 (1.8 fold). Notably, OVOL1 protein levels were upregulated in Harmine- and calcium-treated cultures as well as in Twist1 KO cells (1.8-1.9-fold). With the objective to identify a mechanism through which this OVOL1 induction occurs, we used a siRNA targeting Bmi1, a characteristic downstream target of Twist1 [75]. In Figure 5.3, we show that Harmine treatment indeed results in decreased Bmi-1 levels. Also in this Figure, we observed that Harmine treatment induced expression of p16 (2.3 fold) , E-cadherin (6.6 fold) and OVOL1 (1.2 fold) whereas a 70% decrease in Bmi-1 at 72h also increased both of its downstream targets (2.1 and 4.0 fold respectively) but failed to induce OVOL1.

The siRNA approach was used again but this time targeting OVOL1 to further confirm its involvement in the Harmine-induced differentiation effects observed in keratinocytes. After 72 hours of treatment with siOVOL1 (100nM), there was a reduction in the Harmine-mediated increased protein levels of K1 (2.5 vs 1.9 fold), K10 (1.2 vs 0.7 fold) and Loricrin (6.8 vs 1.5 fold) (Fig 5.4). Unfortunately, due to low basal levels of OVOL1 in these keratinocytes, this experiment did not allow for confirmation of a direct decrease in OVOL1 protein levels after siRNA treatment or increases after Harmine. Nevertheless, the inhibition in Harmine-induced increases of downstream target p21 (1.2 vs 0.7 fold), imply that this system did have a deleterious effect on the OVOL1 pathway.

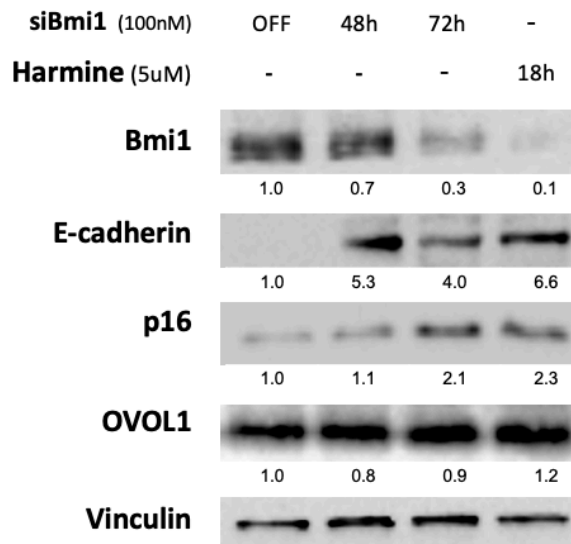


Figure 5.3 Bmi1 inhibition replicates p-16 and E-cadherin increases of Harmine but not OVOL1 induction.

Western blot analysis of Bmi1 downstream targets and OVOL1 in primary keratinocytes from FVB/N mice after an 18 hour treatment with Harmine (5 μ M) alone or with siBmi1 (100nM) for 1 hour and harvested at 48 or 72 hours. Values were normalized to the Vinculin loading control.

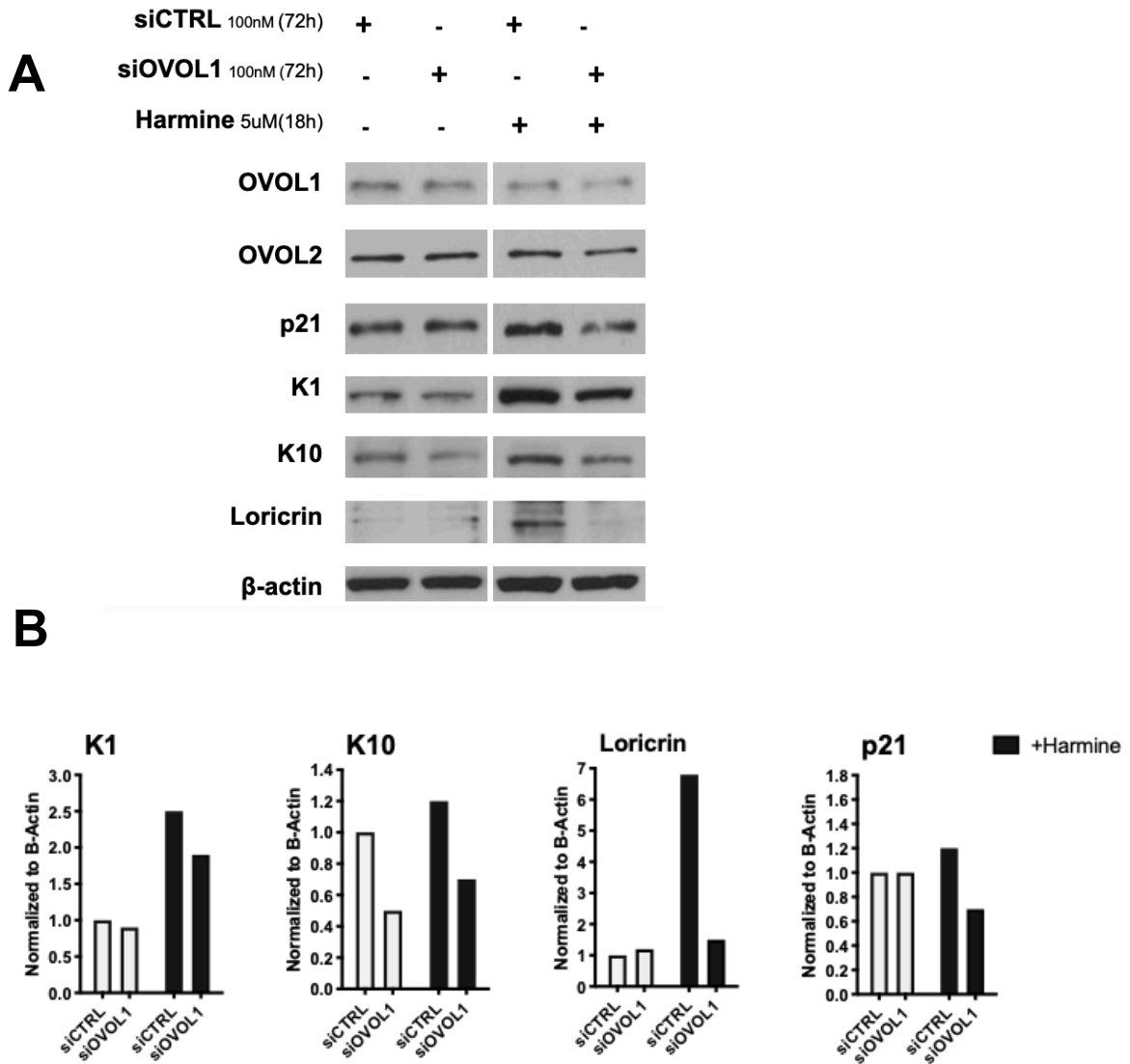


Figure 5.4 OVOL1 inhibition reduces Harmine-induced differentiation.

A. Western blot analysis of differentiation markers in primary keratinocytes from FVB/N mice after an 18 hour treatment with Harmine (5 μ M) and with siOVOL1 (100nM) or siCTRL (100nM) harvested at 72 hours. B. Densitometric quantification for protein targets using values normalized to β -actin.

Twist1 KO in epidermis affects Wnt signaling via PKC activation to induce OVOL1 expression

In order to understand the mechanism behind the activation of OVOL1 in Twist1 deficient and Harmine treated keratinocytes, we analyzed upstream targets of OVOL1. OVOL1 can be considered as a downstream effector of the canonical Wnt signaling pathway, which amongst other functions, governs differentiation of epithelial and hair follicle stem cells [143]. In Figure 5.5A, we found robust decreases in β -catenin levels (70%) in Twist1 KO lysates (used in Chapter 3) that corresponded with an increase in the phosphorylated form of β -catenin (S33/37/T41) (2.90 fold). We proceeded to investigate activators at this phosphorylation site and found that Gwak *et al* reported that PKC phosphorylation has been shown to mediate GSK3 β -independent β -catenin downregulation by phosphorylation β -catenin (S33/37/T41) [144]. Moreover, we show increased protein levels for both S660 and T638/641 phosphorylation sites of PKC. Interestingly, the phosphate that regulates these two, PP2A, was reduced by 78% in the Twist1 KO epidermis (Fig 5.5A). Protein levels for the phosphorylated PKC (T638/641) and β -catenin (S33/37/T41) were accordingly elevated after Harmine and Ca²⁺ treatments in the in vitro Harmine experiment presented before in Figure 5.2 (Figure 5.5B). By utilizing the PKC inhibitor, Bisindoylmaleimide (Bim1), we were able to inhibit phosphorylation sites of PKC by about 30% (Figure 5.6A) which resulted in an inhibition in the Harmine-induced increase of OVOL1 (1.48 vs 0.89 fold) as well as the levels of phosphorylated STAT3 (S727) (1.35 vs 0.98 fold). In the diagram of Figure 5.6B, we present this tentative mechanism for the induction of OVOL1 after Twist1 inhibition via PKC activation and β -catenin degradation.

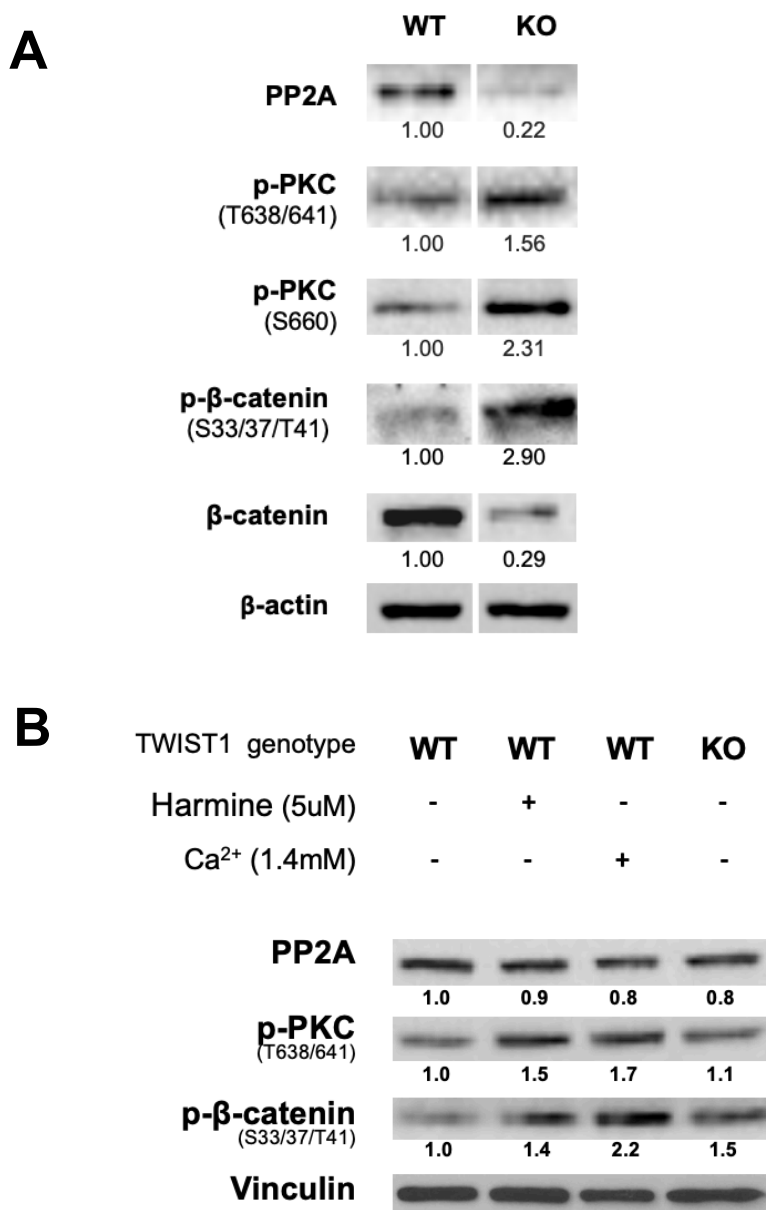


Figure 5.5 Twist1 deletion impacts Wnt pathway via PKC-mediated degradation of β-catenin.

A. Western blot analysis of PKC and Wnt pathway targets in A. epidermal scrapings from K5.Cre^{+/-} x Twist1^{wt/wt} and K5.Cre^{+/-} x Twist1^{flox/flox} mice and B. primary keratinocytes from FVB/N mice after an 18 hour treatment with Harmine (5μM) alone or with Ca²⁺ (1.4mM) alone compared to protein samples from Twist1 KO [K5.Cre^{+/-} x Twist1^{flox/flox}] keratinocytes. Values were normalized to the respective β-actin or Vinculin loading control.

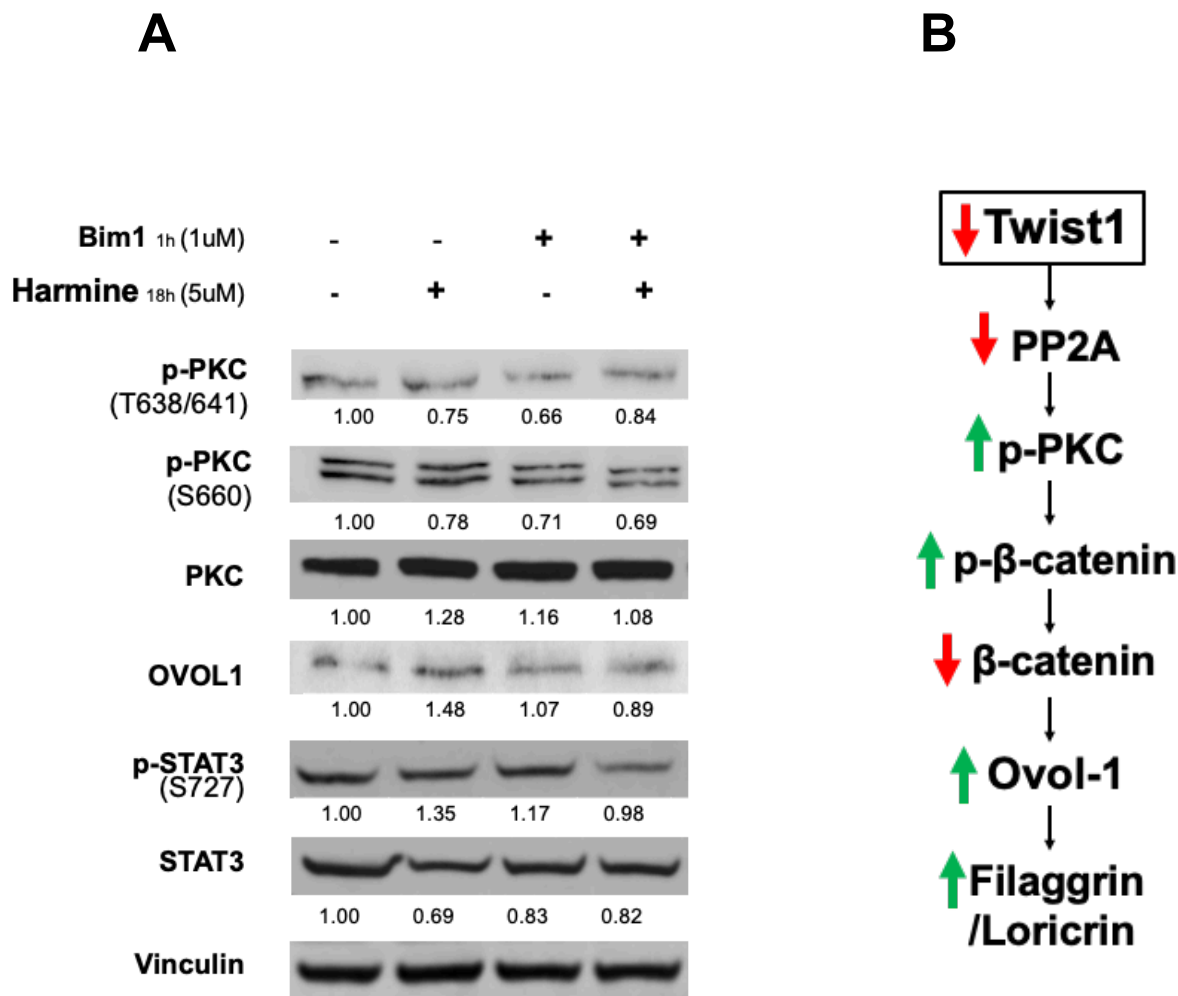


Figure 5.6 PKC inhibition results in reduced Harmine-induced OVOL1 and p-STAT3.

A. Western blot analysis of PKC associated targets in primary keratinocytes from FVB/N mice after a 1 hour treatment with PKC inhibitor Bisindolylmaleimide or Bim1 (1μM) alone or followed by an 18 hour treatment with Harmine (5μM). Values were normalized to loading control Vinculin. B. Diagram showing possible mechanism by which Twist1 induces expression of OVOL1 and differentiation targets through PKC activation.

Harmin treatment in vivo inhibits UVB-induced hyperproliferation

We examined the effect of topical treatment with Harmin on epidermal levels of selected differentiation markers as well as on UVB-induced epidermal proliferation. As shown in Figure 5.7, topical doses of 25, 50 and 75 μ g of Harmin in 0.2mL of acetone to WT FVB/N female mice led to a significant reduction in Twist1 protein levels while protein levels of p21, K1 (except at 75 μ g), K10 and Ovol1 were increased at 24 hours after treatment as determined by Western blot analyses. These preliminary data are surprisingly similar to the effects of Twist1 deletion as shown in Chapter 3 for the selected markers analyzed.

Lastly, we analyzed the effects of Harmin (6 treatments in 2 weeks) in UVB-induced proliferation. Our results in Figure 5.8 show that compared to acetone treatments before UVB radiation, treating with Harmin robustly inhibited UVB-induced increases in protein level of p53 (3.8 vs 2.1 fold), cyclin D1 (13.8 vs 6.8 fold), cdk2 (2.6 vs 0.5 fold), and cdk4 (1.8 vs 0.7 fold). Notably, these treatments also resulted in full depletion of cyclin B1 and p-cdk1 protein levels (Fig 5.8). Correspondingly, Harmin significantly inhibited epidermal proliferation induced by UVB exposure in skin sections (Fig 5.9) as shown by decreased BrdU incorporation and epidermal thickness. These effects of Harmin on sub-chronic UVB-induced hyperproliferation were statistically significant as noted in the quantification graphs of in Figure 5.9B. Collectively, these latter preliminary results suggest that topical application of Harmin may inhibit proliferation and induce differentiation of keratinocytes and thus may inhibit UV skin carcinogenesis.

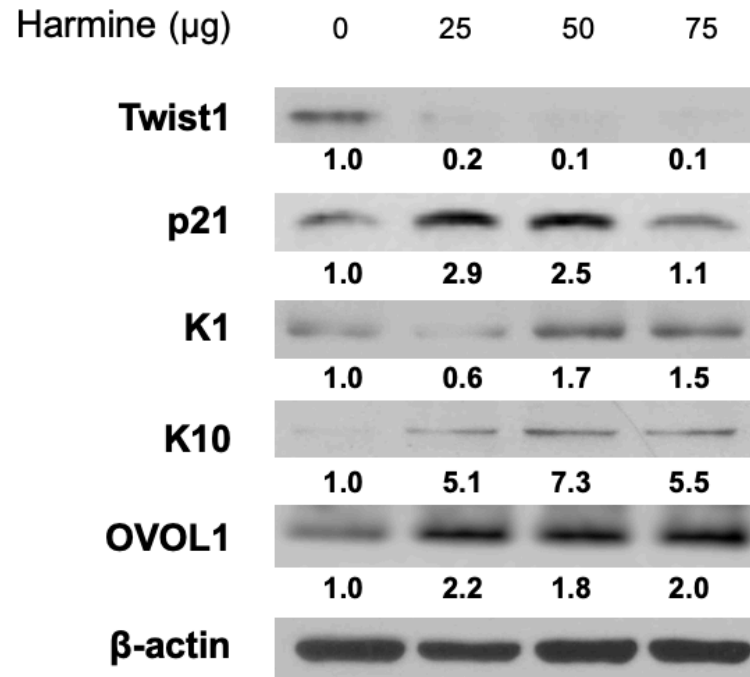


Figure 5.7 Harmine treatment of *in vivo* induces differentiation markers and OVOL1.

Western blot analysis of differentiation makers using epidermal protein lysates from control and Harmine (0-75 μg) topically treated mice (4/group) harvested at 48 hours. Values were normalized to β -actin loading control.

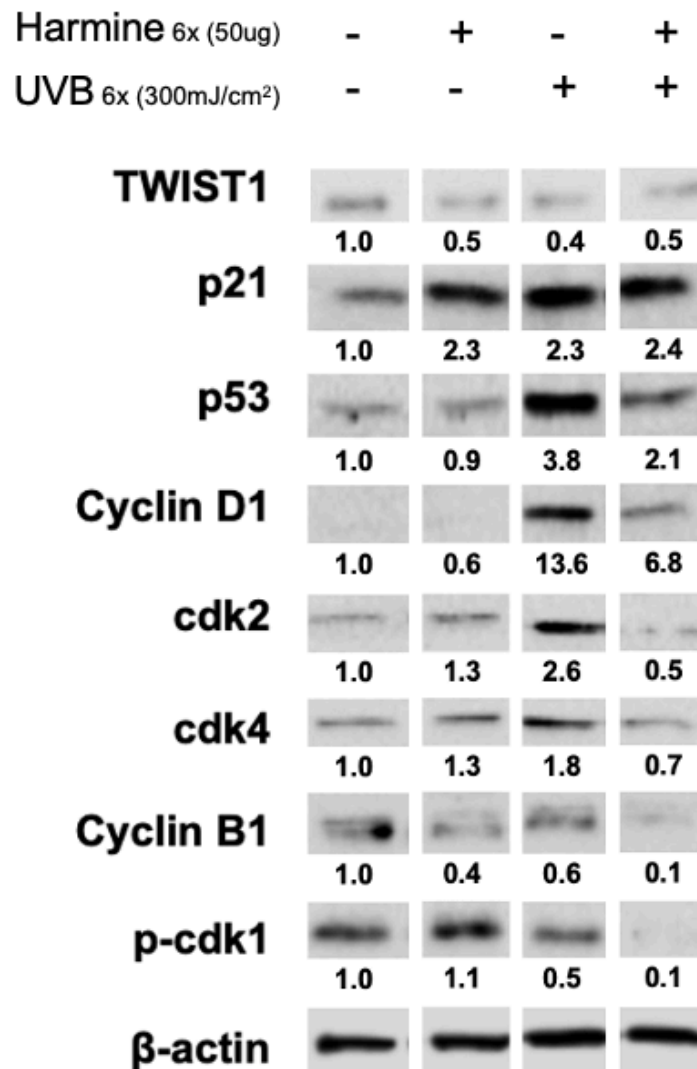


Figure 5.8 Harmine treatment in vivo inhibits UVB-induced activation of cell cycle markers.

Western blot analysis of cell cycle regulators using protein lysates obtained from epidermal scrapings from FVB/N mice treated with 50µg/0.2mL of Harmine (HAR) or Acetone (ACE) and 300mJ/cm² of UV-B 3 times a week for 2 weeks and harvested at 72 hours. Values were normalized to loading control β-actin.

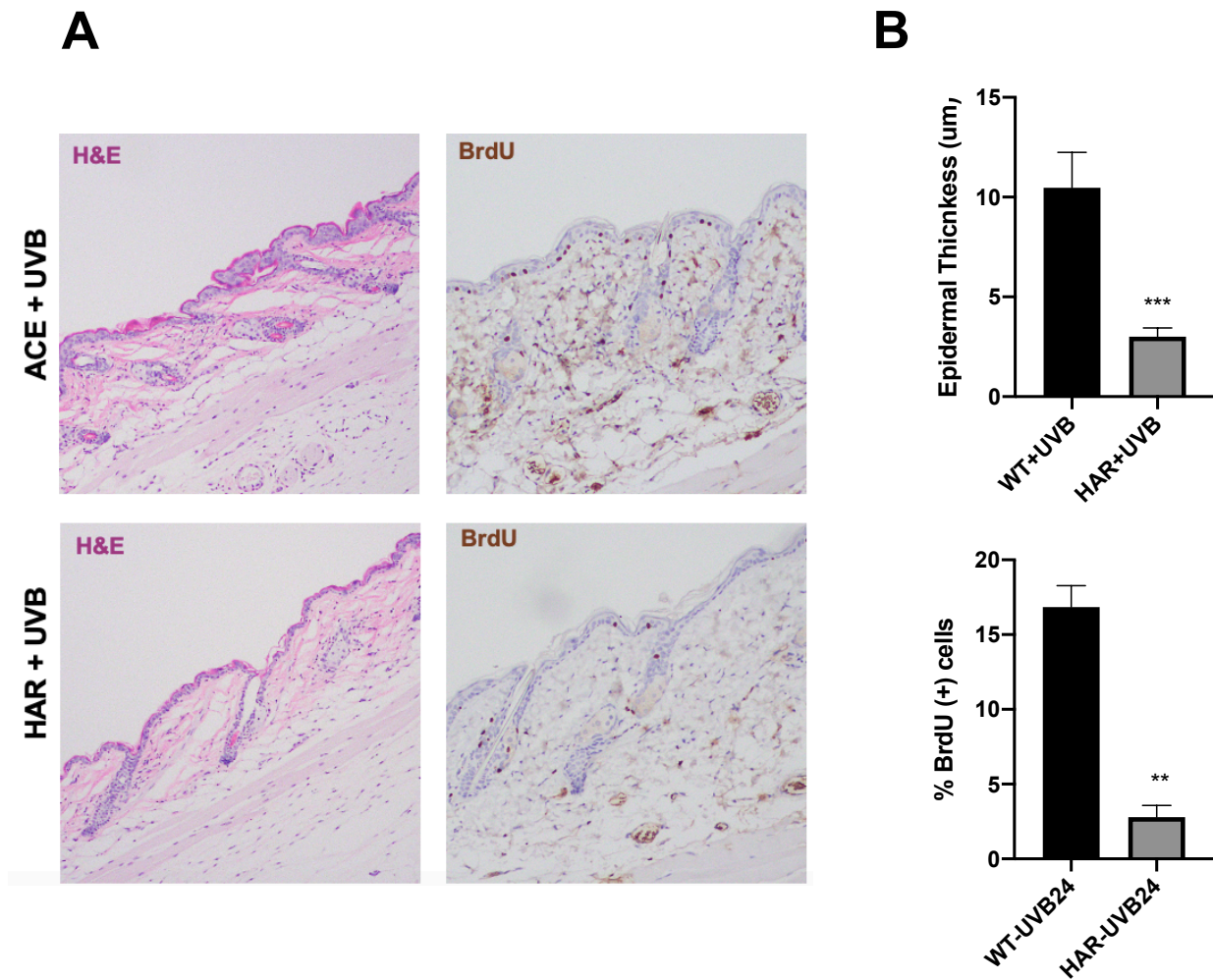


Figure 5.9 Harmine treatment in vivo inhibits UVB-induced increases in epidermal thickness and BrdU incorporation.

A. BrdU and H&E staining of dorsal skin sections harvested at 48 hours from mice exposed to 300mJ/cm² of UVB with or without Harmine (50µg). B. Quantification of epidermal thickness (mean ± SEM) of triplicate measurements from 6 H&E stained skin sections per group. Quantification of positive staining for BrdU in 500 cells per section (mean ± SEM) of 4 sections per treatment group. **p<0.005, ***p<0.0005, Mann Whitney U test.

5.3 DISCUSSION

As shown in Chapter 2, keratinocyte specific deletion of Twist1 (using K5.Cre x Twist1^{flox/flox} mice) resulted in an induction of terminal differentiation, predominantly showing increases in levels of the late stage markers and OVOL1. Accordingly, the overexpression of Twist1 (using doxycycline treated tetO.Twist1 primary keratinocytes) inhibited calcium-induced differentiation *in vitro*. The data presented in this chapter demonstrates that Harmine treatment mimicked the effects of both calcium switch-induced keratinocyte differentiation in primary keratinocytes as well as Twist1 KO-induced differentiation in primary keratinocytes and in epidermis *in vivo*.

We found that treatment of primary keratinocytes with Harmine mimics the effects of high calcium concentrations as well as Twist1 deficiency on keratinocyte differentiation as shown by increases in protein levels of K1, K10, TG1 and p21. Furthermore, inhibition of Twist1 by silencing of Twist1 after lentiviral shRNA infection [58] or Harmine treatment [83] in NSCLC cell lines resulted in the upregulation of p21 and p27. Yochum *et al* recently showed that Harmine promotes Twist1 degradation accompanied by a reciprocal induction of p21 [83], a known TWIST1 repressed transcriptional target gene that was robustly increased in our Twist1 KO keratinocytes. Interestingly, Harmine treatment also led to induction of the differentiation regulator OVOL1, similar to that seen deletion of Twist1. These data are consistent with our observations that both deletion of Twist1 or treatment with Harmine led to upregulation of p21 and OVOL1 and other differentiation markers in mouse keratinocytes.

Several plausible explanations exist to explain the mechanism(s) for how Twist1 KO or Harmine treatment lead to increased protein levels of OVOL1. One potential mechanism involves activation of the PKC-pathway. In this regard, we observed decreased β -catenin protein levels following deletion of Twist1 KO which is consistent with a previous report of the relationship between the β -catenin-AKT axis and Twist1 [145]. The binding of Twist1 to β -catenin enhances the transcriptional activity of the β -catenin/TCF4 complex in epidermal cells [146]. Accordingly, the decreases in Bmi1 expression caused by Twist1 deficiency also correspond to the observed inhibition of β -catenin, as Bmi1 is known to activate the Wnt pathway in other tissues [147]. To explore the mechanism behind the inhibition of the Wnt pathway, we analyzed the induction of a PKC-mediated β -catenin down-regulation. The increased phosphorylation of PKC β II at Ser-660 confirms an activated state that is driving the increased phosphorylation of residues Ser-33, Ser-37, and Ser-45 of β -catenin, which are consistent with previous reports of a proteasomal degradation activation derived from such posttranslational modification. Moreover, the expression of OVOL1 is transcriptionally regulated by the Wnt signaling pathway [103, 143]. Thus, decreased β -catenin signaling would lead to increased expression of OVOL1, as we have observed. Inhibition of the Wnt pathway in Twist1 KO epidermis, may be responsible for the induction of OVOL1 and this may be driven in part by the downregulation of Bmi1 and changes in Akt signaling.

In previous studies, we reported that Twist1 is a regulator of cell cycle progression during tumor promotion through direct transcriptional and post-translational regulation of key cell cycle genes, showing that Twist1 regulates p21 in keratinocytes via a mechanism of nuclear stabilization of p53 [96]. As seen in this Chapter, both in mouse epidermis *in vivo* and in cultured

primary keratinocytes, Twist1 deletion resulted in decreased G2-M cell cycle phase regulators Cyclin B1, and p-cdk1. This indicates that Harmine treatment *in vivo* inhibited UVB-induced proliferation markers, particularly those associated with G2 phase arrest. We also demonstrated that Harmine inhibited UVB-induced increases in epidermal thickness and BrdU incorporation. Altogether, topical application of Harmine *in vivo* proved highly effective in impacting proliferation after UVB exposure.

CHAPTER 6. Conclusions and Future Directions

6.1 CONCLUSIONS

Role of Twist1 in Epidermal Differentiation and Stemness

Twist1 is a bHLH transcription factor involved in EMT, tumor invasion and metastasis. Previous studies have shown a role for Twist1 in chemical carcinogenesis in mouse skin and a potential role in controlling keratinocyte proliferation. In the current studies, the impact of Twist1 deletion in both keratinocyte basal and stem cell compartments on growth properties and related signaling pathways was confirmed. The deletion of Twist1 in K5+ basal keratinocytes led to increased epidermal levels of cell cycle inhibitors (p21, p27, and p16) compared to epidermis from wild-type littermates. Further experiments revealed that Twist1 deletion led to the induction of keratinocyte differentiation shown by increased epidermal protein levels of K1, Loricrin, Filaggrin, TG1 and OVOL1. Accordingly, Twist1 overexpression using as tetO system inhibited calcium-induced differentiation in cultured mouse keratinocytes. The deletion of Twist1 *in vivo* also led to decreased expression of stemness markers, including Sox2, Lgr5, Lgr6 and CD34, which indicated that Twist1 deletion may have a direct effect on the keratinocyte stem cell population in the bulge region. The KSC with Twist1 deletion also showed impaired colony formation capabilities and reduction in stemness markers by flow cytometry. These results further demonstrate that Twist1 deletion alters the behavior of KSC, both in the basal layer and in hair follicle stem cells, possibly by controlling their state of differentiation. This implies that Twist1 may have direct role in regulating proliferative and self-renewal processes in the

epidermis which can explain the inhibition of the UVB-induced hyperproliferation in Twist1 KO mice.

Role of Twist1 in UVB-induced proliferation and tumorigenesis

Our group previously reported that TWIST1 stimulates keratinocyte proliferation in the two-stage chemical carcinogenesis model by preventing the suppressive function of p53. However, the impact of keratinocyte specific TWIST1 deletion on carcinogenesis caused by UVB radiation had not been clarified. In the work presented in this dissertation, we have shown that primary mouse keratinocytes with TWIST1 knockout (KO) displayed an increase in the sub-G1 phase population and an increase in apoptosis as shown by augmented Annexin V staining. Furthermore, deletion of TWIST1 in skin keratinocytes *in vivo* (using K5-Cre x TWIST1^{fllox/fllox} mice) led to increased sensitivity to UVB-induced apoptosis following a single exposure to 300mJ/cm². Additionally, UVB-induced epidermal hyperproliferation was also reduced in the TWIST1 KO mice. Proliferation analysis by Ki67 immunofluorescence staining as well as BrdU incorporation showed a significant decrease in TWIST1 KO epidermis. Correspondingly, protein levels for G2-phase cell cycle regulators were reduced in the absence of TWIST1. Twist1 deficiency significantly increases tumor-free survival in UVB carcinogenesis and reduces cumulative counts of SCC, indicating a robust effect on UVB skin carcinogenesis.

Twist1 inhibition by Harmine replicates effects of Twist1 KO on differentiation and proliferation

As expected, the protein levels of Twist1 were decreased after treatment with the alkaloidal inhibitor Harmine, but interestingly also decreased after calcium-switch. The Harmine treated keratinocytes and those treated only with high calcium showed similar increases in protein levels of p21, TG1 and K1. Notably, OVOL1 protein levels were upregulated in Harmine- and calcium-treated cultures as well as in Twist1 KO cells. Thus, Harmine treatment mimicked the effects of both calcium switch-induced keratinocyte differentiation as well as Twist1 KO-induced differentiation in primary keratinocytes. We also examined the effect of topical treatment with Harmine on epidermal levels of selected differentiation markers as well as on UVB-induced epidermal proliferation. As presented in Chapter 5, topical doses of Harmine led to a significant reduction in Twist1 protein levels while levels of differentiation associated proteins p21, K1, K10 and OVOL1 were increased. Sub-chronic Harmine treatments also significantly inhibited epidermal proliferation induced by UVB exposure with corresponding decreases in G2 phase cell cycle regulators. Collectively, these latter preliminary results suggest that topical application of Harmine may inhibit proliferation and induce differentiation of keratinocytes and thus inhibit UV skin carcinogenesis.

Working Model for the effects of Twist1 Deficiency in Keratinocytes

The diagram below (Figure 6.1) presents a working model of the major changes observed in keratinocytes following deletion of Twist1 that we believe play an important role in the effects on keratinocyte proliferation, differentiation and stemness. As stated above, our current data indicate that OVOL1 is a major downstream effector of Twist1 in maintaining the balance between proliferation and differentiation of keratinocytes and for maintaining stemness of KSC. As shown in Chapter 3, deletion of Twist1 in epidermal keratinocytes led to upregulation of OVOL1. OVOL1 is known to directly regulate levels of both Loricrin and Filaggrin, genes involved in keratinocyte differentiation [108-110] as well as transcriptionally repress c-myc, Zeb1 and Id2 [104, 112-115]. We also observed upregulation of p27 in Twist1 deficient keratinocytes which is consistent with the reduced levels of Id2 we observed as this transcription factor has been shown to transcriptionally repress p27 expression [148, 149]. Another interesting observation from our preliminary experiments is the finding of downregulation of Sox2 in Twist1 deficient keratinocytes. p27 has been shown to be part of a transcriptional repressive complex for Sox2 and this may explain, at least in part, the reduced levels of Sox2 seen in Twist1 deficient keratinocytes [150, 151]. Sox2 is a transcription factor known to play an important role in embryonic development and maintenance of adult stem cells, including keratinocyte stem cells [152]. A role for Sox2 in keratinocyte stem cell maintenance and differentiation has been identified [152, 153]. Furthermore, a role for Sox2 in growth of cSCC was recently reported [154]. Sox2 is known to suppress expression of E-cadherin and ZO-1 and to enhance expression of multiple EMT related genes [155, 156]. Thus, reduction in Sox2 may represent an important mechanism driven by Ovoll upregulation in Twist1 KO mice that

contributes to the effects observed on keratinocyte behavior. It is important to note that Twist1 regulates other pathways that may also play a role in the overall effects seen after its deletion in keratinocytes. Twist1 deletion resulted in an induction in protein levels of cyclin-dependent-kinase (cdk) inhibitors p21 and p16. The mechanism for increased p21 protein level involves the interaction of Twist1 with p53 that leads to increased protein stability as previously shown [96, 102]. The increased protein levels of p16 and E-cadherin are due to reduced levels of Bmi1 seen following deletion of Twist1. Yang *et al* showed the direct binding of Twist1 to the *Bmi1* promoter and the physical interaction between Twist1 and Bmi1 [75]. Also, these two proteins were shown to bind to both *E-cadherin* and *p16INK4A* promoters. Thus, the observed increases in E-cadherin and p16 protein levels are likely due to the loss of transcriptional repression from both Twist1 and Bmi1. Although Bmi1 may play a role in UV skin carcinogenesis, this role may be more related to later stages of the carcinogenic process involving EMT events, while we believe that OVOL1 is a key transcription factor in the effects of Twist1 early in the process of UV skin carcinogenesis and will be the primary focus of our mechanistic studies in the current proposal. Thus, we will further explore the mechanisms linking Twist1 deletion to altered regulation of OVOL1 and the other changes observed in downstream pathways. Currently, the mechanism for OVOL1 upregulation in Twist1 deficient keratinocytes is not known. Twist1 may transcriptionally repress OVOL1 expression and this will be further explored in future experiments describe below. New models (both *in vitro* and *in vivo*) will be used to determine the importance of OVOL1 as a downstream effector of Twist1 during early stages of UV skin carcinogenesis.

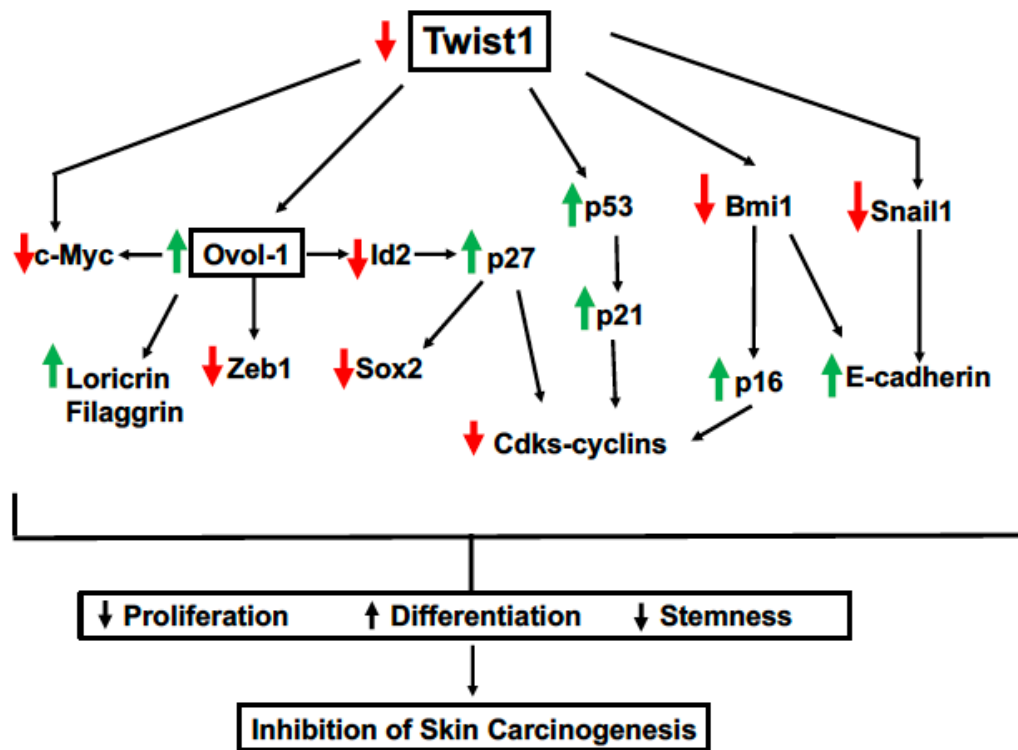


Figure 6.1 Working model for the effects of Twist1 deletion on downstream pathways controlling proliferation, differentiation, stemness and EMT in keratinocytes

6.2 FUTURE DIRECTIONS

Further characterize the role of Twist1 in UVB-induced carcinogenesis with Twist1 overexpression in vivo

For this purpose we will conduct a UVB skin carcinogenesis experiment using the mice with Twist1 overexpression [K5.rTA x tetO.Twist1]. Treatment of these mice with Doxycycline in the drinking water (using recommended standard protocols) will allow us to compare the results with Twist1 deletion as presented in Chapter 4. The expected results from these experiments are that tumors will develop rapidly and progress quickly to aggressive SCCs. In addition, we would perform analyses of effects on differentiation and stem progenitor populations and expect to see that differentiation is blocked *in vivo* and that stem progenitor populations would be expanded.

Determine whether Ovol1 is a direct transcriptional target of Twist1 and the impact of Ovol1 overexpression in vivo on keratinocyte proliferation, differentiation, and UV skin carcinogenesis.

Based on our preliminary data and as shown, we hypothesize that OVOL1 may be a critical downstream effector of Twist1 that plays an important role in regulating the balance between keratinocyte proliferation and differentiation. In future experiments, we will further establish OVOL1 as a critical downstream effector of Twist1 for its effects on keratinocyte

proliferation and differentiation and UV skin carcinogenesis. Firstly, our group plans to perform experiments to determine whether *Ovoll* is a transcriptional target for Twist1. Analysis of the *Ovoll* promoter revealed E-box consensus sequences located 35 and 1468 base-pairs upstream from the transcription start site. This raises the possibility that expression of *Ovoll* may be directly regulated by Twist1. In addition, we will determine the extent to which overexpression of *Ovoll* mimics the effects of Twist1 deletion on keratinocyte behavior both *in vitro* and *in vivo*. For the *in vivo* experiments, we will generate a transgenic mouse model with inducible, keratinocyte specific expression of *Ovoll* in basal keratinocytes. These mice will be used for analyzing the impact of *Ovoll* expression on keratinocyte behavior as well as on UV skin carcinogenesis.

Determine the ability of Harmine to inhibit UVB-induced skin carcinogenesis

We plan to perform UV skin carcinogenesis experiments using our standard UVB skin carcinogenesis protocol for evaluating the impact of Harmine treatment on UV-induced cSCC. We will select the dose of Harmine based on the outcome of experiments to evaluate effects on epidermal proliferation following treatment with UVB. Based on our preliminary data, we expect to find that Harmine given alone will inhibit UVB skin carcinogenesis. We may find that Harmine does not significantly inhibit UVB skin carcinogenesis when given alone. Hence we are considering other compounds (e.g., atalantoflavone, harmol) reported to have similar effects [83, 90] for synergistic combination therapy assessments. It is also important to note that in addition to its effects on Twist1 protein levels, Harmine has been reported to affect other signaling

pathways [81, 157-161] and it may be necessary to explore other mechanisms in addition to those that impact Twist1 protein stability to fully understand the actions of this compound. Finally, mechanistic studies will be performed to further explore how Harmine alters Twist1 levels and whether this mechanism accounts for its primary effects on keratinocytes and tumor formation. The identification of Harmine as a topically applied compound for inhibition of UVB skin carcinogenesis could lead to a whole new class of compounds and a novel approach for prevention of SCCs.

Determine the synergism of Harmine with other phytochemicals

Other groups have found that combining Curcumin and Isovanillin with Harmine showed potent cytotoxicity in cancer cell lines [162]. Our group has reported the efficacy of different combinations of phytochemicals in reducing carcinogenesis of different organ tissues. Examples of those compounds are Ursolic Acid and Curcumin, for which we found that their topical combination significantly inhibited skin tumor promotion by TPA [163]. Furthermore, evidence of Curcumin inducing G2/M cell cycle arrest and apoptosis in a head and neck squamous cell carcinoma model suggests that a combination with Harmine could drive keratinocytes into a mitotic catastrophe mediated cell death [164].

The topical delivery system sometimes is not the first choice for treatments due to the fact that many therapeutic compounds may exhibit poor penetration into skin, especially in a context where the necessary drug concentrations do not meet the treatment requirements. To this end, our group has tested alternative routes and has utilized dietary regimes for cancer prevention

using phytochemicals. We found that Ursolic Acid, Curcumin and Resveratrol given in the diet did not significantly inhibit skin tumor promotion by TPA when compared to the topical experiments [163]. In a recent study, Jiang *et al* developed a topical delivery system for Harmine by using ethosomes [165]. Ethosomes are an efficient delivery vector in the field of transdermal administration, which can delivery drugs rapidly from the stratum corneum into the deeper layers of the skin with excellent deformability [166]. They concluded that this technology exhibited an excellent route for the topical delivery of Harmine in clinical applications as it reduced systemic toxicity and side effects because of low Harmine concentrations in blood.

As we design the future studies to test for the ability of Harmine to inhibit UV-induced skin carcinogenesis, we will implement new technological approaches in drug delivery as well as possible synergistic combinations that yield stronger anti-tumor results and ensure safe dosing for therapeutic solutions using Harmine.

REFERENCES

1. Fuchs, E. and S. Raghavan, *Getting under the skin of epidermal morphogenesis*. Nat Rev Genet, 2002. **3**(3): p. 199-209.
2. Bressler, R.S. and C.H. Bressler, *Functional anatomy of the skin*. Clin Podiatr Med Surg, 1989. **6**(2): p. 229-46.
3. Streilein, J.W. and P.R. Bergstresser, *Langerhans cells: antigen presenting cells of the epidermis*. Immunobiology, 1984. **168**(3-5): p. 285-300.
4. Tumber, T., et al., *Defining the epithelial stem cell niche in skin*. Science, 2004. **303**(5656): p. 359-63.
5. Morris, R.J. and C.S. Potten, *Highly persistent label-retaining cells in the hair follicles of mice and their fate following induction of anagen*. J Invest Dermatol, 1999. **112**(4): p. 470-5.
6. Morris, R.J., et al., *Quantitation of primary in vitro clonogenic keratinocytes from normal adult murine epidermis, following initiation, and during promotion of epidermal tumors*. Cancer Res, 1988. **48**(22): p. 6285-90.
7. Singh, A., et al., *Keratinocyte stem cells and the targets for nonmelanoma skin cancer*. Photochem Photobiol, 2012. **88**(5): p. 1099-110.
8. Kangsamaksin, T., et al., *A perspective on murine keratinocyte stem cells as targets of chemically induced skin cancer*. Mol Carcinog, 2007. **46**(8): p. 579-84.
9. Gerdes, M.J. and S.H. Yuspa, *The contribution of epidermal stem cells to skin cancer*. Stem Cell Rev, 2005. **1**(3): p. 225-31.
10. Potten, C.S. and M. Loeffler, *Epidermal cell proliferation. I. Changes with time in the proportion of isolated, paired and clustered labelled cells in sheets of murine epidermis*. Virchows Arch B Cell Pathol Incl Mol Pathol, 1987. **53**(5): p. 279-85.
11. Sun, T.T. and H. Green, *Differentiation of the epidermal keratinocyte in cell culture: formation of the cornified envelope*. Cell, 1976. **9**(4 Pt 1): p. 511-21.
12. Morris, R.J., S.M. Fischer, and T.J. Slaga, *Evidence that the centrally and peripherally located cells in the murine epidermal proliferative unit are two distinct cell populations*. J Invest Dermatol, 1985. **84**(4): p. 277-81.
13. Watt, F.M. and H. Green, *Stratification and terminal differentiation of cultured epidermal cells*. Nature, 1982. **295**(5848): p. 434-6.
14. Fuchs, E., *Epidermal differentiation and keratin gene expression*. Princess Takamatsu Symp, 1994. **24**: p. 290-302.
15. Mehrel, T., et al., *Identification of a major keratinocyte cell envelope protein, loricrin*. Cell, 1990. **61**(6): p. 1103-12.
16. Watt, F.M., *Involucrin and other markers of keratinocyte terminal differentiation*. J Invest Dermatol, 1983. **81**(1 Suppl): p. 100s-3s.
17. Kanitakis, J., et al., *Filaggrin expression in normal and pathological skin. A marker of keratinocyte differentiation*. Virchows Arch A Pathol Anat Histopathol, 1988. **412**(4): p. 375-82.
18. Yuspa, S.H., et al., *Signal transduction for proliferation and differentiation in keratinocytes*. Ann N Y Acad Sci, 1988. **548**: p. 191-6.

19. Owens, D.M. and F.M. Watt, *Contribution of stem cells and differentiated cells to epidermal tumours*. Nat Rev Cancer, 2003. **3**(6): p. 444-51.
20. Hanahan, D. and R.A. Weinberg, *Hallmarks of cancer: the next generation*. Cell, 2011. **144**(5): p. 646-74.
21. Campos, B., et al., *Differentiation therapy exerts antitumor effects on stem-like glioma cells*. Clin Cancer Res, 2010. **16**(10): p. 2715-28.
22. de Thé, H., *Differentiation therapy revisited*. Nat Rev Cancer, 2018. **18**(2): p. 117-127.
23. Society, A.C., *Cancer Facts & Figures 2019*. 2019: Atlanta.
24. Didona, D., et al., *Non Melanoma Skin Cancer Pathogenesis Overview*. Biomedicines, 2018. **6**(1).
25. Apalla, Z., et al., *Skin Cancer: Epidemiology, Disease Burden, Pathophysiology, Diagnosis, and Therapeutic Approaches*. Dermatol Ther (Heidelb), 2017. **7**(Suppl 1): p. 5-19.
26. Cameron, M.C., et al., *Basal cell carcinoma: Epidemiology; pathophysiology; clinical and histological subtypes; and disease associations*. J Am Acad Dermatol, 2019. **80**(2): p. 303-317.
27. Wong, C.S., R.C. Strange, and J.T. Lear, *Basal cell carcinoma*. BMJ, 2003. **327**(7418): p. 794-8.
28. Que, S.K.T., F.O. Zwald, and C.D. Schmults, *Cutaneous squamous cell carcinoma: Incidence, risk factors, diagnosis, and staging*. J Am Acad Dermatol, 2018. **78**(2): p. 237-247.
29. Fernandez Figueras, M.T., *From actinic keratosis to squamous cell carcinoma: pathophysiology revisited*. J Eur Acad Dermatol Venereol, 2017. **31** Suppl 2: p. 5-7.
30. Ratushny, V., et al., *From keratinocyte to cancer: the pathogenesis and modeling of cutaneous squamous cell carcinoma*. J Clin Invest, 2012. **122**(2): p. 464-72.
31. Thomas-Ahner, J.M., et al., *Gender differences in UVB-induced skin carcinogenesis, inflammation, and DNA damage*. Cancer Res, 2007. **67**(7): p. 3468-74.
32. Moser, U., et al., *Sex-specific differences in patients with nonmelanoma skin cancer of the pinna*. Head Neck, 2020. **42**(9): p. 2414-2420.
33. Ananthaswamy, H.N. and W.E. Pierceall, *Molecular mechanisms of ultraviolet radiation carcinogenesis*. Photochem Photobiol, 1990. **52**(6): p. 1119-36.
34. de Gruijl, F.R., *Photocarcinogenesis: UVA vs. UVB radiation*. Skin Pharmacol Appl Skin Physiol, 2002. **15**(5): p. 316-20.
35. Iannacone, M.R., et al., *Patterns and timing of sunlight exposure and risk of basal cell and squamous cell carcinomas of the skin--a case-control study*. BMC Cancer, 2012. **12**: p. 417.
36. Huang, P.Y. and A. Balmain, *Modeling cutaneous squamous carcinoma development in the mouse*. Cold Spring Harb Perspect Med, 2014. **4**(9): p. a013623.
37. Ibuki, Y., et al., *Radiation sources providing increased UVA/UVB ratios attenuate the apoptotic effects of the UVB waveband UVA-dose-dependently in hairless mouse skin*. J Invest Dermatol, 2007. **127**(9): p. 2236-44.
38. Valejo Coelho, M.M., T.R. Matos, and M. Apetato, *The dark side of the light: mechanisms of photocarcinogenesis*. Clin Dermatol, 2016. **34**(5): p. 563-70.
39. Kim, D.J., et al., *Signal transducer and activator of transcription 3 (Stat3) in epithelial carcinogenesis*. Mol Carcinog, 2007. **46**(8): p. 725-31.

40. Sano, S., et al., *Signal transducer and activator of transcription 3 is a key regulator of keratinocyte survival and proliferation following UV irradiation*. *Cancer Res*, 2005. **65**(13): p. 5720-9.
41. Macias, E., D. Rao, and J. DiGiovanni, *Role of stat3 in skin carcinogenesis: insights gained from relevant mouse models*. *J Skin Cancer*, 2013. **2013**: p. 684050.
42. Chan, K.S., et al., *Forced expression of a constitutively active form of Stat3 in mouse epidermis enhances malignant progression of skin tumors induced by two-stage carcinogenesis*. *Oncogene*, 2008. **27**(8): p. 1087-94.
43. Srivastava, J. and J. DiGiovanni, *Non-canonical Stat3 signaling in cancer*. *Mol Carcinog*, 2016. **55**(12): p. 1889-1898.
44. Jen, W.P., et al., *Twist1 Plays an Anti-apoptotic Role in Mutant Huntingtin Expression Striatal Progenitor Cells*. *Mol Neurobiol*, 2020. **57**(3): p. 1688-1703.
45. Jianwei, Z., et al., *TMPRSS4 Upregulates TWIST1 Expression through STAT3 Activation to Induce Prostate Cancer Cell Migration*. *Pathol Oncol Res*, 2018. **24**(2): p. 251-257.
46. Li, Y., et al., *TPPP3 Promotes Cell Proliferation, Invasion and Tumor Metastasis via STAT3/ Twist1 Pathway in Non-Small-Cell Lung Carcinoma*. *Cell Physiol Biochem*, 2018. **50**(5): p. 2004-2016.
47. Uthaya Kumar, D.B., et al., *TLR4 Signaling via NANOG Cooperates With STAT3 to Activate Twist1 and Promote Formation of Tumor-Initiating Stem-Like Cells in Livers of Mice*. *Gastroenterology*, 2016. **150**(3): p. 707-19.
48. Li, Z., et al., *MKL1 promotes endothelial-to-mesenchymal transition and liver fibrosis by activating TWIST1 transcription*. *Cell Death Dis*, 2019. **10**(12): p. 899.
49. Howard, T.D., et al., *Mutations in TWIST, a basic helix-loop-helix transcription factor, in Saethre-Chotzen syndrome*. *Nat Genet*, 1997. **15**(1): p. 36-41.
50. Franco, H.L., et al., *Redundant or separate entities?--roles of Twist1 and Twist2 as molecular switches during gene transcription*. *Nucleic Acids Res*, 2011. **39**(4): p. 1177-86.
51. Xue, G. and B.A. Hemmings, *Phosphorylation of basic helix-loop-helix transcription factor Twist in development and disease*. *Biochem Soc Trans*, 2012. **40**(1): p. 90-3.
52. Massari, M.E. and C. Murre, *Helix-loop-helix proteins: regulators of transcription in eucaryotic organisms*. *Mol Cell Biol*, 2000. **20**(2): p. 429-40.
53. Castanon, I., et al., *Dimerization partners determine the activity of the Twist bHLH protein during Drosophila mesoderm development*. *Development*, 2001. **128**(16): p. 3145-59.
54. Gordân, R., et al., *Genomic regions flanking E-box binding sites influence DNA binding specificity of bHLH transcription factors through DNA shape*. *Cell Rep*, 2013. **3**(4): p. 1093-104.
55. Zhao, Z., et al., *Multiple biological functions of Twist1 in various cancers*. *Oncotarget*, 2017. **8**(12): p. 20380-20393.
56. Benjamin, B., et al., *Different Levels of Twist1 Regulate Skin Tumor Initiation, Stemness, and Progression*. *Cell Stem Cell*, 2015. **16**(1): p. 67-79.
57. Feng, M.Y., et al., *Metastasis-induction and apoptosis-protection by TWIST in gastric cancer cells*. *Clin Exp Metastasis*, 2009. **26**(8): p. 1013-23.
58. Burns, T.F., et al., *Inhibition of TWIST1 leads to activation of oncogene-induced senescence in oncogene-driven non-small cell lung cancer*. *Mol Cancer Res*, 2013. **11**(4): p. 329-38.

59. Ansieau, S., et al., *TWISTing an embryonic transcription factor into an oncoprotein*. *Oncogene*, 2010. **29**(22): p. 3173-84.
60. Toll, A., et al., *Epithelial to mesenchymal transition markers are associated with an increased metastatic risk in primary cutaneous squamous cell carcinomas but are attenuated in lymph node metastases*. *J Dermatol Sci*, 2013. **72**(2): p. 93-102.
61. Vand-Rajabpour, F., et al., *Differential BMI1, TWIST1, SNAI2 mRNA expression pattern correlation with malignancy type in a spectrum of common cutaneous malignancies: basal cell carcinoma, squamous cell carcinoma, and melanoma*. *Clin Transl Oncol*, 2017. **19**(4): p. 489-497.
62. Morel, A.P., et al., *EMT inducers catalyze malignant transformation of mammary epithelial cells and drive tumorigenesis towards claudin-low tumors in transgenic mice*. *PLoS Genet*, 2012. **8**(5): p. e1002723.
63. Ansieau, S., et al., *Induction of EMT by twist proteins as a collateral effect of tumor-promoting inactivation of premature senescence*. *Cancer Cell*, 2008. **14**(1): p. 79-89.
64. Cheng, G.Z., et al., *Twist is transcriptionally induced by activation of STAT3 and mediates STAT3 oncogenic function*. *J Biol Chem*, 2008. **283**(21): p. 14665-73.
65. Lo, H.W., et al., *Epidermal growth factor receptor cooperates with signal transducer and activator of transcription 3 to induce epithelial-mesenchymal transition in cancer cells via up-regulation of TWIST gene expression*. *Cancer Res*, 2007. **67**(19): p. 9066-76.
66. Li, C.W., et al., *Epithelial-mesenchymal transition induced by TNF-alpha requires NF-kappaB-mediated transcriptional upregulation of Twist1*. *Cancer Res*, 2012. **72**(5): p. 1290-300.
67. Ling, X. and R.B. Arlinghaus, *Knockdown of STAT3 expression by RNA interference inhibits the induction of breast tumors in immunocompetent mice*. *Cancer Res*, 2005. **65**(7): p. 2532-6.
68. Naugler, W.E. and M. Karin, *NF-kappaB and cancer-identifying targets and mechanisms*. *Curr Opin Genet Dev*, 2008. **18**(1): p. 19-26.
69. Sosis, D. and E.N. Olson, *A new twist on twist--modulation of the NF-kappa B pathway*. *Cell Cycle*, 2003. **2**(2): p. 76-8.
70. Sosis, D., et al., *Twist regulates cytokine gene expression through a negative feedback loop that represses NF-kappaB activity*. *Cell*, 2003. **112**(2): p. 169-80.
71. Kang, Y. and J. Massague, *Epithelial-mesenchymal transitions: twist in development and metastasis*. *Cell*, 2004. **118**(3): p. 277-9.
72. Yang, J., S.A. Mani, and R.A. Weinberg, *Exploring a new twist on tumor metastasis*. *Cancer Res*, 2006. **66**(9): p. 4549-52.
73. Peinado, H., D. Olmeda, and A. Cano, *Snail, Zeb and bHLH factors in tumour progression: an alliance against the epithelial phenotype?* *Nat Rev Cancer*, 2007. **7**(6): p. 415-28.
74. Weiss, M.B., et al., *TWIST1 is an ERK1/2 effector that promotes invasion and regulates MMP-1 expression in human melanoma cells*. *Cancer Res*, 2012. **72**(24): p. 6382-92.
75. Yang, M.H., et al., *Bmi1 is essential in Twist1-induced epithelial-mesenchymal transition*. *Nat Cell Biol*, 2010. **12**(10): p. 982-92.
76. Wu, K.J. and M.H. Yang, *Epithelial-mesenchymal transition and cancer stemness: the Twist1-Bmi1 connection*. *Biosci Rep*, 2011. **31**(6): p. 449-55.
77. Vesuna, F., et al., *Twist modulates breast cancer stem cells by transcriptional regulation of CD24 expression*. *Neoplasia*, 2009. **11**(12): p. 1318-28.

78. Schmidt, J.M., et al., *Stem-cell-like properties and epithelial plasticity arise as stable traits after transient Twist1 activation*. Cell Rep, 2015. **10**(2): p. 131-9.
79. Patel, K., et al., *A review on medicinal importance, pharmacological activity and bioanalytical aspects of beta-carboline alkaloid "Harmine"*. Asian Pac J Trop Biomed, 2012. **2**(8): p. 660-4.
80. Berrougui, H., et al., *Vasorelaxant effects of harmine and harmaline extracted from Peganum harmala L. seeds in isolated rat aorta*. Pharmacol Res, 2006. **54**(2): p. 150-7.
81. Zhang, H., et al., *Harmine induces apoptosis and inhibits tumor cell proliferation, migration and invasion through down-regulation of cyclooxygenase-2 expression in gastric cancer*. Phytomedicine, 2014. **21**(3): p. 348-55.
82. Song, Y., et al., *Specific inhibition of cyclin-dependent kinases and cell proliferation by harmine*. Biochem Biophys Res Commun, 2004. **317**(1): p. 128-32.
83. Yochum, Z.A., et al., *A First-in-Class TWIST1 Inhibitor with Activity in Oncogene-Driven Lung Cancer*. Mol Cancer Res, 2017. **15**(12): p. 1764-1776.
84. Demirezer, L.O., et al., *The structures of antioxidant and cytotoxic agents from natural source: anthraquinones and tannins from roots of Rumex patientia*. Phytochemistry, 2001. **58**(8): p. 1213-7.
85. Huang, Q., et al., *Anti-cancer properties of anthraquinones from rhubarb*. Med Res Rev, 2007. **27**(5): p. 609-30.
86. Way, T.D., et al., *Emodin represses TWIST1-induced epithelial-mesenchymal transitions in head and neck squamous cell carcinoma cells by inhibiting the β -catenin and Akt pathways*. Eur J Cancer, 2014. **50**(2): p. 366-78.
87. Chan, C.H., et al., *Pharmacological inactivation of Skp2 SCF ubiquitin ligase restricts cancer stem cell traits and cancer progression*. Cell, 2013. **154**(3): p. 556-68.
88. Ruan, D., et al., *Skp2 deficiency restricts the progression and stem cell features of castration-resistant prostate cancer by destabilizing Twist*. Oncogene, 2017. **36**(30): p. 4299-4310.
89. Posri, P., et al., *A new flavonoid from the leaves of Atalantia monophylla (L.) DC*. Nat Prod Res, 2019. **33**(8): p. 1115-1121.
90. Yuan, T., et al., *A natural product atalantraflavone inhibits non-small cell lung cancer progression via destabilizing Twist1*. Fitoterapia, 2019. **137**: p. 104275.
91. Jaya, S., et al., *Twist1 regulates keratinocyte proliferation and skin tumor promotion*. Molecular Carcinogenesis, 2016. **55**(5): p. 941-952.
92. Chan, K.S., et al., *Disruption of Stat3 reveals a critical role in both the initiation and the promotion stages of epithelial carcinogenesis*. J Clin Invest, 2004. **114**(5): p. 720-8.
93. Kim, D.J., et al., *Targeted disruption of stat3 reveals a major role for follicular stem cells in skin tumor initiation*. Cancer Res, 2009. **69**(19): p. 7587-94.
94. Rao, D., et al., *Constitutive Stat3 activation alters behavior of hair follicle stem and progenitor cell populations*. Mol Carcinog, 2015. **54**(2): p. 121-33.
95. Miyoshi, K., et al., *Stat3 as a therapeutic target for the treatment of psoriasis: a clinical feasibility study with STA-21, a Stat3 inhibitor*. J Invest Dermatol, 2011. **131**(1): p. 108-17.
96. Srivastava, J., et al., *Twist1 regulates keratinocyte proliferation and skin tumor promotion*. Mol Carcinog, 2016. **55**(5): p. 941-52.

97. Izadpanah, M.H., et al., *Ectopic expression of TWIST1 upregulates the stemness marker OCT4 in the esophageal squamous cell carcinoma cell line KYSE30*. Cell Mol Biol Lett, 2017. **22**: p. 33.
98. Chuang, H.Y., et al., *Aminopeptidase A initiates tumorigenesis and enhances tumor cell stemness via TWIST1 upregulation in colorectal cancer*. Oncotarget, 2017. **8**(13): p. 21266-21280.
99. Proestling, K., et al., *Enhanced expression of the stemness-related factors OCT4, SOX15 and TWIST1 in ectopic endometrium of endometriosis patients*. Reprod Biol Endocrinol, 2016. **14**(1): p. 81.
100. Liang, Y., et al., *Epigenetic Activation of TWIST1 by MTDH Promotes Cancer Stem-like Cell Traits in Breast Cancer*. Cancer Res, 2015. **75**(17): p. 3672-80.
101. Jung, H.Y. and J. Yang, *Unraveling the TWIST between EMT and cancer stemness*. Cell Stem Cell, 2015. **16**(1): p. 1-2.
102. Beck, B., et al., *Different Levels of Twist1 Regulate Skin Tumor Initiation, Stemness, and Progression*. Cell Stem Cell, 2015. **16**(1): p. 67-79.
103. Nair, M., et al., *Ovol1 regulates the growth arrest of embryonic epidermal progenitor cells and represses c-myc transcription*. J Cell Biol, 2006. **173**(2): p. 253-64.
104. Ito, T., et al., *Potential role of the OVOL1-OVOL2 axis and c-Myc in the progression of cutaneous squamous cell carcinoma*. Mod Pathol, 2017. **30**(7): p. 919-927.
105. Morris, R.J., et al., *Subpopulations of primary adult murine epidermal basal cells sedimented on density gradients*. Cell Tissue Kinet, 1990. **23**(6): p. 587-602.
106. Zheng, Y., et al., *Isolation of Mouse Hair Follicle Bulge Stem Cells and Their Functional Analysis in a Reconstitution Assay*. Methods Mol Biol, 2016. **1453**: p. 57-69.
107. Kagawa, H., et al., *OVOL1 Influences the Determination and Expansion of iPSC Reprogramming Intermediates*. Stem Cell Reports, 2019. **12**(2): p. 319-332.
108. Tsuji, G., et al., *Aryl hydrocarbon receptor activation restores filaggrin expression via OVOL1 in atopic dermatitis*. Cell Death Dis, 2017. **8**(7): p. e2931.
109. Hashimoto-Hachiya, A., et al., *Upregulation of FLG, LOR, and IVL Expression by*. Int J Mol Sci, 2018. **19**(6).
110. Furue, K., et al., *The IL-13-OVOL1-FLG axis in atopic dermatitis*. Immunology, 2019. **158**(4): p. 281-286.
111. Lasorella, A., et al., *Id2 is a retinoblastoma protein target and mediates signalling by Myc oncoproteins*. Nature, 2000. **407**(6804): p. 592-8.
112. Teng, A., et al., *Strain-dependent perinatal lethality of Ovol1-deficient mice and identification of Ovol2 as a downstream target of Ovol1 in skin epidermis*. Biochim Biophys Acta, 2007. **1772**(1): p. 89-95.
113. Watanabe, K., et al., *Mammary morphogenesis and regeneration require the inhibition of EMT at terminal end buds by Ovol2 transcriptional repressor*. Dev Cell, 2014. **29**(1): p. 59-74.
114. Lee, B., et al., *Transcriptional mechanisms link epithelial plasticity to adhesion and differentiation of epidermal progenitor cells*. Dev Cell, 2014. **29**(1): p. 47-58.
115. Murata, M., et al., *OVOL2-Mediated ZEB1 Downregulation May Prevent Promotion of Actinic Keratosis to Cutaneous Squamous Cell Carcinoma*. J Clin Med, 2020. **9**(3).
116. Nair, M., et al., *Ovol1 represses its own transcription by competing with transcription activator c-Myb and by recruiting histone deacetylase activity*. Nucleic Acids Res, 2007. **35**(5): p. 1687-97.

117. Kulkeaw, K., et al., *Twist1 regulates embryonic hematopoietic differentiation through binding to*. Blood Adv, 2017. **1**(20): p. 1672-1681.
118. Lomas, A., J. Leonardi-Bee, and F. Bath-Hextall, *A systematic review of worldwide incidence of nonmelanoma skin cancer*. Br J Dermatol, 2012. **166**(5): p. 1069-80.
119. American Cancer Society, *Cancer Facts & Figures 2020*. Atlanta: American Cancer Society, 2020.
120. Jerant, A.F., et al., *Early detection and treatment of skin cancer*. Am Fam Physician, 2000. **62**(2): p. 357-68, 375-6, 381-2.
121. Elmets, C.A. and M. Athar, *Milestones in photocarcinogenesis*. J Invest Dermatol, 2013. **133**(E1): p. E13-7.
122. Syed, D.N., F. Afaq, and H. Mukhtar, *Differential activation of signaling pathways by UVA and UVB radiation in normal human epidermal keratinocytes*. Photochem Photobiol, 2012. **88**(5): p. 1184-90.
123. Campbell, C., et al., *p53 mutations are common and early events that precede tumor invasion in squamous cell neoplasia of the skin*. J Invest Dermatol, 1993. **100**(6): p. 746-8.
124. Armstrong, B.K. and A. Kricger, *The epidemiology of UV induced skin cancer*. J Photochem Photobiol B, 2001. **63**(1-3): p. 8-18.
125. Rogers, H.W., et al., *Incidence estimate of nonmelanoma skin cancer in the United States, 2006*. Arch Dermatol, 2010. **146**(3): p. 283-7.
126. Chen, J.G., et al., *Cost of nonmelanoma skin cancer treatment in the United States*. Dermatol Surg, 2001. **27**(12): p. 1035-8.
127. Housman, T.S., et al., *Skin cancer is among the most costly of all cancers to treat for the Medicare population*. J Am Acad Dermatol, 2003. **48**(3): p. 425-9.
128. Brash, D.E., et al., *A role for sunlight in skin cancer: UV-induced p53 mutations in squamous cell carcinoma*. Proc Natl Acad Sci U S A, 1991. **88**(22): p. 10124-8.
129. Criscione, V.D., et al., *Actinic keratoses: Natural history and risk of malignant transformation in the Veterans Affairs Topical Tretinoin Chemoprevention Trial*. Cancer, 2009. **115**(11): p. 2523-30.
130. Hurwitz, R.M. and L.E. Monger, *Solar keratosis: an evolving squamous cell carcinoma. Benign or malignant?* Dermatol Surg, 1995. **21**(2): p. 184.
131. Berlin, J.M., *Current and emerging treatment strategies for the treatment of actinic keratosis*. Clin Cosmet Investig Dermatol, 2010. **3**: p. 119-26.
132. Qian, J., et al., *Twist1 promotes gastric cancer cell proliferation through up-regulation of FoxM1*. PLoS One, 2013. **8**(10): p. e77625.
133. Chen, J., et al., *HDAC5 promotes osteosarcoma progression by upregulation of Twist 1 expression*. Tumour Biol, 2014. **35**(2): p. 1383-7.
134. Maestro, R., et al., *Twist is a potential oncogene that inhibits apoptosis*. Genes Dev, 1999. **13**(17): p. 2207-17.
135. Demontis, S., et al., *Twist is substrate for caspase cleavage and proteasome-mediated degradation*. Cell Death and Differentiation, 2005. **13**(2): p. 4401744.
136. Dae Joon, K., et al., *Targeted disruption of Bcl-xL in mouse keratinocytes inhibits both UVB- and chemically induced skin carcinogenesis*. Molecular Carcinogenesis, 2009. **48**(10): p. 873-885.
137. Tsai, J.H., et al., *Spatiotemporal regulation of epithelial-mesenchymal transition is essential for squamous cell carcinoma metastasis*. Cancer Cell, 2012. **22**(6): p. 725-36.

138. Ookawa, K., et al., *Alterations in expression of E2F-1 and E2F-responsive genes by RB, p53 and p21(Sdi1/WAF1/Cip1) expression*. FEBS Lett, 2001. **500**(1-2): p. 25-30.
139. Dimri, G.P., et al., *Inhibition of E2F activity by the cyclin-dependent protein kinase inhibitor p21 in cells expressing or lacking a functional retinoblastoma protein*. Mol Cell Biol, 1996. **16**(6): p. 2987-97.
140. Gartel, A.L., et al., *A role for E2F1 in Ras activation of p21(WAF1/CIP1) transcription*. Oncogene, 2000. **19**(7): p. 961-4.
141. Yochum, Z.A., et al., *Targeting the EMT transcription factor TWIST1 overcomes resistance to EGFR inhibitors in EGFR-mutant non-small-cell lung cancer*. Oncogene, 2019. **38**(5): p. 656-670.
142. Li, Y., et al., *DH334, a beta-carboline anti-cancer drug, inhibits the CDK activity of budding yeast*. Cancer Biol Ther, 2007. **6**(8): p. 1193-9.
143. Li, B., et al., *The LEF1/beta -catenin complex activates movo1, a mouse homolog of Drosophila ovo required for epidermal appendage differentiation*. Proc Natl Acad Sci U S A, 2002. **99**(9): p. 6064-9.
144. Gwak, J., et al., *Protein-kinase-C-mediated beta-catenin phosphorylation negatively regulates the Wnt/beta-catenin pathway*. J Cell Sci, 2006. **119**(Pt 22): p. 4702-9.
145. Li, J. and B.P. Zhou, *Activation of β -catenin and Akt pathways by Twist are critical for the maintenance of EMT associated cancer stem cell-like characters*. BMC Cancer, 2011. **11**: p. 49.
146. Chang, Y.W., et al., *Diverse Targets of β -Catenin during the Epithelial-Mesenchymal Transition Define Cancer Stem Cells and Predict Disease Relapse*. Cancer Res, 2015. **75**(16): p. 3398-410.
147. Yu, F., et al., *BMI1 activates WNT signaling in colon cancer by negatively regulating the WNT antagonist IDAX*. Biochem Biophys Res Commun, 2018. **496**(2): p. 468-474.
148. Simbulan-Rosenthal, C.M., et al., *Id2 protein is selectively upregulated by UVB in primary, but not in immortalized human keratinocytes and inhibits differentiation*. Oncogene, 2005. **24**(35): p. 5443-58.
149. Trabosh, V.A., et al., *Sequestration of E12/E47 and suppression of p27KIP1 play a role in Id2-induced proliferation and tumorigenesis*. Carcinogenesis, 2009. **30**(7): p. 1252-9.
150. Chen, Y. and G.L. Sen, *SOX2 expression inhibits terminal epidermal differentiation*. Exp Dermatol, 2015. **24**(12): p. 974-6.
151. Wu, F., et al., *Sox2 suppresses the invasiveness of breast cancer cells via a mechanism that is dependent on Twist1 and the status of Sox2 transcription activity*. BMC Cancer, 2013. **13**: p. 317.
152. Boumahdi, S., et al., *SOX2 controls tumour initiation and cancer stem-cell functions in squamous-cell carcinoma*. Nature, 2014. **511**(7508): p. 246-50.
153. Li, H., et al., *p27(Kip1) directly represses Sox2 during embryonic stem cell differentiation*. Cell Stem Cell, 2012. **11**(6): p. 845-52.
154. Li, X.M., et al., *KLF4 suppresses the tumor activity of cutaneous squamous cell carcinoma (SCC) cells via the regulation of SMAD signaling and SOX2 expression*. Biochem Biophys Res Commun, 2019. **516**(4): p. 1110-1115.
155. Bigdelou, Z., et al., *Role of Oct4-Sox2 complex decoy oligodeoxynucleotides strategy on reverse epithelial to mesenchymal transition (EMT) induction in HT29-ShE encompassing enriched cancer stem-like cells*. Mol Biol Rep, 2020. **47**(3): p. 1859-1869.

156. Herreros-Villanueva, M., et al., *SOX2 promotes dedifferentiation and imparts stem cell-like features to pancreatic cancer cells*. *Oncogenesis*, 2013. **2**: p. e61.
157. Gao, J., et al., *Harmine suppresses the proliferation and migration of human ovarian cancer cells through inhibiting ERK/CREB pathway*. *Oncol Rep*, 2017. **38**(5): p. 2927-2934.
158. Hai-Rong, C., H. Xiang, and Z. Xiao-Rong, *Harmine suppresses bladder tumor growth by suppressing vascular endothelial growth factor receptor 2-mediated angiogenesis*. *Biosci Rep*, 2019. **39**(5).
159. Liu, J., et al., *Harmine induces cell cycle arrest and mitochondrial pathway-mediated cellular apoptosis in SW620 cells via inhibition of the Akt and ERK signaling pathways*. *Oncol Rep*, 2016. **35**(6): p. 3363-70.
160. Liu, X., et al., *Harmine is an inflammatory inhibitor through the suppression of NF- κ B signaling*. *Biochem Biophys Res Commun*, 2017. **489**(3): p. 332-338.
161. Zhang, P., et al., *Harmine Hydrochloride Triggers G2 Phase Arrest and Apoptosis in MGC-803 Cells and SMMC-7721 Cells by Upregulating p21, Activating Caspase-8/Bid, and Downregulating ERK/Bad Pathway*. *Phytother Res*, 2016. **30**(1): p. 31-40.
162. Vishwakarma, V., et al., *Potent Antitumor Effects of a Combination of Three Nutraceutical Compounds*. *Sci Rep*, 2018. **8**(1): p. 12163.
163. Tremmel, L., et al., *Inhibition of skin tumor promotion by TPA using a combination of topically applied ursolic acid and curcumin*. *Mol Carcinog*, 2019. **58**(2): p. 185-195.
164. Hu, A., et al., *Curcumin induces G2/M cell cycle arrest and apoptosis of head and neck squamous cell carcinoma*. *Oncotarget*, 2017. **8**(31): p. 50747-50760.
165. Jiang, J., et al., *The transdermal performance, pharmacokinetics, and anti-inflammatory pharmacodynamics evaluation of harmine-loaded ethosomes*. *Drug Dev Ind Pharm*, 2020. **46**(1): p. 101-108.
166. Touitou, E., et al., *Ethosomes - novel vesicular carriers for enhanced delivery: characterization and skin penetration properties*. *J Control Release*, 2000. **65**(3): p. 403-18.